UNIVERSITY OF CALIFORNIA,
IRVINE

Streptavidin as a Host for Cu(II) Complexes

DISSERTATION

submitted in partial satisfaction of the requirements
for the degree of

DOCTOR OF PHILOSOPHY

in Chemistry

by

Jonathan D. Paretsky

Dissertation Committee:
Professor Andrew S. Borovik, Chair
Professor Jennifer A. Prescher
Professor David Van Vranken

2015

DEDICATION

To Jessica, my wife,

for purpose and

endless patience.

To my parents,

for steadfast support.

To Andy,

for inspiration, expectation,

and opportunity.

And, finally, to my unborn child,

your future is the reason I do eveything.

TABLE OF CONTENTS

LIST OF FIGURES

LIST OF SCHEMES

LIST OF TABLES

ACKNOWLEDGEMENTS

Before I started research at UCI, I came to Andy to express my interest in his research, even though I had no background in bioinorganic chemistry. We discussed my interest in organic chemistry, and my desire to incorporate transition metals into my research. Naïvely I told him I had no interest in working with proteins or running gel electrophoresis, as that is what I thought bioinorganic chemistry was. He assured me that was not the case. Little did I know in a few short years I would be initiating a project that, for the first time in Andy's group history, used a protein as a ligand scaffold. Andy is great that way. When he saw an opportunity to try a new research project that was dear to his heart and fundamentally different from his lab's ouevre—if only in experiment if not in goal—he did not hesitate to give me a crack at it. It turned out to be a long and tortuous road. Andy and I disagreed at times, in our own passive ways, but every time I thought I had hit the end of my rope, he would reel me back in and set me on my path again. Every time I stopped believing in myself, he would believe in me, and that was enough

One of Andy's gifts is the ability to attract interesting and talented researchers, and because of this I have been surrounded by a phenomenal group of coworkers throughout my stay at UCI. Our workspace makes for a uniquely cozy environment. We share one lab, one office, our science, our successes, and our failures. Over the years there have been numerous graduate students and postdocs who have had a tremendous influence in shaping me both as a scientist and person. Dr. Dave Marsh kept me company as we were both soloing projects, and he, Dr. Sonja Peterson, and I climbed the highest mountain in the contiguous United States. Dr. Nate Sickermann showed me the importance of scientific curiosity. Dr. Dave Lacy always got me excited about my own science. Sarah and Ethan have been dear friends, confidants, and coffee (or chai… or scotch…) mates. Hannah Boonski was a stimulating mentoring experience. A special acknowledgment goes out to Sam, who joined me on the Artificial Metalloprotein Project and who has been an excellent teammate and colleague while developing chemistry. Thanks also to the only graduate student I shared a cubby with, Victoria, for discussions of science and pop culture, and for shared admiration of Dwayne "The Rock" Johnson. I could write at length on each and every one of you; rest assured you all hold a special place in my heart.

The faculty and resources at UCI are outstanding, and they have always been a point of pride when I think upon this institution. John and Biniam have been a huge help in understanding mass spectrometry, and Phil Dennison keeps the NMR instrumentation in tiptop condition. Prof. Dave Van Vranken allowed me to come to his group meetings when I wanted to brush up on my organic chemistry, and he was a huge help when I was trying to understand chiral HPLC analysis, which did not make into this document; special thanks to both him and Prof. Jen Prescher for serving on my advancement and dissertation committees.

The Ward lab at the University of Basel in Switzerland took me in for a month to show me how to work with Streptavidin and think about research with the protein. Dr. Tillmann Heinisch especially deserves much credit for solving many a crystal structure and sharing a Feldschlösschen.

The Poulos lab, especially Sarvind, has been incredibly supportive in my efforts to learn how to perform protein crystallography and has generously shared their equipment, instrumentation, and time. Sarvind has been an invaluable resource in my efforts, and always kept me asking "Why?" when something unexpected occurred.

UCI is a great school, but it is the students who make it so special. I am fortunate to have had what is possibly the greatest graduate school cohort of all time—you will have to take my word for it. Never has there been such a talented and compassionate group of students striving to make it in the sciences. I am continually humbled by the talent, hard work, and dedication displayed by classmates, and they have served as a constant source of inspiration. From this group of people I have found some of my closest friends. Alex, Avi, Justin, and Wes have been wonderful companions, and even my physicist roommate, Elliot, turned out to be okay—for a physicist, at least.

My family has supported me in all my efforts and has always had my back. From sage words of wisdom (and frequent, unsolicited life advice) from my father to packages of homemade chocolate chip cookies from my mother and moments of laughter with my sister Rachel, all of what you have done for me has made this possible. Brother Matt took me in and helped make California a home when I first moved to Irvine. Sister Eve has always had an open door when I needed an escape.

And what can be said of my wife Jessica? She has born every burden, ridden every high, suffered every low, and savored every victory alongside me. She waited patiently for me every night I said I would be home by six and got in at eight because I misjudged how long it would take to run a column. She listened to all of my technical explanations of my daily research with genuine interest even though I spoke what was virtually a different language. I cannot say enough how fortunate I am to have her as my wife and friend. She made my dream her own, and whenever I could not see the forest but for the trees, she showed me the way. With the completion of my degree, Jessica and I are headed off on a new adventure, and I cannot wait to see what life brings us next. (Spoiler alert: It's a baby.)

It is not in the stars to hold our destiny but in ourselves.

-William Shakespeare

CURRICULUM VITAE

Jonathan D Paretsky

EDUCATION

Ph.D., Chemistry, September 2015
University of California, Irvine, Irvine, CA
Research Advisor: Prof. A. S. Borovik

B.A., Chemistry, German, May 2009
Ripon College, Ripon, WI
magna cum laude

TEACHING EXPERIENCE

TA Professional Development Program, Department of Chemistry,
University of California, Irvine 2013, 2014
Taught new teachers a two-day Chemistry-specfic training program of interactive workshops to provide new Chemistry TAs with a foundation to begin their instructional careers.
Personally developed workshops for training TAs on diversity and microteaching.

Pedagogical Fellow, University of California, Irvine 2013–2014
Awarded the position of being one of three chemistry Pedagogical Fellows.
Designed and executed workshops on topics ranging from active learning to managing diversity in the classroom for a 2 day training program as part of the TA Professional Development and Training program
Took three courses on advanced pedagogy and career development
Reviewed applications and conducted interviews in the recruitment process for the next class of pedagogical fellows.
"Each year the [Teaching, Learning and Technology Center] selects a cadre of excellent and highly experienced TA mentors from across disciplines as part of the Pedagogical Fellows (PF) Program. Fellows receive advanced pedagogical training in preparation for the services they will provide to new TAs during the annual TA Professional Development Program held during Welcome Week. They also participate in a six-unit course in Advanced Pedagogy and Academic Job Preparation" - www.tltc.uci.edu/pfProgram.html

Undergraduate Mentor, University of California, Irvine 2011, 2013–Present
Mentored a UCI undergraduate on an ongoing research project within the Borovik lab.
Designed a laboratory project based upon the artificial metalloprotein research, supervised the synthesis of organic ligands, transition metal complexes, and artificial metalloproteins.
Supervised a visiting undergraduate for 10 weeks, mentored organic synthesis and laboratory technique.

Teaching Assistant, University of California, Irvine
General Chemistry Discussion 2010–2013
3 quarters of Chemistry 1A, 2 quarters of Chemistry 1C, 4–6 sections per quarter
Average enrollment: 350 per lecture, 20 per discussion section.
Served as a substitute lecturer for three lectures. Lectured on new material and led in class problem solving sessions.
Led discussion sections, designed problem sets, held office hours and review sessions.
Responsible for grading exams and maintaining class website.

Inorganic Chemistry Lab 2012
1 quarter upper division Chemistry 107L, 1 section, 12 students
Conducted one 7 hour lab section per week
Graded full laboratory reports, maintained grade book, prepared chemicals for experiments

Honors and Majors General Chemistry Lab 2012
1 quarter Chemistry 2L, two sections.
Average enrollment: 20 students per section.
Conducted laboratory sections. Prepared brief presentations on experiments, led experiments, graded homework, maintained a grade-book.

Organic Chemistry Discussion
2012
1 quarter Chemistry 51B, 4 discussion sections.
400 students in lecture, average 30 per discussion.
Prepared worksheets for discussion sections, led small group discussions, gave short presentations on course material, held office hours, graded exams.

Organic Chemistry Lab 2009–2011
2 quarters Chemistry 51LA, 1 quarter 51LB, two sections per quarter, 20 students per section.
Conduct laboratory sessions for organic chemistry. Instructed students on essential techniques, graded work, maintained a gradebook, and held regular office hours. (20 students per section).

Laboratory Assistant and Tutor, Ripon College 2007–2009
Assisted in conducting two sections of undergraduate organic chemistry lab.
Tutored students in organic and analytical chemistry, developed study aids.

RESEARCH EXPERIENCE

Graduate Student Researcher, University of California, Irvine
2009–Present
Adviser: Dr. A. S. Borovik
Synthesized a series of biotinylated ligands with a modular linker capable of being bound by the protein Streptavidin in a site-specific and reproducible fashion.
Prepared copper complexes with these ligands and studied their solution properties when bound by the protein using UV-Vis and EPR spectroscopy.
Crystallized Streptavidin and studied the metal binding site with X-ray crystallography
Synthesized a bis-biotinylated Salen compound and studied its complexes with copper and ability to bridge two biotin binding pockets.
Investigated the application of Fe(II) complexes bearing ligands with intramolecular H–bond donating groups toward intramolecular C—H amination reactions.

Visiting Scholar, University of Basel, Basel, Switzerland August 2012
Adviser: Dr. T. R. Ward
Learned techniques for manipulating Streptavidin including protein crystallography, circular dichroism, and gel electrophoresis.

Undergraduate Research Assistant, Ripon College 2006–2009
Adviser: Dr. M. Iimura
Synthesized a tridentate podant thioether ligand and studied its coordination chemistry with ruthenium.
Investigated the application of a series of thioether ligands toward Cu–catalyzed C–N bond-forming reactions.

Visiting Undergraduate Scholar, University of Bonn, Bonn, Germany 2008
Adviser: Dr. A. K. Lützen
Made progress toward the synthesis of chiral dissymetric 9,9'-spirobifluorenes.
Developed German reading, writing and verbal skills in a laboratory setting.

NSF–REU, Coe College, Cedar Rapids, IA 2007
Adviser: Dr. S. Stoudt
Completed a five-step synthesis of a ligand to support a hyper-valent organotin species.
Began initial studies of using the ligand to form Sn complexes.

PRESENTATIONS

1) **J. D. Paretsky**, T. Heinisch, V. Köhler, J. Jones, T. R. Ward. Streptavidin as a host for copper complexes.
Abstracts of Papers. 248th ACS National Meeting, San Francisco, CA, August 10–14, **2014** (Presentation)
UCI Student Inorganic Seminar Series, Irvine, CA, April 10, **2014** (Presentation)

2) **J. D. Paretsky**, T. Heinisch, V. Köhler, J. Jones, T. R. Ward. Streptavidin as a host for developing artifical metalloproteins. Bioinorganic Gordon Research Seminar, January 30–February 2, **2014** (Poster)

3) B. P. Nell, **J. D. Paretsky**, M. Iimura. Synthesis of organometallic compounds bearing tridentate podand thither ligands. Abstracts for Papers. 237th ACS National Meeting, Salt Lake City, UT, March 22–26, **2009** (Poster)

HIGHLIGHTS

An organic chemist with a multidisciplinary background in ligand design, inorganic synthesis, and manipulation of artificial metalloproteins.
Assisted in developing and expanding a new research program within my graduate research group.
Experienced in collaborative environments with multinational team members as part of two visiting scholar experiences with skills in German reading, writing, and conversation.
Capable of developing workshops and symposia for training educators and communicating scientific information.

SKILLS

Organic Synthesis
Inorganic Synthesis
Schlenk Line Techniques
Glove Box
Air-Free Manipulations
Column Chromatography
Protein Crystallography
NMR Spectroscopy
UV-Vis Spectroscopy
ESI Mass Spectrometry
Chiral HPLC
FT-IR Spectroscopy
EPR Spectroscopy
Pymol (3D protein software)
German (Intermediate)
Advanced Pedagogical Techniques
Symposium Planning

PROFESSIONAL EXPERIENCE

American Chemical Society Graduate Student Symposium Planning Committee
University of California, Irvine 2011–2013
Worked as part of a six-person team to develop, plan, and organize a daylong symposium entitled “From Benchtop to Business: Energy Solutions for a Green Future” at the ACS National Meeting in New Orleans in April, 2013.
Developed flyers, programs, posters, and a banner for advertisement and use during the symposium.
Participated in developing symposium theme, contacting speakers, and soliciting funding from academic organizations and industry.

SELECT AWARDS

UC Irvine Pedagogical Fellow	2013–Present
Magna Cum Laude	2009
Honors in Chemistry and German	2009
Ripon College Award for Writing in German	2009
Knop Scholarship - Ripon College full-tuition science scholarship	2007–2009
Pickard Scholarship - Ripon College partial tuition scholarship	2005–2007

AFFILIATIONS

American Chemical Society	2008–Present
ACS Graduate Student Symposium Planning Committee	2011–2012
Phi Beta Kappa	2009
Eka Francian Chemistry Honor Society	2008–2009
Delta Phi Alpha German Language Honor Society	2008–2009
Laurel Society of Academic Excellence	2008
Phi Sigma Iota International Foreign Language Honor Society	2006

ABSTRACT OF DISSERTATION

Streptavidin as a Host for Copper(II) Complexes

By

Jonathan D. Paretsky

Doctor of Philosophy in Chemistry

University of California, Irvine, 2015

Professor Andrew S. Borovik, Chair

In nature, metal ions are utilized in many proteins and enzymes in order to perform a variety of chemical transformations that are essential to maintaining human life. The range of selectivity and functionality can be attributed to the unique environment surrounding each active site, which allow for control over not only the primary coordination sphere—containing atoms covalently bound to the metal ion, but also the secondary coordination sphere (microenvironment)—made up of non-covalent interactions such as hydrogen bonds (H-bonds). Although nature is very efficient at these chemical processes, achieving the same level of selectivity is difficult in synthetic systems. In order to reproduce the functions found in metalloproteins it is necessary to maintain control over both the primary and secondary coordination spheres of synthetic systems as seen within active sites. To accomplish this, typically a rigid organic framework is constructed that will coordinate to a metal ion and additionally provide a supporting network of non-covalent interactions: intramolecular H-bonds.

The Borovik group has performed extensive research the area of secondary coordination sphere effects around transition metal complexes and has developed a multitude of ligand frameworks that bind metal ions and incorporate intramolecular H-

bond donors or acceptors that can stabilize exogenous ligands bound to the transition metal (TM) complexes. While these systems have been extremely effective and have been used to prepare unique high-valent metal-oxo/hydroxo species, they fall short in being able to provide extensive networks of H-bonds and long-range interactions found in microenvironments of metalloproteins. To address these challenges and gain further control over the secondary coordination sphere, this dissertation presents the development of new research program within the Borovik group in collaboration with the Ward lab: the development of artificial metalloproteins using biotin-Streptavidin (Sav) technology. Although Sav does not naturally contain metal ions, TM complexes of interest can be attached to biotin and inserted into the protein. This is an attractive feature, because of Sav's exceptionally high affinity for biotin , which can be exploited for the use of installing biotinylated metal complexes. Furthermore, the selective binding of biotin provides a reproducible anchor for TM complexes within the active site of protein. In addition to being able to chemically modify a ligand, the protein is amenable to site directed mutagenesis, which allows for alterations of the microenvironment around the TM complexes. This combined chemogenetic approach allows for enhanced control over primary and secondary coordination spheres of TM complexes.

The first portion of this document describes the study of biotinylated copper(II) complexes with varied linker lengths between the Cu(II) complex and biotin. Utilizing different linker lengths was proposed to allow for: 1) to design discrete monomeric species confined within separate subunits or 2) to create a bimetallic systems at the

dimer interface. Additionally, different mutants of Sav varying the amino acid residue at a site proximal to the Cu(II) complex were investigated to observe the protein effects on the secondary coordination sphere of the TM complex. Changing the serine at the112 position to either lysine, aspartate, or cysteine had drastic effects on the microenvironment of the Cu(II) complex. This was studied through Uv-Vis and electronic paramagnetic resonance (EPR) spectroscopies, and X-ray diffraction studies (XRD). XRD studies explicitly showed the molecular structures of the Cu(II) complexes bound within Sav and the effects of linker length changes and site directed mutagenesis. This research has shown proof of concept that Cu(II) complexes can be prepared within Sav and different microenvironments can be reproducibly attained with different linker lengths and protein mutants, and my work has established this methodology as a promising new research program within the group.

Another way of harnessing the dimer-of-dimers nature of Sav would be to prepare a TM complex linked to two biotin molecules to potentially bridge across two subunits of the protein. As reproducibility and rigidity of a binding environment is essential to selectivity in chemical transformations, this was envisioned as a method of firmly anchoring a TM complex within the protein to be studied further. To probe this hypothesis a bis-biotinylated Schiff-base was prepared and its binding to Sav studied using HABA titrations and gel electrophoresis. It was shown that instead of bridging two subunits in a homotetramer, the ligand and its complexes bridged separate Sav molecules to form oligomers of proteins.

Prior to developing the biotin-Sav program, I investigated the use of well-established tripodal, tetradentate ligands within the Borovik lab. Previous research within the lab had shown that the Fe(II) complexes of these ligands were capable of activating aryl azides to form Fe(III)-amido compounds via a putative Fe(IV)-imido intermediates. It was proposed that this would be amenable to a catalytic system wherein a C–H bond within an aryl azide substrate could be activated by an Fe(IV)-imido and I anticipated subsequent radical rebound would form a new C–N bond. However, the system did not demonstrate the ability to perform C–H amination.

CHAPTER 1

Introduction

Purpose of Dissertation Research

Nature performs chemical reactions with the help of a variety of proteins and enzymes, many of which contain metal cofactors in their active sites that are crucial to function.[1] These metalloproteins and metalloenzymes are responsible for innumerable processes and transformations that are essential to life as we know it. Examples include the metalloproteins that are essential for aerobic respiration: these include myoglobin (Mb) and hemoglobin (Hb) (Figure 1-1a), which are two iron-containing, heme proteins that are responsible for the storage and transport of O_2 in mammals. Also included is the dicopper protein hemocyanin, which transports O_2 for some crustaceans and arthropods (Figure 1-1b).[2,3] The photosynthesis of plants relies on the oxygen-evolving complex (OEC) in Photosystem II, which consists of a Mn_4CaO_4 cluster that performs one of the most life-essential reactions of all: the conversion of water to O_2 (Figure 1-1c).[4] Nitrogenase, which contains a cluster of Fe and Mo ions bridged by sulfides, is a metalloenzyme that is critical to nitrogen fixation.[5-7] Manganese superoxide dismutase serves the role of protector of cells by catalyzing the disproportionation of the radical superoxide ($O_2^{-\bullet}$) into H_2O_2 and O_2 (Figure 1-1d).[8,9] These are just a few examples of among thousands of life-essential metal-containing biomolecules.

a) Hemoglobin b) Hemocyanin c) The OEC d) Mn SOD

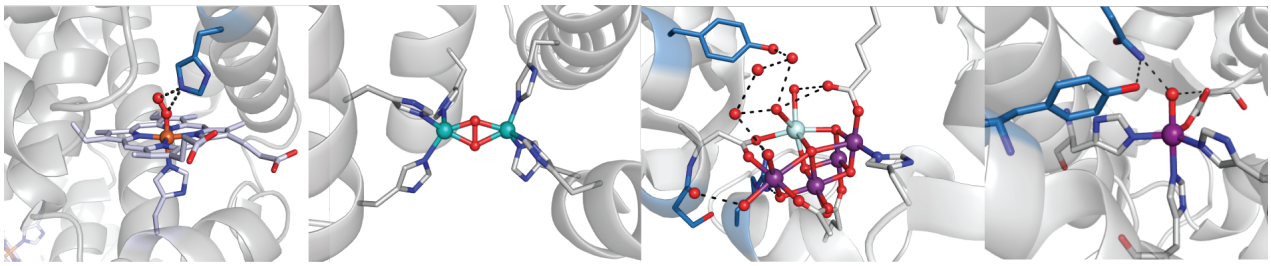

PDB: 1HHO PDB: 3IXV PDB: 3BZ1 PDB: IGV3

Figure 1-1 Examples of the active sites of some metalloproteins and metalloenzymes. Orange = Fe; teal = Cu, violet = Mn; aquamarine = Ca. Hydrogen-bonding networks are indicated by dashed lines, and participating amino acid residues are highlighted in blue. Portions of protein have been omitted for clarity.

Close examination of the active sites of metalloproteins reveals two main coordination spheres that govern reactivity and selectivity at the metal center.[10,11] The primary coordination sphere includes those ligands that are covalently bonded to the metal ion, such as amino acid residues with donor atoms, water molecules, and other substrates. The primary sphere governs the coordination geometry and electronic properties of the complex. In contrast, the secondary coordination sphere consists of the myriad of noncovalent interactions that surround the metal cofactor, providing steric interactions, hydrophilic and hydrophobic effects, and hydrogen bonds (H-bonding). These interactions are individually much weaker than the primary sphere effects, but nonetheless are vital for orienting substrates in active sites, shuttling protons and electrons, and stabilizing reactive species.

The interplay between the two coordination sphere is illustrated by SyrB2, which is a non-heme iron metalloenzyme that catalyzes the chlorination of threonine, an important transformation in the biosynthesis of the antifungal peptide syringomycin E.[12-18] The active site of SyrB2 consists of a ferric center bound by two histidine

residues, *α*-ketoglutarate (*α*KG), a chloride ion, and a water molecule, all of which define the primary sphere and establish a six-coordinate metal center (Figure 1-2). The orientation of the *α*KG is structured by an H-bonding network with arginine (Arg248), threonine (Thr113), and tryptophan (Trp145) residues. A network of intramolecular H-bonds also exists between the chloride ion and neighboring amino acid residues (Asn123, Thr143, Arg 254) and water molecules. The secondary sphere built by amino acid residues allows for appropriate orientation of the substrate, threonine, as it approaches the active site. With the introduction of threonine to the active site, it is proposed that the water molecule is displaced, generating a five-coordinate Fe^{II} center. Dioxygen then attacks the Fe^{II} center, and subsequent decarboxylation of *α*KG to succinate effects oxidation to an Fe^{IV}=O species. Hydrogen atom abstraction from the gamma position of the threonine by the iron-oxo results in an Fe(III)-OH species that H-bonds to the threonine hydroxyl group, orienting the substrate such that the methyl radical rebounds with the chloride ion rather than the hydroxide ligand, which is the common mechanism observed in other non-heme iron metalloproteins. After the selective chlorination of the substrate and its displacement by water, the metalloprotein returns to its Fe^{II} resting state.

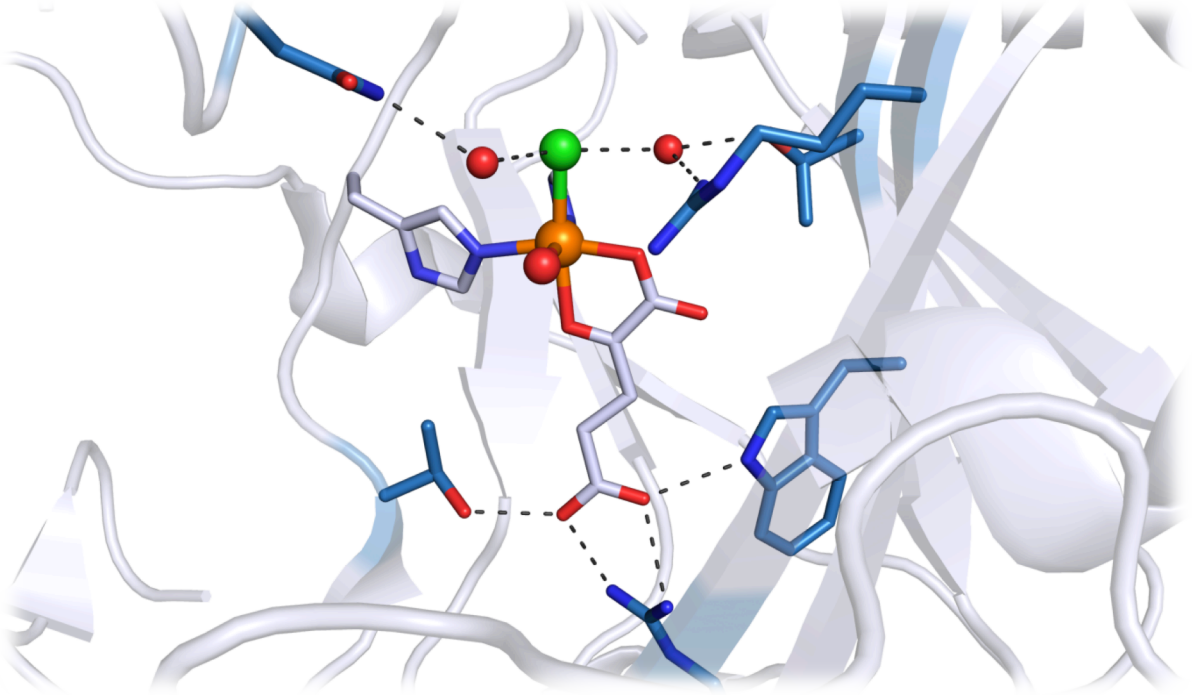

Figure 1-2 The active site of SyrB2 (PDB: 2FCT) depicting the binding environment of the non-heme Fe(II) cofactor. The ***α***KG is shown coordinated to the Fe center. Fe = orange, chlorine = green, oxygen = red, nitrogen = blue. H-bonds depicted as dashed black lines. Obscuring sidechains omitted for clarity.

The importance of the finely tuned H-bonding networks of metalloproteins is revealed upon mutation of residues within the active sites that are involved in H-bonding interactions, which often results in a dramatic reduction of activity or in some cases, a complete loss of function. For example, in the previously mentioned protein hemoglobin, substitution of the distal histidine (Figure 1-1a) for a different residue drastically decreases the ability of the protein to transport O_2.[19-22] Similarly, substituting the H-bond donating glutamine for an H-bond accepting glutamate in the active site of MnSOD (Figure 1-1d) inhibits the function of the enzyme.[8]

The ability of metalloproteins and enzymes to perform chemical transformations under ambient conditions with high selectivity and rapid reaction rates has been the

envy of synthetic chemists. Many attempts have been made to develop systems that are capable of including secondary sphere interactions, especially H-bonds, in order to mimic Nature's success. However, the inherently low strength of H-bonds (1-10 kcal/mol)[23-26] makes it difficult to prepare synthetic complexes that can reproducibly position intramolecular H-bonding donors or acceptors around the metal ion. An early example of such a system that incorporated such secondary sphere interactions is the "picket fence porphyrin", originally prepared by Collman (Figure 1-3a). [27-30] Metal porphyrins units are frequently found in metalloproteins including Mb and Hb, which contain isolated Fe^{II}-porphyrin cofactors that reversibly bind O_2. In the absence of the protein scaffold, treatment of a heme with O_2 results in the irreversible formation of dimeric structures with bridging oxo units.[31] Collman's system prevents this dimerization by including bulky pivalamido groups at the meso positions of the porphyrin, which effectively blocks approach of another porphyrin unit. Furthermore, Reed demonstrated that substitution of a pivalamide group for a urea-modified arm permits for intramolecular H-bonding between the urea N-H and an O_2 ligand (Figure 1-3b).[32]

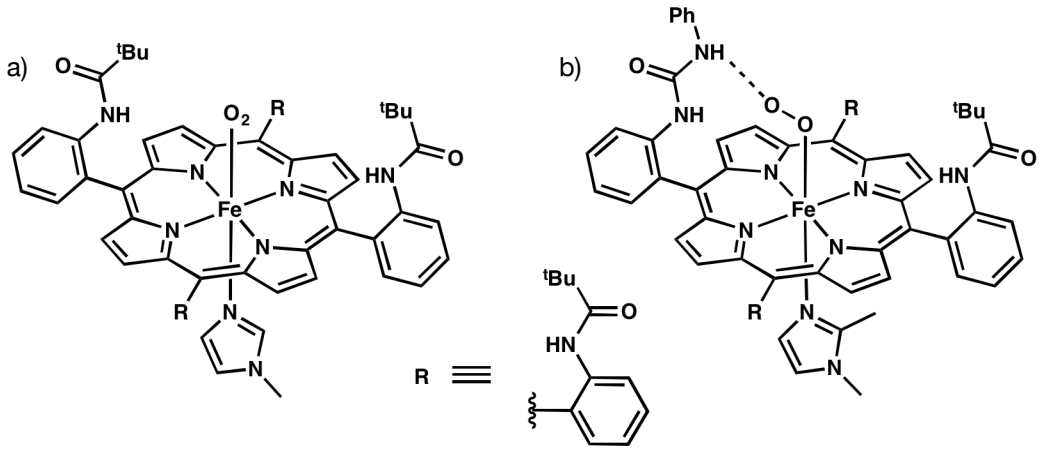

Figure 1-3 (a) Diagram of Collman's "picket fence porphyrin" depicting an Fe-O_2 adduct. (b) Reed's modified picket fence porphyrin incorporates a urea in place of pivalamide, allowing for formation of an intramolecular H-bond to the O_2 ligand1.

The Borovik lab has endeavored to incorporate the concepts of metal ion isolation and intramolecular H-bonding to design bio-inspired metal complexes. This is accomplished by utilizing a rigid organic framework that can chelate a transition metal ion and also simultaneously poise H-bond donor or acceptor groups around a vacant coordination site.[33] One such example is the urea-based ligand $[H_3buea]^{3-}$ and its corresponding complexes [M-H_3buea] (Figure 1-4), which have been utilized to synthesize and characterize high valent transition metal species such as $Mn^{V}=O$[34] and $Fe^{IV}=O$[35] complexes. These systems are analogous to proposed biologically relevant intermediates in the OEC and in SyrB2, respectively, among other metalloenzymes. Figure 1-4 provides several other examples of metal complexes with H-bond donors or acceptors that have been developed in the Borovik lab to study the effects of H-bonding networks.[36-39]

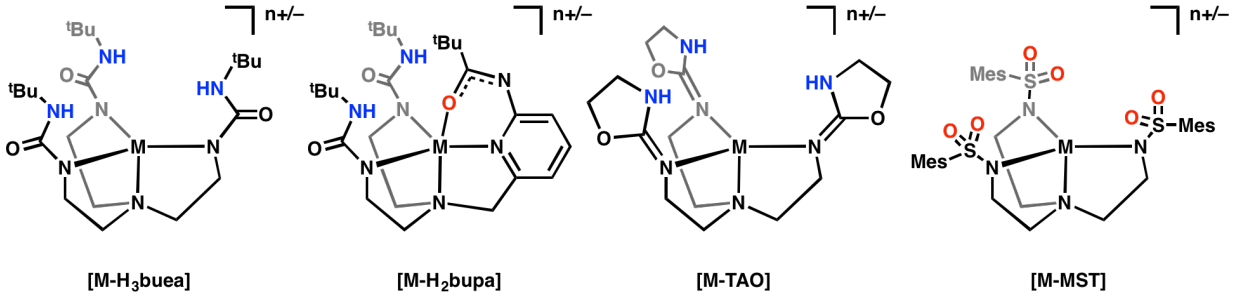

Figure 1-4 Some of the transition metal complexes of ligands bearing intramolecular H-bond donors or acceptors in the secondary sphere developed by the Borovik group.

The difficulty of precisely positioning functional groups to govern secondary sphere interactions makes preparing larger (e.g. higher molecular weight) and more complex systems a significant challenge. One method the Borovik lab has investigated previously to address this area is the use of methods to prepare molecularly imprinted polymers as scaffolds for metal complexes.[40-42] Using this methodology, a metal complex bearing polymerizable groups was incorporated into a porous polymer matrix. A removable "blocking group" is included as a ligand to ensure a binding pocket will be formed within the polymer. Removal of the initial metal ion eliminates the blocking group and generates a void space; subsequently incorporation of a different metal ion produced a new immobilized metal complex with enough space to bind external ligands (e.g, substrates). Moreover, the local environment around the metal complex can be tuned by using different linkers, ligands, and solvents. One such system features a salen imprinted polymer bearing cobalt ions that are capable of reversibly binding O_2 (Scheme 1-1). Because the Co(salen) complexes are immobilized and isolated within the polymer matrix, undesirable dimerization or formation of oxygen bridged species—which often hinders reversible O_2 binding in molecular systems—is

avoided.

Scheme 1-1 Representation of the formation of imprinted polymers. The squiggly lines denote the polymer matrix.

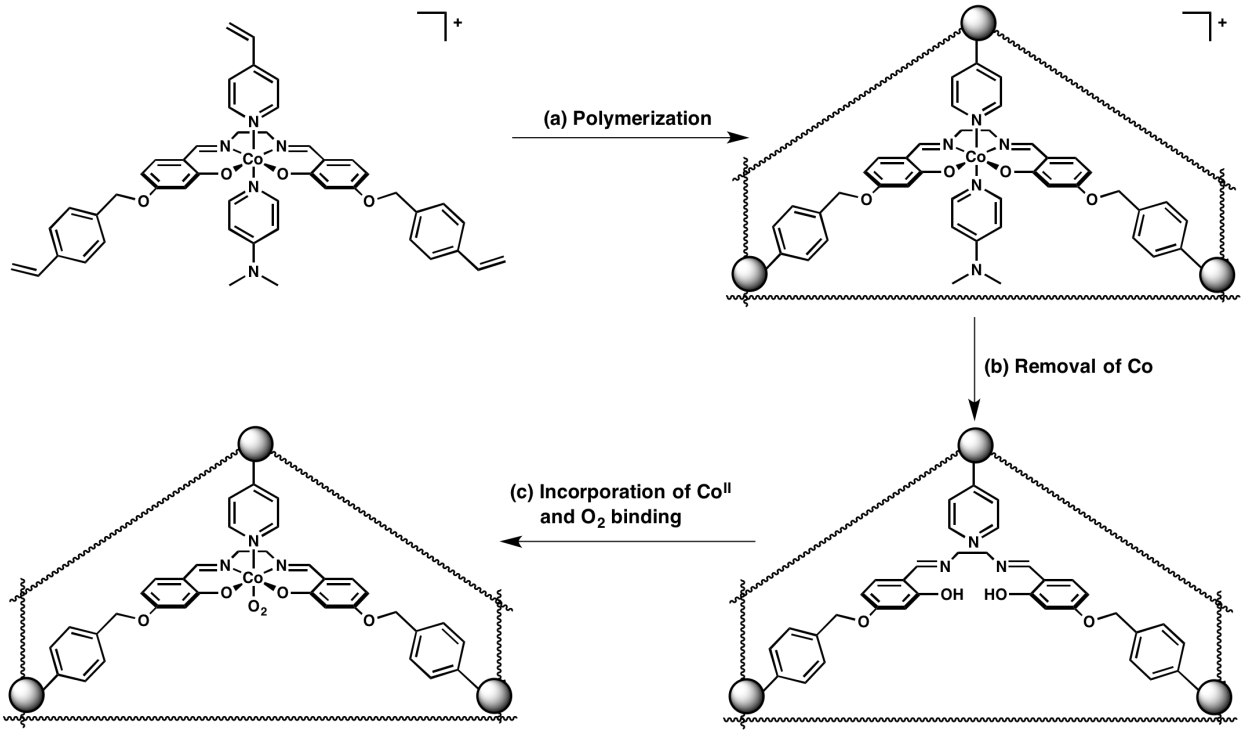

Recently, the Borovik lab has focused efforts toward a new direction of controlling secondary sphere interactions: artificial metalloproteins (AMPs). We view the protein scaffold as an alternative form of a molecular ligand or polymeric organic framework that can support transition metal ions. Embedding a non-native metal ion into a protein matrix can produce a complex possessing new reactivity that is tuned by the local environment provided by the protein. The work of other research groups has paved our entry into this field, as there are many different methods for preparing AMPs.[43-54] Relevant examples include *de novo* design, rational design of scaffold proteins, and non-covalent anchoring.

The first, *de novo* design, is a method that allows for the generation of a new

polypeptide not found in Nature. Computational modeling allows for the prediction of a peptide sequence that will form a given folded structure, which can then be synthesized using a variety of techniques. Structural cues are drawn from known metalloproteins, such as α-helix bundles bearing histidine triads, that are capable of binding ions. Among those who employ this method are the groups of Degrado[55-58] and Pecoraro.[59-62] Pecoraro has shown that a *de novo* designed α-helix bundle containing a His_3Cu site can reduce NO_2 to NO in the presence of a sacrificial reductant.[63] This model system serves as a mimic to nitric oxide reductase, highlighting the strides that synthetic chemists have made in developing functional enzymes from scratch (Figure 1-5a).

Although *de novo* design is a powerful tool for creating new AMPs, the method is currently limited in the number of accessible protein folding styles. Most *de novo* constructed systems employ bundles of α-helices, whereas natural metalloproteins utilize α-helices, β sheets and barrels, or various combinations of these and other folding patterns. To capitalize on the surfeit of naturally available protein matrices, existing metalloproteins can be modified through rational design of active sites, once again with the aid of computer modeling. An elegant example comes from the work of Lu and coworkers.[64,65] Their study utilizes the metalloenzyme nitric oxide reductase (NOR), a diiron protein containing one heme site and one non-heme site in close proximity. In an effort to study the structure and properties of the metalloenzyme, which is difficult to obtain in large quantities, crystallize, or alter through mutagenesis, Lu and coworkers reconstructed the active site using myoglobin (Mb) as a scaffold protein (Figure 15b). Lu identified amino acid residues in proximity to the heme that

were then altered through site-directed mutagenesis to introduce an artificial non-heme iron site. By selectively tuning the metal environment, they were able to construct a structural and functional mimic of NOR and demonstrate the importance of certain amino acid residues in the active site.

The third method involves anchoring an artificial metal cofactor into a host protein through non-covalent interactions. A prime example of this methodology is the use of biotin and the protein streptavidin. Biotin is a naturally occurring molecule that is bound with unusually high affinity (K_a = ~10^{15} M^{-1}) by the homotetrameric protein streptavidin (Sav). The pioneering work of Wilson and Whitesides[66] demonstrated that covalently attaching biotin to a metal complex would allow for the incorporation of a catalyst into the protein host. The inherently chiral environment provided by the protein structure surrounding the biotin-binding pocket, referred to as the vestibule, was shown to transfer chiral information in asymmetric hydrogenation reactions, albeit at modest enantiomeric excess. The Ward lab has since modified this methodology to generate a variety of homogenous catalysts based on the biotin-Sav interaction, this time using a chemogenetic approach. The ligand and linker used to bind a metal ion can be modified through standard chemical syntheses to modulate the primary coordination sphere of a given complex, whereas the binding vestibule can be modified via site-directed mutagenesis to provide a library of mutants of Sav for tuning of secondary sphere interactions of the AMPs (Figure 1-5c). The Ward lab has successfully demonstrated the use of Sav systems to catalyze asymmetric transfer hydrogenations of cyclic imines[67-72], allylic alkylations[73], and dihydroxylations[74], among other transformations. [75-82]

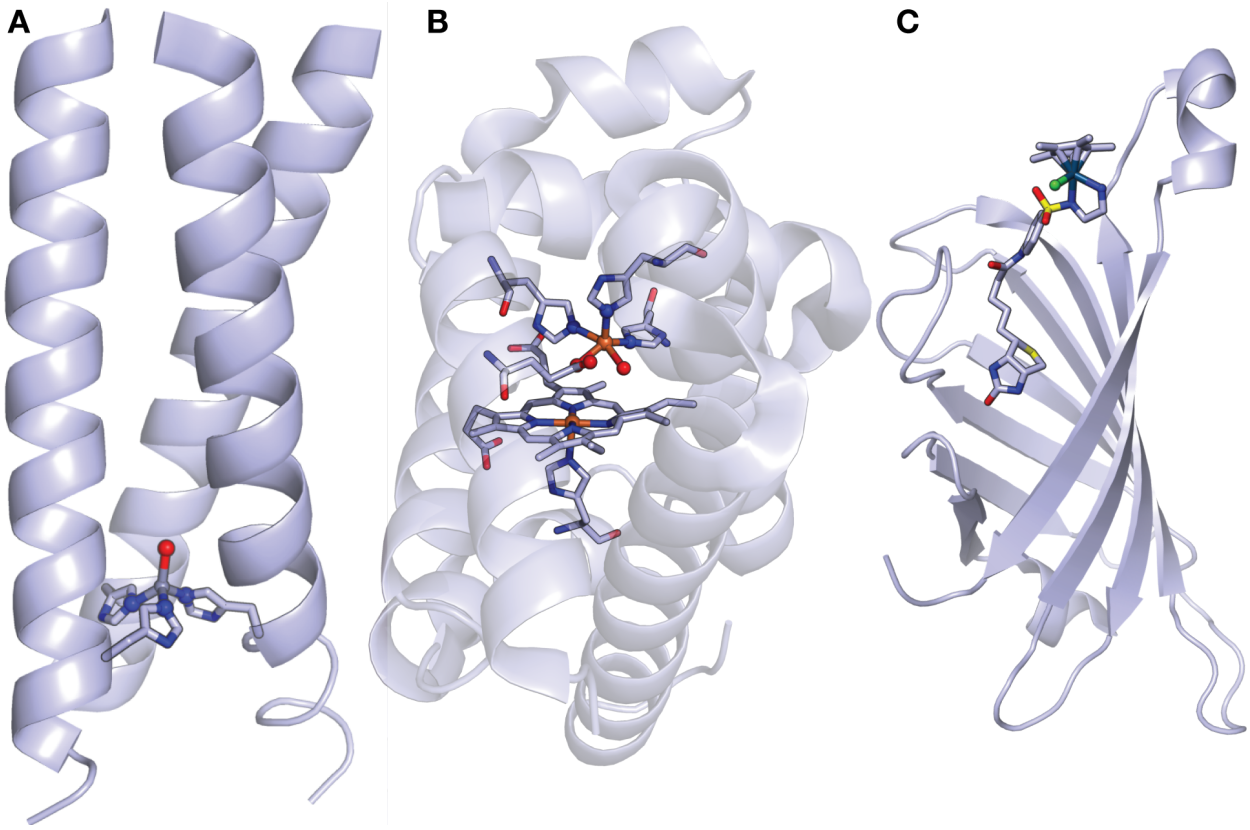

Figure 1-5 Examples of Artificial metalloproteins. (a) A de novo designed three-helix bundle (PDB: 3PBJ). (b) Myoglobin with an additional metal-binding site engineered via rational design (PDB: 2C9V). (c) A transfer hydrgogenation catalyst anchored in a protein using biotin-streptavidin technology (PDB: 3PK2).

We have selected the biotin-streptavidin system as the scaffold to generate AMPs and study secondary sphere effects on transition metal complexes. The chemical versatility of attaching biotin to different ligand frameworks (biotinylation) combined with the ability to probe a library of protein mutants in collaboration with the Ward lab were two of the main advantages of this approach. Additionally, streptavidin is remarkably robust for a protein and is compatible with a wide range of temperatures, pH's, and organic solvents. The remaining chapters of this dissertation will describe my efforts towards the use of biotin-Sav as a scaffold for metal complexes, utilizing the protein matrix as an organic framework to supply hydrogen bonds and other noncovalent interactions to the immobilized complex. The final chapter entails work I

initially performed on investigating the use of traditional Borovik ligands to mediate intramolecular C–H bond amination reactions.

Description of Chapter 2 The use of biotin-Streptavidin technology as a framework with which to prepare TM complexes represents a new direction of research within the Borovik lab. This chapter describes a chemogenetic approach to preparing Cu(II) complexes confined within Sav. Biotinylated ligands with linkers of ethyl, propyl, or butyl chains between biotin and the metal-binding moiety were synthesized, and their binding to Sav was studied with optical and EPR spectroscopy. Additionally, X-ray diffraction studies were performed on the artificial metalloproteins to attain molecular structures. Mutants of Sav prepared by my collaborators via site-directed mutagenesis were used to further investigate the role of the surrounding amino acids in controlling the microenvironments around the protein-confined Cu(II) complexes. It was also observed that by replacing a neighboring serine with an aspartate, a second point of anchoring to the Cu(II) center could be observed by coordination of the carboxylate to the Cu(II) center. Spectroscopic evidence was also observed for thiolate coordination to the Cu(II) center when the same serine was replaced with a cysteine residue. The research in this chapter established biot-Sav technology as method within the Borovik lab for preparing artificial metalloproteins to study secondary coordination spheres and reactivity of TM complexes.

Description of Chapter 3 The alignment of two biotin-binding sites of two Sav subunits across the dimer interface appears ideal for positioning a TM complex with

multiple points of anchoring within Sav. I proposed a bis-biotinylated salen framework that could potentially bridge across two biotin-binding sites and anchor a TM complex firmly within the Sav active site. Such rigid placement of a TM complex would allow for greater selectivity in organic transformations. The bis-biotinylated Schiff base was prepared along with its Cu(II) complexes, and their binding to Sav was studied with HABA titrations and gel electrophoresis. Through this investigation, I determined that the bis-biotinylated species did not link two subunits in a single Sav molecule, but rather cross-linked protein molecules to make dimers and other oligomers.

Description of Chapter 4 Previous research within the Borovik lab established the tripodal, tetradentate urea- and amidate hybrid-based ligands as capable of forming Fe(II) complexes that react with *p*-tolyl azide to form an Fe(III)-amido via a putative Fe(IV)-imido intermediate. As this is a species that is proposed to exist along the pathway of forming C–N bonds through C–H bond amination, I proposed using these Fe(II) complexes to investigate a C–H amination reaction. I used an aryl azide substrate that included C—H bond that would react to via intramolecular C–H bond activation to form indole or indoline products. My investigation into this area showed these Fe(II) complexes to not be effective in mediating this transformation, likely due to steric encumbrance.

References

1 R. H. Holm and E. I. Solomon, *Chem. Rev.*, 2004, **104**, 347–348.
2 K. A. Magnus, H. Ton-That and J. E. Carpenter, *Chem. Rev.*, 1994, **94**, 727–735.
3 M. E. Cuff, K. I. Miller, K. E. van Holde and W. A. Hendrickson, *J. Mol. Biol.*, 1998,

278, 855–870.
4 Y. Umena, K. Kawakami, J.-R. Shen and N. Kamiya, *Nature*, 2011, **473**, 55–60.
5 Y. Hu and M. W. Ribbe, *J. Biol. Inorg. Chem.*, 2014, **19**, 731–736.
6 T. Spatzal, M. Aksoyoglu, L. Zhang, S. L. A. Andrade, E. Schleicher, S. Weber, D. C. Rees and O. Einsle, *Science*, 2011, **334**, 940–940.
7 K. M. Lancaster, M. Roemelt, P. Ettenhuber, Y. Hu, M. W. Ribbe, F. Neese, U. Bergmann and S. DeBeer, *Science*, 2011, **334**, 974–977.
8 A.-F. Miller, *Curr. Op. Chem. Bio.*, 2004, **8**, 162–168.
9 W. Atzenhofer, G. Regelsberger, U. Jacob, G. A. Peschek, P. G. Furtmüller, R. Huber and C. Obinger, *J. Mol. Biol.*, 2002, **321**, 479–489.
10 A. Werner, *Ber. Dtsch. Chem. Ges.,* 1912, **45**, 121–130.
11 H. M. Colquhoun, J. F. Stoddart and D. J. Williams, *Angew. Chem. Int. Ed.*, 1986, **25**, 487–507.
12 S. D. Wong, M. Srnec, M. L. Matthews, L. V. Liu, Y. Kwak, K. Park, C. B. Bell, E. E. Alp, J. Zhao, Y. Yoda, S. Kitao, M. Seto, C. Krebs, J. M. Bollinger and E. I. Solomon, *Nature*, 2013, **499**, 320–323.
13 T. Borowski, H. Noack, M. Radoń, K. Zych and P. E. M. Siegbahn, *J. Am. Chem. Soc.*, 2010, **132**, 12887–12898.
14 M. L. Matthews, C. S. Neumann, L. A. Miles, T. L. Grove, S. J. Booker, C. Krebs, C. T. Walsh and J. M. Bollinger, *Proc. Natl. Acad. Sci. U.S.A.*, 2009, **106**, 17723–17728.
15 H. J. Kulik, L. C. Blasiak, N. Marzari and C. L. Drennan, *J. Am. Chem. Soc.*, 2009, **131**, 14426–14433.
16 A. Butler and M. Sandy, *Nature*, 2009, **460**, 848–854.
17 S. Pandian, M. A. Vincent, I. H. Hillier and N. A. Burton, *Dalton Trans.*, 2009, 6201–6207.
18 L. C. Blasiak, F. H. Vaillancourt, C. T. Walsh and C. L. Drennan, *Nature*, 2006, **440**, 368–371.
19 P. J. Condon and J. W E Royer, *Journal of Biological Chemistry*, 1994, **269**, 25259–25267.
20 S. Huang, J. Huang, A. P. Kloek, D. E. Goldberg and J. M. Friedman, *Journal of Biological Chemistry*, 1996, **271**, 958–962.
21 J. Yang, A. P. Kloek, D. E. Goldberg and F. S. Mathews, *Proc. Natl. Acad. Sci. U.S.A.*, 1995, **92**, 4224–4228.
22 B. Shaanan, *Nature*, 1982, **296**, 683–684.
23 M. Meot-Ner Mautner, *Chem. Rev.*, 2005, **105**, 213–284.
24 C. L. Perrin and J. B. Nielson, *Annu Rev Phys Chem*, 1997, **48**, 511–544.
25 J. Emsley, *Chem. Soc. Rev.*, 1980, **9**, 91–124.
26 G. C. Pimentel and A. L. McClellan, *Annu. Rev. Phys. Chem.*, 1971, **22**, 347–385.
27 J. P. Collman, J. I. Brauman, E. Rose and K. S. Suslick, *Proc. Natl. Acad. Sci. U.S.A.*, 1978, **75**, 1052–1055.
28 J. P. Collman, J. I. Brauman and K. M. Doxsee, *J. Am. Chem. Soc.*, 1980, **102**, 4182–4192.
29 J. P. Collman and L. Fu, *Acc. Chem. Res.*, 1999, **32**, 455–463.

30 J. P. Collman, *Acc. Chem. Res.*, 1977, **10**, 265–272.
31 D. M. Kurtz Jr, *Chem. Rev.*, 1990, **90**, 585–606.
32 G. E. Wuenschell, C. Tetreau and D. Lavalette, *J. Am. Chem. Soc.*, 1992, **114**, 3346–3355.
33 A. S. Borovik, *Acc. Chem. Res.*, 2005, **38**, 54–61.
34 T. Taguchi, R. Gupta, B. Lassalle-Kaiser, D. W. Boyce, V. K. Yachandra, W. B. Tolman, J. Yano, M. P. Hendrich and A. S. Borovik, *J. Am. Chem. Soc.*, 2012, **134**, 1996–1999.
35 D. C. Lacy, R. Gupta, K. L. Stone, J. Greaves, J. W. Ziller, M. P. Hendrich and A. S. Borovik, *J. Am. Chem. Soc.*, 2010, **132**, 12188–12190.
36 R. L. Shook, S. M. Peterson, J. Greaves, C. Moore, A. L. Rheingold and A. S. Borovik, *J. Am. Chem. Soc.*, 2011, **133**, 5810–5817.
37 Y. J. Park, N. S. Sickerman, J. W. Ziller and A. S. Borovik, *Chem. Commun.*, 2010, **46**, 2584–2586.
38 Y. J. Park, S. A. Cook, N. S. Sickerman, Y. Sano, J. W. Ziller and A. S. Borovik, *Chem. Sci.*, 2013, **4**, 717–726.
39 Y. J. Park, J. W. Ziller and A. S. Borovik, *J. Am. Chem. Soc.*, 2011, **133**, 9258–9261.
40 L. L. Welbes and A. S. Borovik, *Acc. Chem. Res.*, 2005, **38**, 765–774.
41 A. C. Sharma and A. S. Borovik, *J. Am. Chem. Soc.*, 2000, **122**, 8946–8955.
42 J. F. Krebs and A. S. Borovik, *J. Am. Chem. Soc.*, 1995, **117**, 10593–10594.
43 J. C. Lewis, *ACS Catal.*, 2013, 2954–2975.
44 M. T. Reetz, *Chem. Record*, 2012, **12**, 391–406.
45 M. T. Reetz and N. Jiao, *Angew. Chem. Int. Ed. Engl.*, 2006, **45**, 2416–2419.
46 M. T. Reetz, J. J.-P. Peyralans, A. Maichele, Y. Fu and M. Maywald, *Chem. Commun. (Camb.)*, 2006, 4318–4320.
47 C. Cavazza, C. Bochot, P. Rousselot-Pailley, P. Carpentier, M. V. Cherrier, L. Martin, C. Marchi-Delapierre, J. C. Fontecilla-Camps and S. Ménage, *Nature Chem*, 2010, **2**, 1069–1076.
48 J. Oelerich and G. Roelfes, *Chem. Sci.*, 2013, **4**, 2013–2017.
49 J. Bos, A. García-Herraiz and G. Roelfes, *Chem. Sci.*, 2013, **4**, 3578–3582.
50 J. Bos, F. Fusetti, A. J. M. Driessen and G. Roelfes, *Angew. Chem.,* 2012, **124**, 7590–7593.
51 J. Bos, F. Fusetti, A. J. M. Driessen and G. Roelfes, *Angew. Chem. Int. Ed.*, 2012, **51**, 7472–7475.
52 V. Köhler and N. J. Turner, *Chem. Commun.*, 2015, **51**, 450–464.
53 A. Pordea and T. Ward, *Synlett*, 2009, **2009**, 3225–3236.
54 R. J. Radford, J. D. Brodin, E. N. Salgado and F. A. Tezcan, *Coord. Chem. Rev.*, 2011, **255**, 790–803.
55 J. Kaplan and W. F. DeGrado, *Proc. Natl. Acad. Sci. U.S.A.*, 2004, **101**, 11566–11570.
56 R. B. Hill, D. P. Raleigh, A. Lombardi and W. F. DeGrado, *Acc. Chem. Res.*, 2000, **33**, 745–754.
57 H. C. Fry, A. Lehmann, J. G. Saven, W. F. DeGrado and M. J. Therien, *J. Am.*

Chem. Soc., 2010, **132**, 3997–4005.
58 C. B. Bell, J. R. Calhoun, E. Bobyr, P.-P. Wei, B. Hedman, K. O. Hodgson, W. F. DeGrado and E. I. Solomon, *Biochemistry*, 2009, **48**, 59–73.
59 M. L. Zastrow and V. L. Pecoraro, *Coord. Chem. Rev.*, 2013, **257**, 2565–2588.
60 M. L. Zastrow and V. L. Pecoraro, *J. Am. Chem. Soc.*, 2013, **135**, 5895–5903.
61 M. L. Zastrow, A. F. A. Peacock, J. A. Stuckey and V. L. Pecoraro, *Nature Chem*, 2012, **4**, 118–123.
62 F. Yu, V. M. Cangelosi, M. L. Zastrow, M. Tegoni, J. S. Plegaria, A. G. Tebo, C. S. Mocny, L. Ruckthong, H. Qayyum and V. L. Pecoraro, *Chem. Rev.*, 2014, **114**, 3495–3578.
63 M. Tegoni, F. Yu, M. Bersellini, J. E. Penner-Hahn and V. L. Pecoraro, *Proc. Natl. Acad. Sci. U.S.A.*, 2012, **109**, 21234–21239.
64 Y. Lu, S. M. Berry and T. D. Pfister, *Chem. Rev.*, 2001, **101**, 3047–3080.
65 N. Yeung, Y.-W. Lin, Y.-G. Gao, X. Zhao, B. S. Russell, L. Lei, K. D. Miner, H. Robinson and Y. Lu, *Nature*, 2009, **462**, 1079–1082.
66 M. E. Wilson and G. M. Whitesides, *J. Am. Chem. Soc.,* 1978, **100**, 306–307.
67 J. R. Carey, S. K. Ma, T. D. Pfister, D. K. Garner, H. K. Kim, J. A. Abramite, Z. Wang, Z. Guo and Y. Lu, *J. Am. Chem. Soc.*, 2004, **126**, 10812–10813.
68 V. M. Robles, M. Dürrenberger, T. Heinisch, A. Lledós, T. Schirmer, T. R. Ward and J.-D. Maréchal, *J. Am. Chem. Soc.*, 2014, **136**, 15676–15683.
69 J. M. Zimbron, T. Heinisch, M. Schmid, D. Hamels, E. S. Nogueira, T. Schirmer and T. R. Ward, *J. Am. Chem. Soc.*, 2013, **135**, 5384–5388.
70 M. Dürrenberger, T. Heinisch, Y. M. Wilson, T. Rossel, E. Nogueira, L. Knörr, A. Mutschler, K. Kersten, M. J. Zimbron, J. Pierron, T. Schirmer and T. R. Ward, *Angew. Chem. Int. Ed.*, 2011, **50**, 3026–3029.
71 M. Creus, A. Pordea, T. Rossel, A. Sardo, C. Letondor, A. Ivanova, I. LeTrong, R. E. Stenkamp and T. R. Ward, *Angew. Chem. Int. Ed.*, 2008, **47**, 1400–1404.
72 C. Letondor, A. Pordea, N. Humbert, A. Ivanova, S. Mazurek, M. Novič and T. R. Ward, *J. Am. Chem. Soc.*, 2006, **128**, 8320–8328.
73 J. Pierron, C. Malan, M. Creus, J. Gradinaru, I. Hafner, A. Ivanova, A. Sardo and T. R. Ward, *Angew. Chem.*, 2008, **120**, 713–717.
74 V. Köhler, J. Mao, T. Heinisch, A. Pordea, A. Sardo, Y. M. Wilson, L. Knörr, M. Creus, J.-C. Prost, T. Schirmer and T. R. Ward, *Angew. Chem. Int. Ed.*, 2011, **50**, 10863–10866.
75 A. Pordea, M. Creus, J. Panek, C. Duboc, D. Mathis, M. Novic and T. R. Ward, *J. Am. Chem. Soc.*, 2008, **130**, 8085–8088.
76 M. Skander, N. Humbert, J. Collot, J. Gradinaru, G. Klein, A. Loosli, J. Sauser, A. Zocchi, F. Gilardoni and T. R. Ward, *J. Am. Chem. Soc.*, 2004, **126**, 14411–14418.
77 C. M. Thomas, C. Letondor, N. Humbert and T. R. Ward, *J. Organomet. Chem.,* 2005, **690**, 4488–4491.
78 M. Skander, C. Malan, A. Ivanova and T. R. Ward, *Chem. Commun.*, 2005, 4815–4817.
79 A. Pordea, D. Mathis and T. R. Ward, *J. Organomet. Chem.*, 2009, **694**, 930–936.
80 C. Mayer, D. G. Gillingham, T. R. Ward and D. Hilvert, *Chem. Commun.*, 2011, **47**,

12068–12070.
81 C. Lo, M. R. Ringenberg, D. Gnandt, Y. Wilson and T. R. Ward, *Chem. Commun.*, 2011, **47**, 12065.
82 T. K. Hyster, L. Knorr, T. R. Ward and T. Rovis, *Science*, 2012, **338**, 500–503.

CHAPTER 2

Streptavidin as a Host for Copper Complexes

I. Introduction

Reproducible control over noncovalent interactions surrounding transition metal (TM) ions and the study of these secondary sphere effects has been of ongoing interest to the Borovik lab.[1,2] The interest in these phenomena stems from the structure and function of natural metalloproteins which feature numerous noncovalent interactions, especially hydrogen bonds (H-bonds), through amino acid residues and structural water molecules surrounding TM ions in the active site.[3] The Borovik research program has incorporated these types of interactions in synthetic systems using porous polymer hosts[4-6] and rigid organic ligand scaffolds[7-11] that support TM ions (see Chapter 1 for greater detail). Both of these systems position intramolecular H-bond donors or acceptors such that they can interact with exogenous ligands bound to the metal center. Although these methodologies have yielded success in areas such as stabilization of biologically relevant high-valent Fe- and Mn-O(H) compounds and heterobimetallic systems,[7,12-14] there are certain limitations to the synthetic frameworks:

- The organic ligand frameworks are unable to reliably reproduce extended networks of H-bonding interactions (e.g. structural water molecules)
- Scaffolds capable of supporting bimetallic species are difficult to prepare[15] and often require bridging moieties not generally observed in natural systems.
- The ligand systems are sensitive to water.

This chapter presents a new research program in the Borovik lab, which uses artificial metalloproteins (AMPs) to address the limitations of synthetic systems discussed above. AMPs allow for further control over structure and function of TM complexes utilizing extended networks of H-bonds and allowing access to aqueous media. AMPs have been generated previously by other groups through such methods as adding metallo-porphyrins and related compounds to apo-myoglobin[16-18] or adding Fe complexes to NikA[19]. Although these methods are effective, they are limited to either certain types of TM complexes or have difficulty reproducibly binding TM ions in a site-specific fashion.

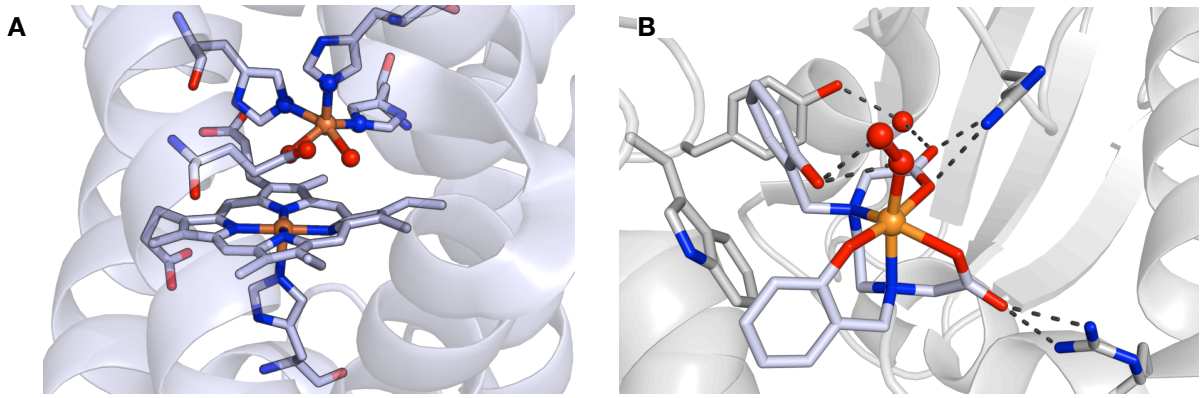

Figure 2-1 Two examples of artificial metalloproteins. **(A)** A myoglobin-based artificial nitric oxide reductase designed by the Lu group using *in silico* methodologies to predict amino acid mutations necessary to generate a secondary metal binding site within proximity to a heme. (PDB 3K9Z).[20] **(B)** The molecular structure of an intermediate along the intamolecular arene oxidation pathway of a prosthetic iron complex anchored in NikA. Ménage and coworkers were able to crystallographically characterize four of the intermediates of the catalytic cycle along with the final product, which implicated the role of Fe^{III}–OOH intermediate, pictured above (PDB 3MVZ).[19]

Another method is the exploitation of the biotin-streptavidin (Sav) interaction. Streptavidin is a homotetrameric (four identical subunits) protein that is isolated from *Streptomyces avidinii* and it binds biotin with extraordinarily high affinity, $K_a \sim 10^{14}$ M^{-1}.[21] By synthetically affixing biotin to a metal complex, AMPs can be prepared by

treating Sav with the biotinylated complexes (Figure 2-2). This method has been most notably explored by the Ward group which has used this approach to prepare a number of artificial metalloenzymes capable of performing catalytic transformations, such as asymmetric transfer hydrogenations[22-24] and olefin metatheses[25] which derive stereochemical information from the chiral protein active site.

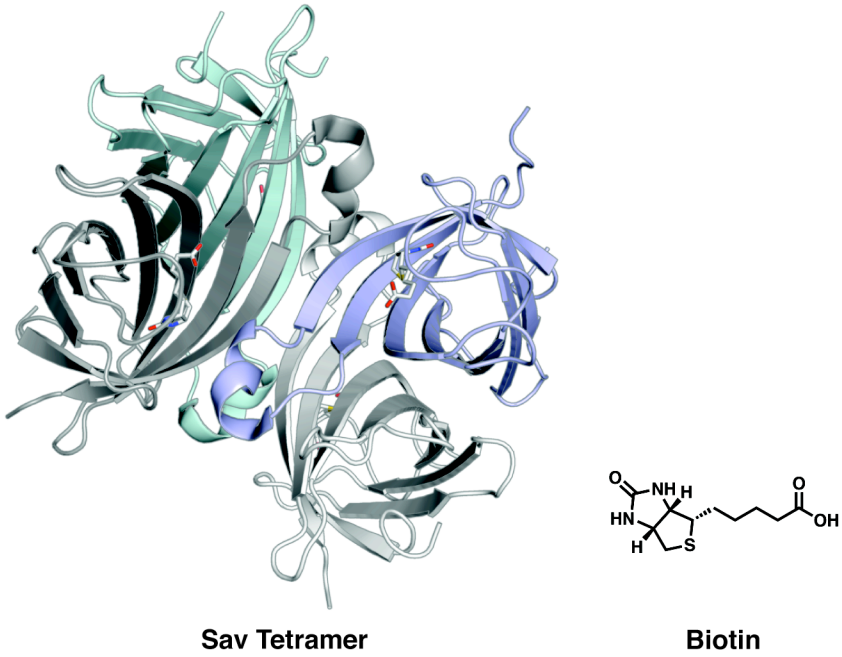

Figure 2-2 The four β-barrels of a Sav tetramer, depicted in different colors to highlight the individual subunits. Each subunit binds one biotin molecule.

For my research, the biotin-Sav interaction was utilized for the following reasons:

- Affixing biotin to an organic ligand allows for reproducible and site-specific placement of TM ions

- The molecular biology of Sav is well understood, allowing for the preparation of protein mutants through site-directed mutagenesis
- Sav is tolerant to a wide range of pHs and relatively high concentrations of nonaqueous solvents (Sav remains soluble and binds biotin in 50% ethanol).[26]
- Native (or apo) Sav crystallizes well, which allows for determination of molecular structure through X-ray diffraction methods.

Properties of Sav. The homotetrameric structure of Sav assembles into a "dimer of dimers" configuration, which brings two biotin-binding sites into alignment across from each other at one dimer interface (Figure 2-3). Once Sav binds biotin, the tethered TM complex sits within the vestibule (the bowl-like cavity formed by two subunits of the dimer), and the environment of the TM complex is controlled by protein effects within this area. By using biotinylated TM complexes with variable linker lengths, it is proposed that the M•••M distance can be tuned to provide for either discrete, monomeric metal complexes where each metal complex is isolated within a subunit, or bimetallic systems in which the metal complexes confined within the dimer are capable of either directly interacting with each other or can cooperatively perform chemistry (Figure 2-4).

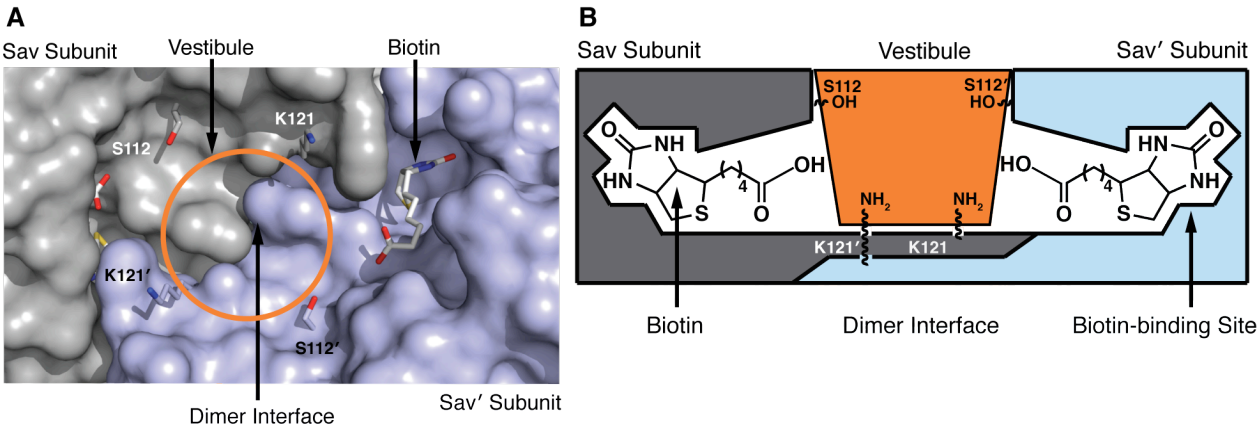

Figure 2-3 **(A)** A Pymol representation of a Sav dimer. One subunit is depicted in grey and the other in light blue for contrast. One biotin binding pocket has had obscuring amino acid residues removed to reveal the biotin within. The vestibule is the bowl-like area between the opposing biotin binding sites of the dimer. The amino acids at the 112 and 121 positions are exposed. **(B)** A schematic representation of the Sav dimer, again indicating the location of the vestibule between the biotin binding sites.

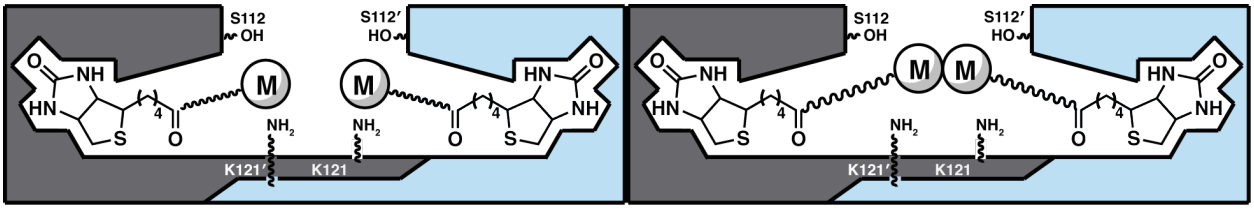

Figure 2-4 Depiction of how varying the linker length between the metal binding moiety and biotin will increase or decrease the inter-metal ion distance.

The initial focus of the study was to prepare AMPs using biotin-Sav technology to reproducibly position TM ions with controlled M•••M distances and to study their structure both spectroscopically and crystallographically. To this end a series of biotinylated tri-dentate ligands with varying linker lengths have been prepared (Figure 2-5). Dipicolylamine (dpa) was chosen as its coordination chemistry has been well established, and will also produce complexes with an open coordination site allowing for the binding of additional ligands.[27,28] Cu(II) was selected for initial studies because of its stability in aqueous media, optical spectroscopic features, and a spin state of

S = ½, which allows it to be probed by electron paramagnetic resonance (EPR) spectroscopy. Our collaborators in the Ward lab provided Sav mutants, as well as performed the X-ray diffraction studies on some of the AMPs we provided them.

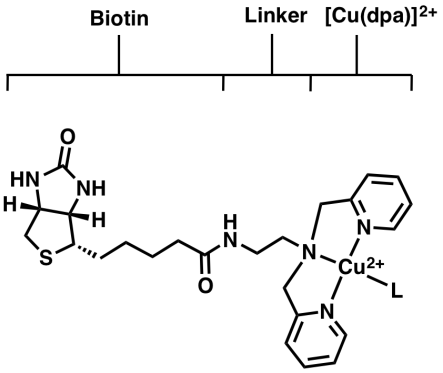

Figure 2-5 Figure depicting the proposed ligand design concept. A modular linker between biotin and the metal-binding moiety will be modified to adjust the location of the Cu(II) complexes within the vestibule. Ethyl (shown here), propyl, and butyl linkers have all been prepared.

II. Results and Discussion

Ligand Synthesis

The ligands were prepared based on the premise that a modular spacer is required between the metal-binding moiety and biotin to control the position of the TM ion within Sav. Simple alkyl chains were used as a starting point, as the synthesis would be straightforward. Starting with dipicolylamine (DPA) prepared according to literature procedure,[29] reaction with bromo-alkyl phthalimides with varying alkyl chain lengths in the presence of potassium carbonate and potassium iodide in acetonitrile (MeCN)[30] generated the corresponding N-phthalimide protected dpa derivatives in yields ranging 69—80% (Scheme 2-1). The phthalimides were then deprotected with an excess of

hydrazine monohydrate to unveil the primary amines in high yields. Finally, the primary amines were allowed to react with biotin pentafluorophenol ester (biotin-PFP) to give the biotinylated ligands Biotin-n-dpa (n = 2 (ethyl, et), 3 (propyl, pr), 4 (butyl, bu)) as tan solids (Scheme 2-1).

Scheme 2-1 Synthesis of biotinylated ligands.

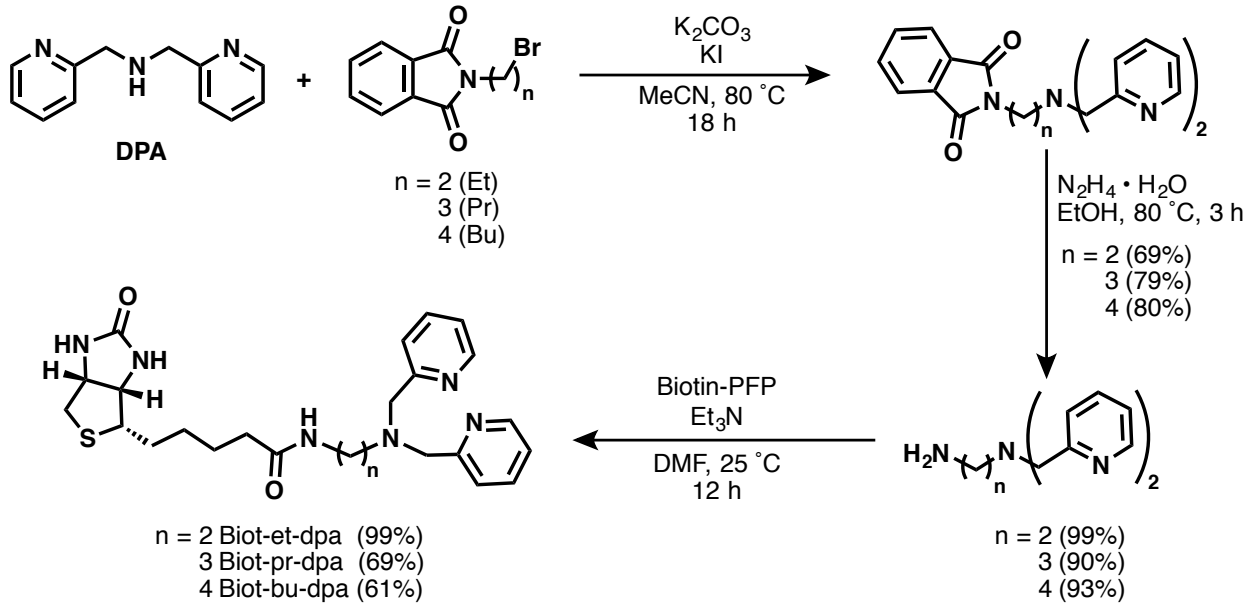

Synthesis of Cu^{II} Complexes

[Cu(Biot-ethyl-dpa)(NO_3)](NO_3), **[Cu(Biot-propyl-dpa)(NO_3)](NO_3)**, **[Cu(Biot-butyl-dpa)(NO_3)](NO_3)** and analogous ClO_4^- complexes were prepared by treating a solution of **Biot-n-dpa** in ethanol with $Cu(NO_3)_2 \cdot 3H_2O$ or $Cu(ClO_4)_2 \cdot 6H_2O$. The complexes were precipitated from the reaction mixture with diethylether and isolated as putative [Cu(Biotin-n-dpa)(NO_3)(EtOH)](NO_3) salts, according to previously reported procedures to prepare copper dpa complexes.[27] The electronic absorption spectra of these Cu^{II} complexes display weak d-d bands at λ_{max} = 654 nm (ε ~ 100 $M^{-1}cm^{-1}$), which

is consistent with $Cu(DPA)^{2+}$ complexes. Mass spectrometry of the complexes gives molecular ion peaks corresponding to $[Cu(Biot\text{-}n\text{-}dpa)\text{-}H]^{+}$, $[Cu(Biot\text{-}n\text{-}dpa)]^{2+}$, and $[Cu(biot\text{-}n\text{-}dpa)(NO_3)]^{+}$, which suggests that at least one nitrate binds to the Cu(II) center. Perpendicular mode EPR spectroscopy features a signal at $g_{\perp} = 2.04$, which is consistent with the expected mononuclear Cu(II) center with an S = ½ spin ground state (Figure 2-6). All attempts of obtaining X-ray quality crystals of the biotinylated copper complexes from either DMF/diethylether vapor diffusion or layering techniques were unsuccessful, likely due to the flexible nature of both the alkyl spacer and long alkyl chain off biotin.

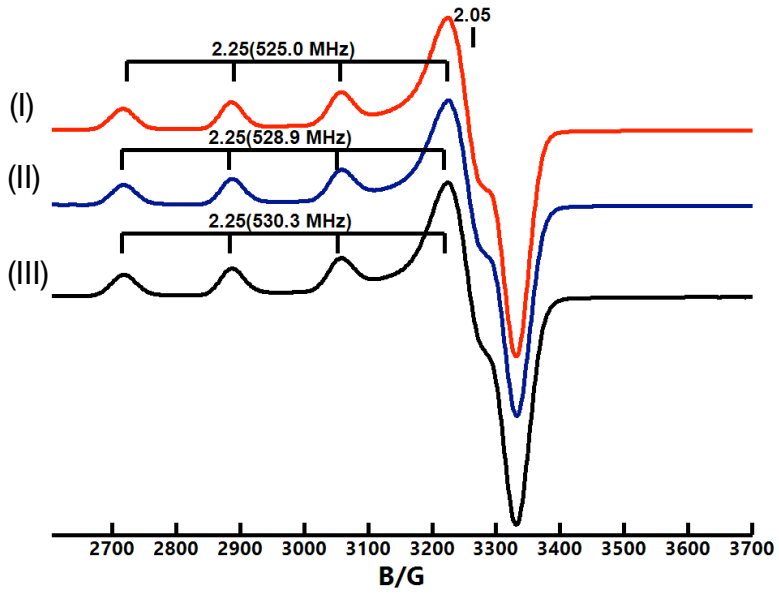

Figure 2-6 Perpendicular mode EPR spectra of (I) **$[Cu(Biot\text{-}bu\text{-}dpa)(NO_3)](NO_3)$**, (II) **$[Cu(Biot\text{-}pr\text{-}dpa)(NO_3)](NO_3)$**, and (III) **$[Cu(Biot\text{-}et\text{-}dpa)(NO_3)](NO_3)$** in DMF/THF at 77 K.

HABA Titrations

Having prepared biotinylated metal complexes, the next step was to determine how many equivalents of metal complex were necessary to saturate the biotin binding sites of the Sav tetramer. It is known that unsubstituted biotin occupies the binding sites of tetrameric Sav in a four to one manner; that is, there is one biotin per biotin-binding site within a subunit. After substituting biotin with additional moieties it must be determined if the biotinylated complexes will still be bound by the Sav host protein in a similar fashion. This was determined using the 2-(4′-hydroxyazobenzene)benzoic acid (HABA) titration method. Using this technique, a solution of Sav is saturated by HABA, which has a binding affinity for Sav of $K_a \sim 10^{3.5}\ M^{-1}$, and therefore requires a large excess of HABA to fully saturate the binding sites of Sav. The HABA⊂Sav interaction generates a diagnostic absorption in the visible spectrum at $\lambda_{max} = 506$ nm. Adding equivalents of a solution of the biotinylated complex displaces HABA from the biotin binding sites, causing a decrease in the absorption at 506 nm. Once no further change in absorbance is observed, it is assumed that the number of equivalents of complex added corresponds to the amount required to fully occupy the binding sites of the Sav tetramer. For this project, it has been shown **[Cu(Biot-et-DPA)]$^{2+}$**, **[Cu(Biot-pr-DPA)]$^{2+}$,** and **[Cu(Biot-bu-DPA)]$^{2+}$** all require approximately 3.5 equivalents to saturate a Sav tetramer, binding in the predicted fashion (Figure 2-7).

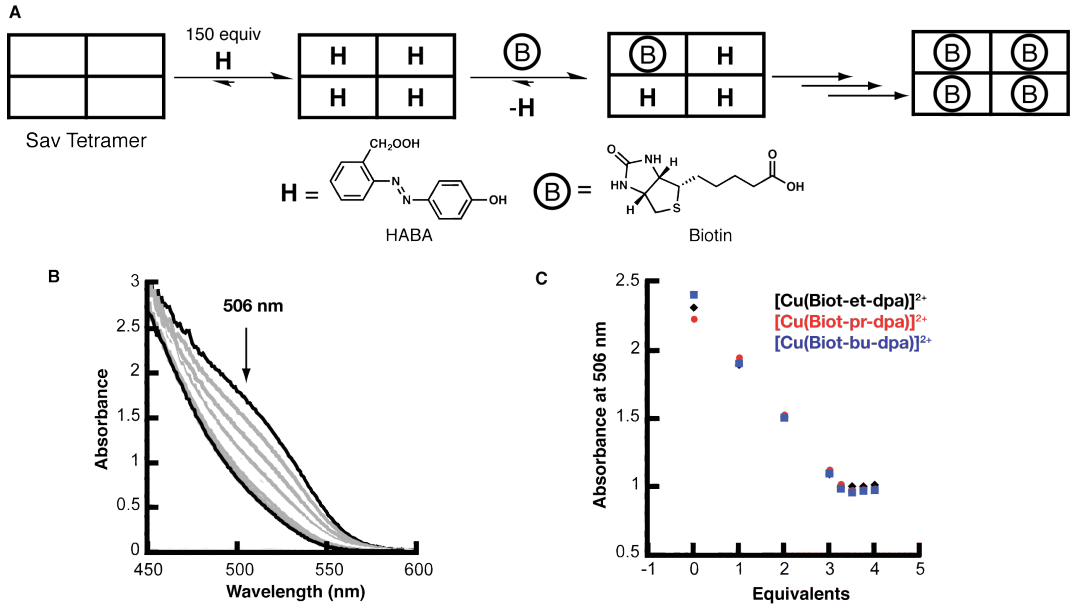

Figure 2-7 A) A schematic description of the HABA titration methodology. Apo-streptavidin is loaded with an excess of HABA to ensure occupation of all four biotin binding sites. Biotinylated species displace HABA from the binding site due to the large affinity of Sav for biotin. B) The titration is complete when the absorption at 506 nm corresponding to the HABA⊂Sav complex stops decreasing. C) A plot of the absorption of the HABA⊂Sav complex versus equivalents of $[Cu(Biot\text{-}n\text{-}DPA]^{2+}$ added. This data indicates that it requires approximately 3.5 equivalents of complex to occupy all Sav binding sites and is consistent between all three linker lengths.

Preparation of Artificial Metalloproteins

After confirming with HABA titrations that the biotinylated Cu^{2+} complexes occupy the biotin binding sights of Sav, artificial metalloproteins were prepared by treating solutions of Sav in either buffer or water with a solution of **$[Cu(Biot\text{-}n\text{-}DPA)]^{2+}$**. The electronic absorption spectra display a shift to higher energy, from λ_{max} = 654 nm for the free complexes to λ_{max} = 630 nm in the AMPs (**Figure 2-8**). Perpendicular mode EPR spectroscopy of frozen solutions of the artificial metalloproteins feature a axial spectrum centered around $g_{\perp}$ = 2.04 with four-line hyperfine splitting that is indicative of

an $S = ½$ $^{63}Cu^{2+}$ ion. Slight variations in the EPR spectra for the different linker lengths could suggest the proximity of two paramagnetic species in solution.

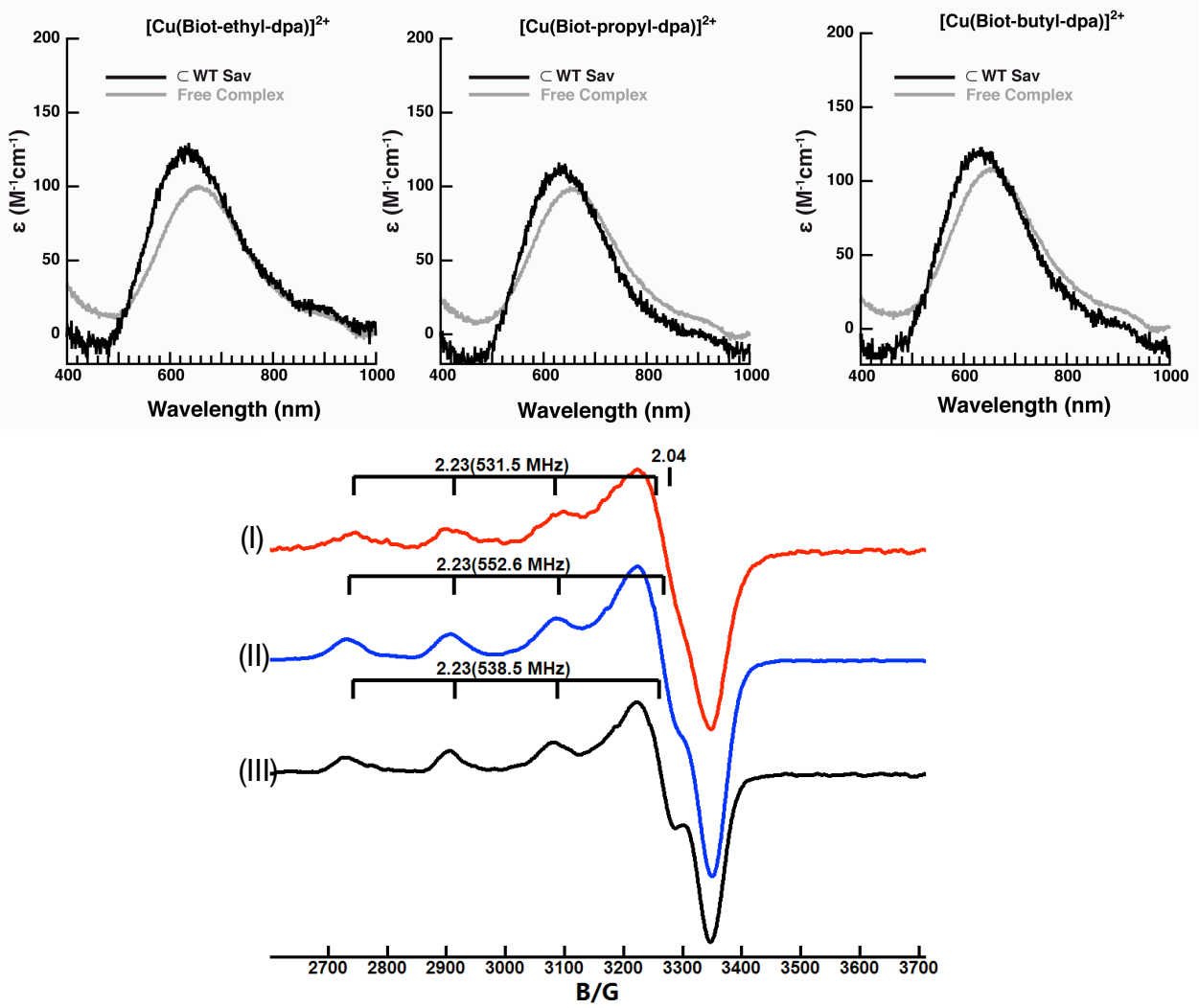

Figure 2-8 A) Optical spectra of **[Cu(Biot-n-DPA)]$^{2+}$** as free complexes overlayed with the corresponding **[Cu(Biot-n-dpa)]$^{2+}$⊂WT Sav .** B) Perpendicular mode EPR Spectra in 200 mM phosphate buffer at 77 K of (I) **[Cu(Biot-butyl-dpa)]$^{2+}$⊂WT Sav,** (II) **[Cu(Biot-propyl-dpa)]$^{2+}$⊂WT Sav,** (III) **[Cu(Biot-ethyl-dpa)]$^{2+}$⊂WT Sav.**

Preparation of Protein Crystals

With copper complexes in hand, X-ray diffraction studies of the AMPs were undertaken. X-ray quality single crystals of Sav and its mutants were obtained through

hanging drop vapor diffusion using a droplet of protein in water and precipitation buffer (2.6 M $(NH_4)_2SO_4$ and 0.1 M NaOAc at pH 4.0) allowed to equilibrate against a solution of the precipitation buffer in a reservoir at room temperature. Slow diffusion of water out of the droplet allows the protein to slowly crystallize. Artificial metalloproteins were prepared *in crystallo* by incubating apo-Sav crystals in 10 mM solutions of $[Cu(Biot\text{-}n\text{-}DPA)]^{2+}$ for approximately one hour. Molecular structures of the artificial metalloproteins were obtained through X-ray diffraction of the incubated crystals.

Analysis of Molecular Structure of WT Sav

The goal of X-ray diffraction studies of the biotinylated copper complexes was to determine the effect of increased linker length on the positioning of Cu^{II} complexes within the binding vestibule of the Sav dimer. The hypothesis was that a short linker length would lead to copper complexes positioned further away from each other, and that increasing the linker length would decrease the Cu•••Cu distance, thereby allowing for control over discrete monomeric copper complexes or potentially the cooperative chemistry of dinuclear copper species.

The initial structural refinements of **$[Cu(Biot\text{-}et\text{-}DPA)]^{2+}\subset$WT Sav** show a Cu•••Cu distance of ~12 Å (Figure 2-99 A). This is in agreement with the hypothesis that the shortest linker length would provide for monomeric Cu species. This early result also highlights the effectiveness of the AMP system in providing for long-range H-bonding interactions, as a channel of hydrogen bound water molecules is observed passing through the center of the vestibule between the two copper complexes.

In the case of **[Cu(Biot-propyl-DPA)]$^{2+}$⊂ WT Sav** structures, the complex is capable of adopting two conformations rotated approximately 90˚ apart, with a Cu•••Cu distance of ~7 Å (Figure 2-9 B). This suggests that the slightly longer linker positions the Cu complexes in an open pocket where there is greater flexibility to adopt different conformations. Unlike the structure of the ethyl linker, no water molecules are observed in the molecular structure of **[Cu(Biot-propyl-DPA)]$^{2+}$⊂ WT Sav** between the complexes, which indicates that the freedom of rotation of the complexes prevents a well-defined secondary sphere around the metal centers.

[Cu(Biot-Bu-DPA)]$^{2+}$⊂ WT Sav has a Cu•••Cu distance of 6.7 Å (Figure 2-99 C). This complex has the longest spacer length, however Cu•••Cu distance decreases only minimally compare to the AMP with the propyl spacer. Similar to the propyl complex, a H-bonding network can be observed around and between the complexes, however in this case there is a sulfate ion from the buffer that is coordinated to the Cu center in a monodentate fashion. This sulfate is also hydrogen-bound to the lysine at the 121 position. The combination of this H-bond interaction and the coulombic repulsion of the two dicationic metal centers could prevent the metal complexes from getting closer and thus suggest that an aliphatic linker may be too flexible to further decrease the Cu•••Cu distance as planned.

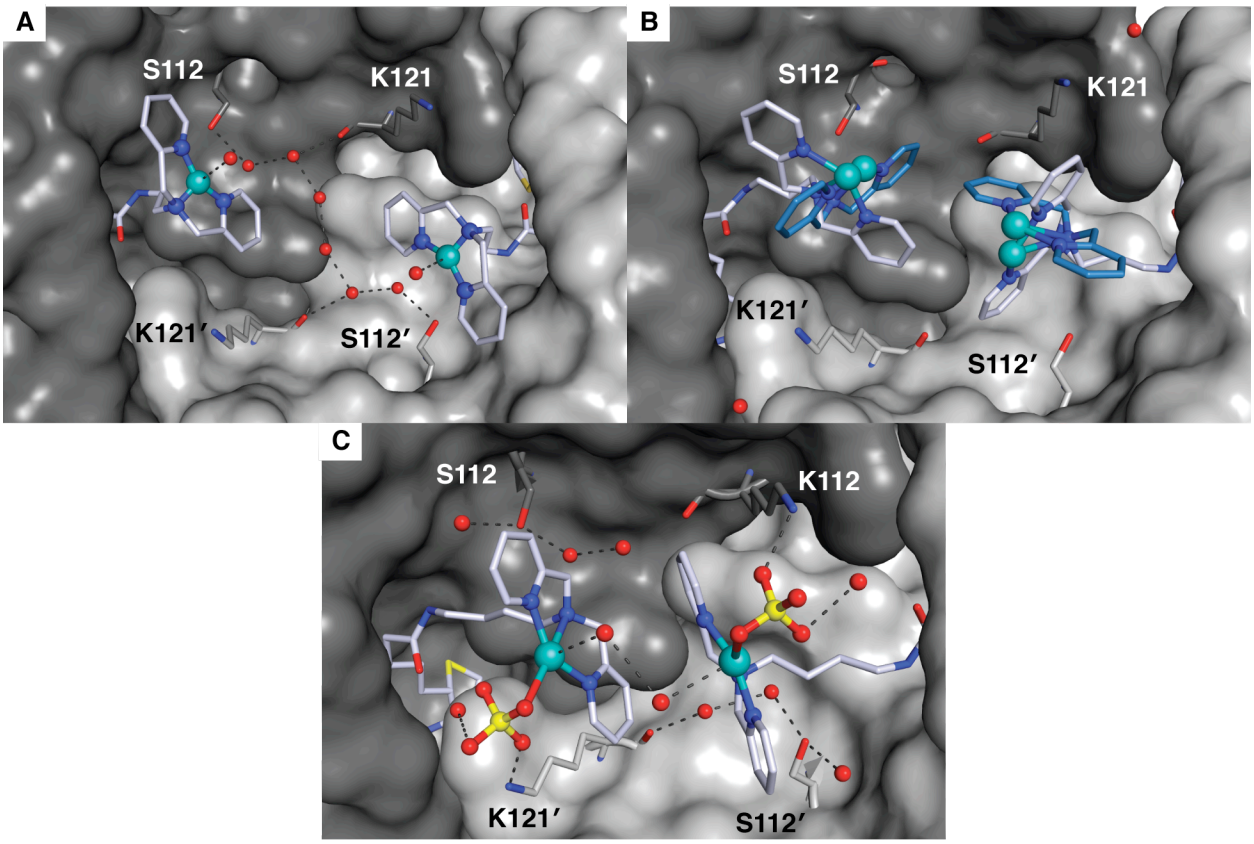

Figure 2-9 Molecular structures displaying the binding interfaces of (A) $[Cu(Biot\text{-}ethyl\text{-}dpa)]^{2+}\subset$WT Sav, (B) $[Cu(Biot\text{-}propyl\text{-}dpa)]^{2+}\subset$WT Sav, (C) $[Cu(Biot\text{-}butyl\text{-}dpa)]^{2+}\subset$WT Sav. Dashed lines represent H-bonds, and red spheres are water molecules. Cu^{2+} is shown in cyan, and sulfur is yellow. Only two subunits are shown, one in dark grey and the other in light grey.

Effects of Site Directed Mutagenesis

Mutants of Sav prepared by the Ward lab were also used to obtain molecular structures of complexes with L124V, L121R, L121M, S112V, S112M, S112D, and S112K. They found that most of the molecular structures featured only minor changes in conformation, Cu•••Cu distance, or H-bond networks. However, **$[Cu(Biot\text{-}propyl\text{-}DPA)]^{2+}$** with S112D and S112K mutants provided significant changes from the WT structure.

In the **[Cu(Biot-Pr-DPA)]$^{2+}$⊂ WT Sav** structure, the complex was capable of adopting two conformations rotated approximately 90˚ apart, with a Cu•••Cu distance of ~7 Å. By replacing the serine residue at 112 position with the larger amino residue, either aspartate or lysine, a single conformation was enforced. In the case of **[Cu(Biot-Pr-DPA)]$^{2+}$⊂Sav S112D** the Cu•••Cu distance decreases to 6.2 Å, the shortest observed in this study. This appears to prevent structural water molecules from situating between the copper centers, although an H-bonding network remains in place around the Cu(II) complexes (Figure 2-10 A). For **[Cu(Biot-Pr-DPA)]$^{2+}$⊂ S112K Sav**, the inter-copper distance is similar to that of the wild-type at 7.0 Å, however, an H-bonding network between water molecules and sulfate ions from the buffer can be observed between the complexes (Figure 2-10 B).

Interestingly, the **[Cu(Biot-Bu-DPA)]$^{2+}$⊂Sav S112D** structure shows a complex which adopts two conformations (Figure 2-10 C). One conformation is similar to the wild-type structure with a Cu•••Cu distance of 6.9 Å (not shown), but the second is rotated ~180˚ and allows the 112D aspartate to coordinate directly to the copper center. This is a significant achievement as it shows that the complexes can be bound to Sav both through the supermolecular Sav-biotin interaction but also a direct bond to an amino acid residue on the protein surface. Such dual anchoring methods have been shown in the case of Sav[31] and other proteins[18] to firmly anchor complexes in place. Similarly to the case of the **[Cu(Biot-Pr-DPA)]$^{2+}$⊂Sav WT** where multiple

conformations are possible, no structural water molecules are observed around the Cu(II) complexes.

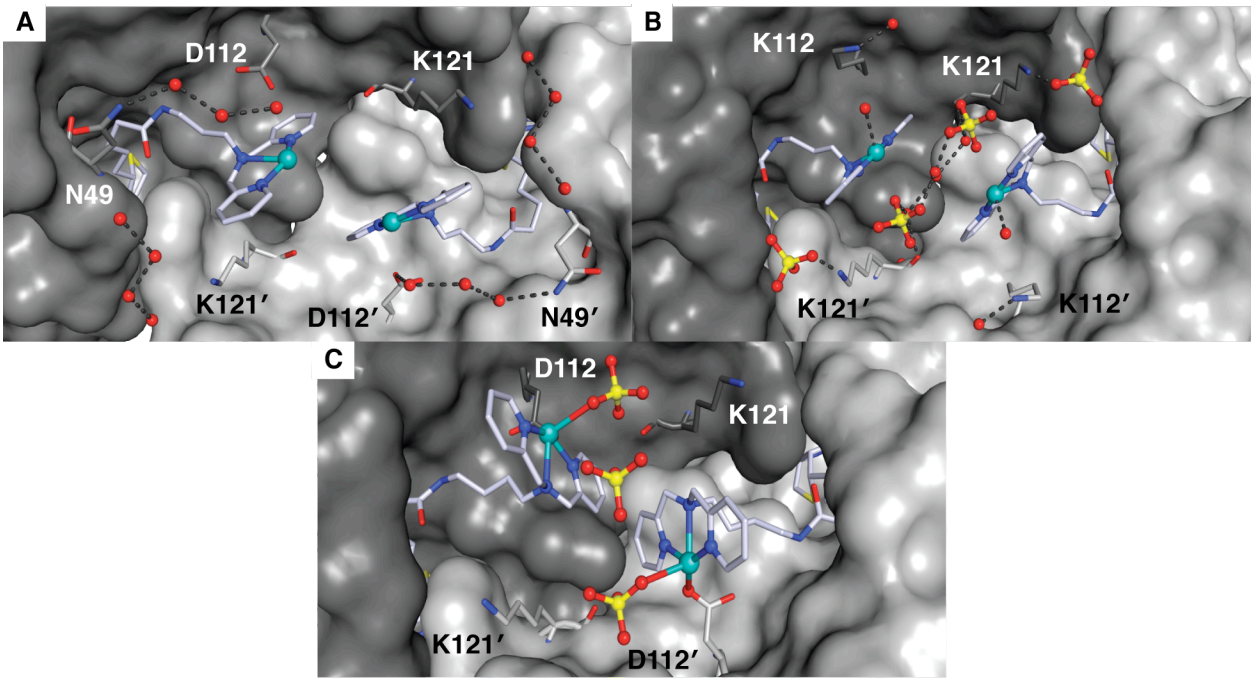

Figure 2-10 Molecular structures displaying the binding interfaces of (A) [Cu(Biot-propyl-dpa)]$^{2+}$⊂ S112D Sav, (B) [Cu(Biot-propyl-dpa)]$^{2+}$⊂ S112K Sav, (C) [Cu(Biot-butyl-dpa)]$^{2+}$⊂ S112D Sav. Dashed lines represent H-bonds, and red spheres are water molecules. Cu^{2+} is shown in cyan, and sulfur is yellow. Only two subunits are shown.

Cysteine Interaction

Structural information of the Cu^{2+} AMPs was most readily obtained from the crystallographic studies, however some interesting mutants of Sav eluded crystallization attempts, including the S112C variation. It was predicted that the thiol of cysteine would be capable of interacting with the Cu(II) centers. By adding solutions of **[Cu(Biot-n-DPA)]$^{2+}$** to S112C Sav, strong new absorptions were observed in the visible spectra of **[Cu(Biot-et-dpa)]$^{2+}$⊂S112C Sav**, **[Cu(Biot-pr-dpa)]$^{2+}$⊂S112C Sav**,

[Cu(Biot-bu-dpa)]$^{2+}$⊂ S112C Sav λ_{max} = 402 nm (ε = 3400 $M^{-1}cm^{-1}$), 389 nm (ε = 3200 $M^{-1}cm^{-1}$), 384 nm (ε = 4100 $M^{-1}cm^{-1}$), indicative of the thiolate to Cu^{II} charge transfer (Figure 2-11).[32] Additionally, the perpendicular EPR spectrum taken at 77 K shows a compression of the hyperfine coupling constant, A, versus WT Sav (A = 553 MHz in WT Sav compared to 383 MHz in **[Cu(Biot-et-dpa)]$^{2+}$⊂S112C Sav**) which provides further evidence for a cysteine-coordinated copper center (Figure 2-12).

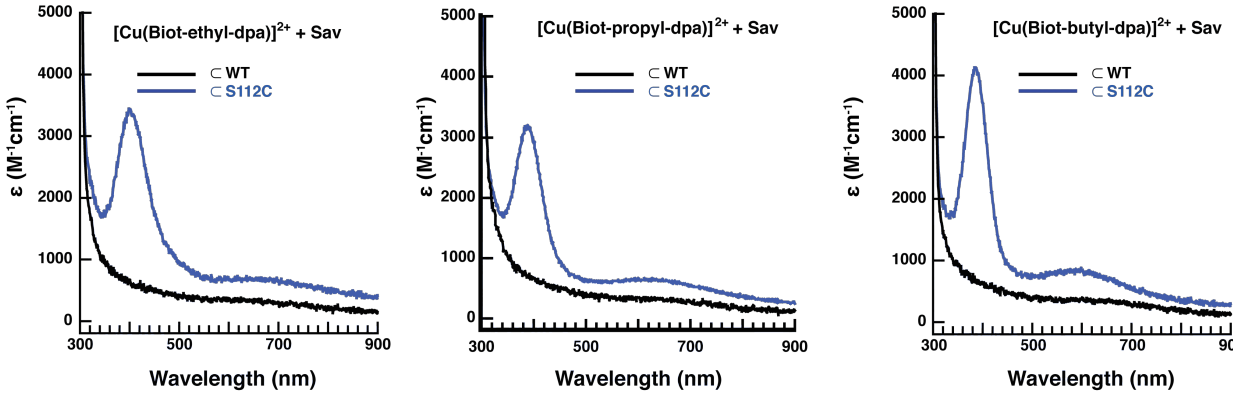

Figure 2-11 Optical spectra of **[Cu(Biot-n-DPA)]$^{2+}$** as free complexes overlayed with the corresponding **[Cu(Biot-n-dpa)]$^{2+}$⊂S112C** Sav AMPs .

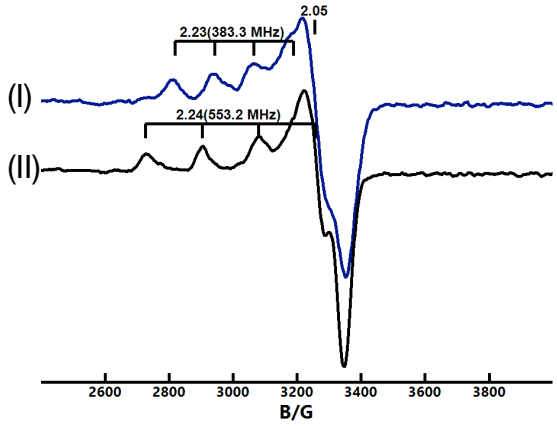

Figure 2-12 Perpendicular mode EPR Spectra in 200 mM phosphate buffer at 77 K of **(I) [Cu(Biot-et-dpa)]$^{2+}$⊂S112C Sav**, **(II) [Cu(Biot-et-dpa)]$^{2+}$⊂WT Sav**

Conclusion

The studies of AMPs described here solidify the utility of biotin-Sav technology as a viable means for generation of discrete metal complexes with a vast array of secondary interactions provided by the protein host. From the initial X-ray structural studies, it was shown that by controlled ligand modification, the distance of the metal ions can be modulated within the vestibule of the Sav dimer interface. In the future, incorporation of more rigid ligand linkers should be used to place the metal ions even closer together to produce cooperative chemistry across the dimer interface.

In addition, the modification of the protein through site-directed mutagenesis demonstrated a secondary source of influencing the metal complexes. First, by incorporating an aspartate within close proximity to the metal ion, the complex can be anchored in a specific position within the binding pocket. And second, the mutation of Sav to include a cysteine amino acid within the vestibule provided spectroscopic evidence of a Cu—S bond evidenced by intense charge-transfer transitions in the optical spectrum. These types of amino acid interactions with metal ions provide a route to the production of hybrid complexes that incorporate not only the biotinylated ligand but also direct contact with the protein host and paves the way for new and exciting artificial metalloproteins.

IV. Experimental

General Experimental Details. All commercially available reagents were used as received except the following: dimethylsulfoxide, *N,N*-dimethylformamide, toluene, and ether were degassed with argon and dried by vacuum filtration through activated alumina according to the procedure by Grubbs.[34] Triethylamine was distilled over potassium hydroxide. Thin-layer chromatography (TLC) was performed on Whatman 250 μm layer 6 Å glass-backed silica gel plates. Eluted plates were visualized using either UV light, I_2, potassium permanganate, or DACA stains. Silica gel chromatography was performed with the indicated solvent system using Fisher reagent silica gel 60 (230-400 mesh).

Instrumentation: Fourier Transform infrared spectra were collected on a Varian 800 Scimitar Series FTIR spectrometer. ^{1}H and ^{13}C NMR spectra were recorded at 500/600 and 125 MHz, respectively. ^{1}H NMR spectra were reported in ppm on the δ scale and referenced to tetramethylsilane. The data are presented as follows: chemical shift, multiplicity (s = singlet, d = doublet, t = triplet, q = quartet, m = multiplet, b = broad, app = apparent), coupling constant(s) in Hertz (Hz), and integration. ^{13}C NMR spectra were reported in ppm relative to $CDCl_3$ (77.23 ppm) or DMSO-d_6 (39.52 ppm). Mass spectra were measured on a MicroMass AutoSpec E, a MicroMass Analytical 7070E, or a MicroMass LCT Electrospray instrument. Electronic absorbance spectra were recorded with a Cary 50 spectrophotometer. X-band EPR spectra were collected using a Bruker EMX spectrometer equipped with an ER041XG microwave bridge.

Preparation of Compounds

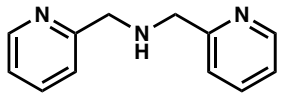

Di-(2-picolyl)amine (DPA).[29] To a solution of 2-picolylamine (9.617 g, 88.93 mol) in 100 mL EtOH was added a solution of pyridine carboxyaldehyde (9.519 g, 88.87 mmol) in 70 mL EtOH dropwise with stirring. After 15 min, $NaBH_4$ (8.443 g, 223.2 mmol) was added in small portions and the reaction was heated to reflux for 1 h. The mixture was cooled in an ice bath for 30 min, and a solution of concentrated HCl (15 mL) in EtOH (10 mL) was added via addition funnel over ca 15 min. The reaction mixture was then cooled in a refrigerator at 4 ˚C overnight. The resulting white precipitate was removed via filtration, and the filtrate was evaporated to dryness under reduced pressure. Next the crude residue was dissolved in a solution of 75 mL diethyl ether and 120 ml EtOH. To this was added 30 mL concentrated HCl, which precipitated the DPA•3HCl salt from the solution. The white crystals were collected via vacuum filtration. The free base was obtained by dissolving the salt in 100 mL water, transferring it to a separatory funnel, and adding a solution of sodium hydroxide (24 g, 0.60 mol) in 60 mL water, resulting in a two-phase system. The product was extracted with DCM (3 x 50 mL), washed with 50 mL water, 50 mL brine, dried over $MgSO_4$, and concentrated under reduced pressure to give a pale yellow oil (16.05 g, 91%). ^{1}H NMR ($CDCl_3$, 500 MHz) δ 8.56 (d, 2H, *J* = 4.8), 7.64 (dt, 2H, *J* = 7.2, 1.2 Hz), 7.36 (d, 2H, *J* = 7.8 Hz), 7.16 (dd, 2H, *J* = 4.8, 2.4 Hz), 3.99 (s, 4H), 2.44 (bs, 2H). ^{13}C NMR ($CDCl_3$, 126 MHz) δ[ppm]:

159.9, 148.5, 136.7, 122.5, 122.1, 55.0. HRMS calcd for $[M+Na]^+$ 222.1007, found 222.0999.

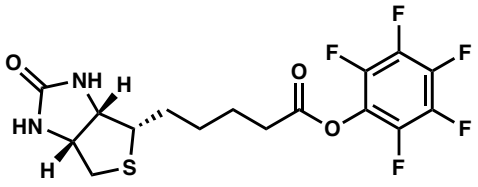

Biotin-pentafluorophenol ester (Biotin-PFP).[33] Biotin (3.034 g, 12.42 mmol) and 60 mL DMF were combined in a round bottom flask and heated at 70 ˚C until the biotin dissolved. The solution was cooled to room temperature in a water bath. Et_3N (3.6 g, 5.0 mL, 36 mmol) was added followed by pentafluorophenyltrifluoroacetate (4.842 g, 17.29 mmol), which caused the reaction mixture to turn pink. The reaction was allowed to stir under nitrogen at room temperature for 30 min. The solvent was removed in vacuo, and the crude residue was transferred to a frit and washed with diethyl ether. After drying under reduced pressure, the product was obtained as a white powder (4.790 g, 93%). ^{1}H NMR (DMSO-d_6, 500 MHz) δ[ppm]: 6.44 (s, 1H), 6.36 (s, 1H), 4.32–4.30 (m, 1H), 4.16–4.14 (m, 1H), 2.84 (dd, 1H, J = 12, 4.9 Hz), 2.79 (t, 2H, J = 7.4), 2.59 (d, 1H, J = 12 Hz), 1.70–1.63 (m, 3H), 1.54–1.41 (m, 3H). MS calcd for $[M+Na]^+$ 433.06, found 433.05.

Synthesis of phthalimide-protected alkyl dipicolyl amines (Phth-n-DPA).[30]

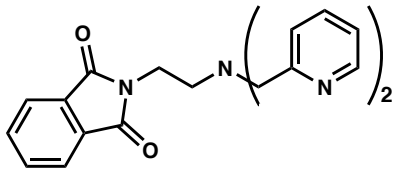

Phth-et-DPA. This compound was prepared using a modified literature procedure. Anhydrous potassium carbonate (3.050 g, 22.06 mmol) and potassium iodide (0.1876 g, 1.130 mmol) were suspended in dry acetonitrile (350 mL). DPA (1.103 g, 5.554 mmol) was added to this suspension, followed by 2-bromoethylphthalimide (1.482 g, 5.832 mmol). The mixture was refluxed for 24 h, filtered, and concentrated under vacuum to yield a red oil that was dissolved in DCM (200 mL) and was washed with saturated $NaHCO_3$ solution (3 × 200 mL) and with water (2 × 200 mL). Then the solvent was evaporated *in vacuo*, and to the resulting dark oil was added 1 M HCl (140 mL). The aqueous solution was washed with DCM (5 × 50 mL), and then it was carefully basified with solid sodium bicarbonate. An orange solid precipitated. It was extracted into DCM (3 × 50 mL), and concentrated under vacuum to yield a dark brown solid. The crude product was purified via flash chromatography (10% methanol in DCM as eluent). The product was obtained as a tan solid (1.431 g, 69%). ^{1}H NMR ($CDCl_3$, 600 MHz) δ[ppm]: 8.44 (bd, 2H, *J* = 4.8 Hz), 7.82 (dd, 2H, *J* = 5.4, 3.0 Hz), 7.73 (dd, 2H, *J* = 5.4, 3.0 Hz), 7.41 (td, 2H, *J* = 7.8, *J* =1.8 Hz), 7.34 (d, 2H, *J* = 8.4 Hz), 7.06 (dt, 2H, *J* = 6.0, 2.4 Hz), 3.86 (s, 4H), 3.84 (t, 2H, *J* = 6.0 Hz), 2.86 (t, 2H, 6.0 Hz). ^{13}C NMR ($CDCl_3$, 126 MHz) δ[ppm]: 168.3, 159.5, 149.1, 136.4, 134.0, 132.5, 123.3, 123.2, 122.1, 60.5, 51.9, 36.3. HRMS calcd for $[M+Na]^+$ 395.1484, found 395.1483.

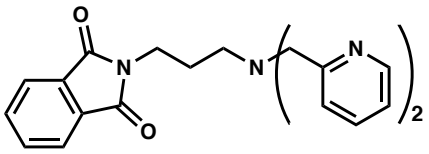

Phth-pr-DPA. This was compound was prepared using the above conditions with sodium carbonate (4.456 g, 41.85 mmol), potassium iodide (0.3644 g, 21.95 mmol), DPA (2.085 g, 1.046 mmol), and 3-bromopropylphthalimide (2.947 g, 10.99 mmol). The product was obtained as a red brown solid (3.185 g, 79%) and was used without further purification. ^{1}H NMR ($CDCl_3$, 600 MHz) δ[ppm]: 8.48 (d, 2H, *J* = 3.6 Hz), 7.82 (dd, 2H, *J* = 5.4, 3.0 Hz), 7.71 (dd, 2H, *J* = 5.4, 3.0 Hz), 7.63 (dt, 2H, *J* = 7.8, 1.8 Hz), 7.54 (d, 2H, *J* = 7.8 Hz), 7.11 (dd, 2H, *J* = 7.2, 1.2 Hz), 3.82 (s, 4H), 3.70 (t, 2H, *J* = 7.2 Hz), 2.64 (t, 2H, *J* = 7.2 Hz), 1.93 (q, 2H, *J* = 7.2 Hz). 13C NMR? HRMS calcd for $[M+H]^+$ 387.1821 found 387.1812.

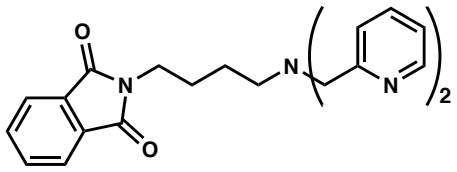

Phth-bu-DPA. This compound was prepared using the above conditions with sodium carbonate (4.456 g, 41.85 mmol), potassium iodide (1.113 g, 6.703 mmol), DPA (6.6173 g, 33.20 mmol), and 4-bromobutylphthalimide (10.30 g, 36.50 mmol). The product was obtained as a red brown solid (10.58 g, 80%) and was used without further purification.^{1}H NMR ($CDCl_3$, 600 MHz) δ[ppm]: 8.50 (d, 2H, *J* = 4.8 Hz), 7.66 (t, 2H, *J* = 7.68), 7.52 (d, 2H, *J* = 7.8 Hz), 7.15 (t, 2H, *J* = 5.6), 3.81 (s, 4H), 2.66 (t, 2H, *J* = 6.9 Hz)

2.55 (t, 2H, *J* = 7.1 Hz), 1.86 (bs, 2H), 1.58 (q, 2H, *J* = 7.0 Hz), 1.44 (q, 2H, *J* = 7.1 Hz). MS calcd for $[M+Na]^+$ 123.18 found 423.25.

Preparation of aminoalkyl dipicolyl amines (NH_2-n-DPA).

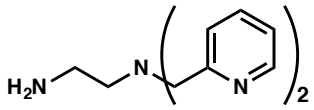

NH_2-et-DPA. To a round bottom flask charged with DPA-et-Phth (1.43 g. 3.84 mmol) and 100 mL ethanol was added five equivalents of $N_2H_4 \bullet H_2O$ (0.9 mL, 0.02 mol). The reaction mixture was brought to reflux with vigorous stirring. The phthalhydrazide byproduct forms as voluminous white precipitate over time. After three hours, the reaction mixture was cooled to room temperature and filtered through a frit. The filtrate was concentrated under reduced pressure to give a white residue, which was washed over a pad of Celite on a frit with DCM (3 x 50 mL) to separate the desired amine from the insoluble phthalhydrazide. The combined DCM washes were concentrated *in vacuo* to give the product as a pale yellow oil, which was used without further purification (0.93g, 99%). ^{1}H NMR ($CDCl_3$, 500 MHz) δ[ppm]: 8.54 (d, 2H, *J* = 4.0 Hz), (dt, 2H, *J* = 7.7, 1.6 Hz), 7.49 (d, 2H, 7.7 Hz), 7.16 (t, 2H, *J* = 5.3 Hz), 3.85 (s, 4H), 2.80 (t, 2H, *J* = 6.0 Hz), 2.67 (t, 2H, *J* = 6.1 Hz), 1.72 (bs, 2H). ^{13}C NMR ($CDCl_3$, 126 MHz) δ[ppm]: 159.8, 149.3, 136.6, 123.2, 60.9, 57.6, 39.8. HRMS calcd for $[M+H]^+$ 243.16, found 243.08.

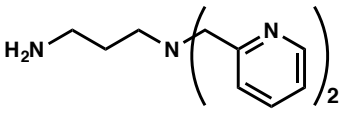

NH_2-pr-DPA. Was prepared using the above conditions with DPA-pr-Phth (5.693 g. 17.73 mmol), 125 mL ethanol, and $N_2H_4 \bullet H_2O$ (3.736 g, 74.63 mmol) to afford the desired product (1.60 g, 93%). ^{1}H NMR ($CDCl_3$, 600 MHz) δ[ppm]: 8.57 (d, 2H, *J* = 5.6 Hz), 7.65 (t, 2H *J* = 7.2 Hz), 7.45 (d, 2H, *J* = 7.8 Hz), 7.16 (t, 2H, *J* = 6.0 Hz), 3.82 (s, 4H), 2.83 (t, 2H, *J* = 6.6 Hz), 2.63 (t, 2H, *J* = 6.6 Hz), 1.75 (p, 2H, *J* = 6.6 Hz).

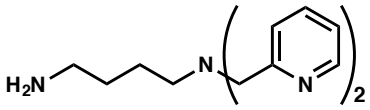

NH_2-bu-DPA. Was prepared using the above conditions with DPA-bu-Phth (2.548 g. 6.362 mmol), 60 mL ethanol, and $N_2H_4 \bullet H_2O$ (1.697 g, 33.90 mmol) to afford the desired product (1.60 g, 93%). ^{1}H NMR ($CDCl_3$, 500 MHz) δ[ppm]: 8.54 (d, 2H, *J* = 4.5 Hz), 7.66 (t, 2H, *J* = 7.7 Hz), 7.52 (d, 2H, *J* = 7.8 Hz), 7.15 (t, 2H, *J* = 5.6 Hz), 3.81 (s, 4H), 2.66 (t, 2H, *J* = 6.9), 2.55 (t, 2H, *J* = 7.1 Hz), 1.58 (p, 2H, *J* = 7.0), 1.44 (p, 2H, *J* = 7.1). HRMS *m/z* calcd for $[M+H]^+$ 271.1923, found 271.1924.

Synthesis of biotinylated ligands (Biot-n-DPA)

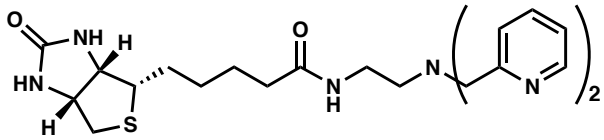

Biotin-et-DPA. In round bottom flask, NH_2-et-DPA (0.810 g, 3.34 mmol) was dissolved in 15 mL DMF. To this was added 1.5 equiv Et_3N (1.9 g, 1.4 mL, 2.6 mmol) and biotin-

PFP (1.371, 3.341 mmol). The reaction mixture was allowed to stir at room temperature for 18 h. The mixture was then concentrated under reduced pressure, and the crude mixture was lixiviated with diethylether to give the product as a brown, hygroscopic powder (1.596 g, 99%). ^{1}H NMR ($CDCl_3$, 500 MHz) δ[ppm]: 8.56 (d, 2H, *J* = 4.4 Hz), 7.68 (bs, 1H), 7.64 (t, 2H, *J* = 7.7 Hz), 7.33 (d, 2H, *J* = 7.8 Hz), 7.18 (t, 2H, *J* = 6.3 Hz), 5.83 (bs, 1H), 5.14 (bs, 1H), 4.49 (m, 1H), 4.32 (m, 1H), 3.89 (s, 4H), 3.33 (m, 2H), 3.16 (q, 1H, *J* = 4.6 Hz), 2.91 (dd, 1H, *J* = 12.8, 5.0 Hz), 2.74 (m, 3H), 2.26 (t, 2H , *J* = 7.4 Hz), 1.70 (bm, 4H), 1.48 (m, 2H). ^{13}C NMR ($CDCl_3$, 126 MHz) δ[ppm]: 173.1, 163.5, 159.3, 149.3, 149.3, 136.8, 123.6, 122.5, 61.9, 60.3, 60.1, 55.6, 52.7, 40.8, 37.7, 36.2, 28.4, 28.3, 25.9. HRMS *m/z* calcd for $[M+Na]^+$ 491.2205, found 491.2206.

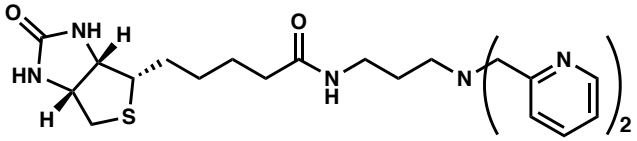

Biot-pr-DPA. Was prepared using the same conditions above with NH_2-pr-DPA (1.160 g, 4.524 mmol), biotin-PFP (1.757 g, 4.281 mmol), triethyl amine (0.90 mL, 6.4 mmol) 69%. ^{1}H NMR ($CDCl_3$, 600 MHz) δ[ppm]: 8.54 (d, 2H, *J* = 4.2 Hz), 7.70 (bt, 1H), 7.65 (t, 2H, *J* = 6.6 Hz), 7.18 (t, 2H, *J* = 5.4 Hz), 6.00 (s, 1H), 5.34 (s, 1H), 4.50 (t, 1H, *J* = 6.6 Hz), 4.31 (t, 1H, *J* = 4.8), 3.28 (q, 2H, *J* = 6.0 Hz), 3.15 (q, 1H, *J* = 4.8 Hz), 2.90 (dd, 1H, *J* = 13, 4.8 Hz), 2.73 (d, 1H, *J* = 13 Hz), 2.64 (t, 2H, *J* = 6.0 Hz), 2.25 (t, 2H, *J* = 7.2 Hz), 1.78–1.62 (m, 7H), 1.46–1.43 (m, 3H). ^{13}C NMR (DMSO, 126 MHz) δ[ppm]: 171.8, 162.7, 159.4, 149.7, 136.5, 122.6, 122.1, 61.0, 59.6, 59.2, 55.4, 51.5, 36.7, 35.3, 28.2, 28.0, 26.7, 25.3. HRMS *m/z* calcd for $[M+Na]^+$ 505.2362, found 505.2360.

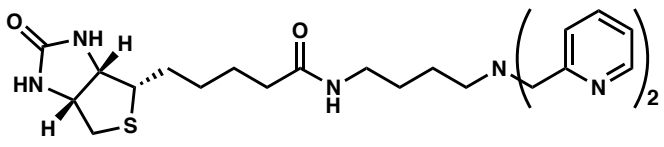

Biot-bu-DPA Was prepared using the same conditions above with NH_2-bur-DPA (0.700 g, 2.59 mmol), biotin-PFP (1.040 g, 2.53 mmol), triethyl amine (0.44 mL, 3.2 mmol) 74% ^{1}H NMR ($CDCl_3$, 600 MHz)) δ[ppm]: 8.52 (d, 2H, *J* = 4.2 Hz), 7.66 (dt, 2H, *J* = 7.8, 1.8 Hz), 7.47 (d, 2H, *J* = 7.8 Hz), 7.17 (bdt, 2H, *J* = 5.4, 1.8 Hz), 6.62 (bs, 1H), 6.18 (s, 1H), 5.40 (s, 1H), 4.50–4.48 (m, 1H), 4.31–4.29 (m, 1H), 3.83 (s, 4H), 3.20–3.17 (m, 2H), 3.16–3.12 (m, 2H), 2.89 (dd, 1H, *J* = 13, 4.8 Hz), 2.72 (d, 1H, *J* = 13 Hz), 2.59 (t, 2H, *J* = 6.6 Hz), 2.20 (t, 2H, *J* = 7.2 Hz), 1.77–1.572 (m, 6H), 1.49 (q, 2H, *J* = 6.6 Hz), 1.43 (q, 2H, *J* = 7.2 Hz) ^{13}C NMR ($CDCl_3$, 126 MHz) δ[ppm]:193.4, 173.4, 163.6, 149.2, 136.8, 123.6, 122.42, 62.0, 60.3, 55.6, 53.9, 40.8, 39.1, 36.1, 28.3, 28.2, 27.3, 25.9, 23.8. HRMS m/z calcd for $[M+H]^+$ 497.2699, found 497.2689.

Synthesis of Cu^{II} Complexes

[Cu(Biot-et-dpa)(ClO_4)](ClO_4) To a solution of $Cu(ClO_4)_2 \cdot 6H_2O$ (0.0620 g, 0.236 mmol) in EtOH (5 mL) was added Biot-et-dpa (0.0997 g, 0.213 mmol) in EtOH. Upon mixing a blue precipitate formed. After 30 min the reaction mixture was concentrated, and the remaining complex was precipitated with diethyl ether. The product was recovered on a glass frit and washed with diethyl ether to recover a blue, hygroscopic solid (0.1251, 75%). FTIR (Nujol mull, cm^{-1}, selected bands): 3353, 1658, 1611, 1270, 1095, 768, 722. HRMS m / *z* calcd for $[M-H]^+$ 530.1525, found 530.1527.

[Cu(Biot-pr-dpa)(ClO_4)](ClO_4) Prepared analogously to the above procedure (84%). FTIR (Nujol mull, cm^{-1}, selected bands): 3373, 1612, 1269, 1099**.** HRMS m / *z* calcd for $[M-H]^+$ 544.1682, found 544.1668.

[Cu(Biot-bu-dpa)(ClO_4)](ClO_4) Prepared analogously to the above procedure (79%). FTIR (Nujol mull, cm^{-1}, selected bands): 3376, 1665, 1613, 1269, 1097 MS *m* / *z* calcd for $[M+ClO_4]^+$ 658.14, found 658.11.

[Cu(Biot-et-dpa)(NO_3)](NO_3) Prepared according to the above procedure substituting $Cu(NO_3)\cdot 3H_2O$ for $Cu(ClO_4)_2\cdot 3H_2O$ (32%) FTIR (KBr pellet, cm^{-1}, selected bands): 3380, 3080, 2934, 2862, 1659, 1612, 1482, 1384, 1290, 1157, 1116, 1033, 769. MS *m* / *z* calcd for $[M+NO_3]^+$ 593.15, found 593.14.

[Cu(Biot-pr-dpa)(NO_3)](NO_3) Prepared according to the above procedure substituting $Cu(NO_3)_2\cdot 3H_2O$ for $Cu(ClO_4)_2$. (40%) FTIR (KBr pellet, cm^{-1}, selected bands): 3301, 3074, 2930, 2871, 1659, 1610, 1384, 1288, 1156, 1115, 1010, 320, 766. MS *m* / *z* calcd for $[M+NO_3]^+$ 607.16, found 607.13.

[Cu(Biot-bu-dpa)(NO_3)](NO_3) Prepared according to the above procedure substituting $Cu(NO_3)_2\cdot 3H_2O$ for $Cu(ClO_4)_2$. (87%) MS *m* / *z* calcd for $[M+NO_3]^+$ 621.18, found 621.31.

HABA Titrations. A solution of protein (1 mg/mL) was prepared in 200 mM phosphate buffer at pH 7 and transferred to a 1 cm cuvette. 150 equivalents of a 25 mM solution of HABA in phosphate buffer were added. A solution of ligand or metal complex in DMF was added in 4 µL portions until at least 5 equivalents had been added. The titration was monitored by UV-Visible spectroscopy at λ_{max} = 506 nm.

Crystallographic Studies of Biot-n-DPA⊂ Sav. Sav protein was crystallized by hanging drop vapor diffusion method. Diffraction quality crystals were grown at room temperature by mixing 2 μL of 356 μM protein (ca 20 mg/mL) and 2 μL of reservoir solution containing 2.6 M $(NH_4)_2SO_4$ and 0.1 M NaOAc at pH 4 (precipitation buffer). Crystals were soaked in solubilized $[Cu(Biot\text{-}n\text{-}dpa)]^{2+}$ in DMF:precipitation buffer for one hour before being transferred to cryo-protectant (30% glycerol in precipitation buffer) and a set of data collected at 100 K from single crystals using a RIGAKU 007HF X-ray source equipped with a Saturn 344+ CCD detector. The diffraction images were indexed, integrated, and scaled by using MOSFLM.[34]

PDB 2QCB[35] was used as a search model to solve the structure by molecular replacement calculations using the program Phaser[36] implemented in CCP4 package. The transformed model was subjected to refinement using Phenix[37]. The phases were improved and extended to 2.5 Å incrementally. The $2F_o - F_c$ and $F_o - F_c$ electron density maps were visualized using the program COOT[38], which was used for model building. The crystallographic *R*-factor and *R*-free were monitored at each stage to avoid any bias. Water molecules were added by the automatic water-picking algorithm of COOT and inspected manually. **Uv-vis Experiments** A solution of protein (ca 10 mg/mL) was prepared in either water or 200 mM phosphate buffer at pH 7 and transferred to 1 cm cuvette. To this was added 3.5 equiv of the appropriate Cu^{II} complex from a 30 mM stock solution in DMF.

EPR Experiments. A solution of protein (ca 1 mg/mL) was prepared in either water or 200 mM phosphate buffer at pH 7 and transferred to an EPR tube. Four equivalents of

metal complex were added from a 30 mM solution in DMF. The samples were then frozen at 77 K in liquid nitrogen and used for data collection.

Table 2-1 Metric parameters for crystallographic data.

Sav Mutant	[Cu(Biot-bu-dpa)]$^{2+}$ ⊂WT Sav	[Cu(Biot-bu-dpa)]$^{2+}$ ⊂S112D Sav	[Cu(Biot-pr-dpa)]$^{2+}$ ⊂S112K Sav	[Cu(Biot-pr-dpa)]$^{2+}$ ⊂S112D Sav	[Cu(Biot-pr-dpa)]$^{2+}$ ⊂WT Sav
			Data processing statistics		
Unit cell dimensions	57.3 Å, 57.3 Å, 174.8 Å, α=β=γ=90°	57.4 Å, 57.4 Å, 174.6 Å, α=β=γ=90°	57.3 Å, 57.3 Å, 175.5 Å, α=β=γ=90°	57.4 Å, 57.4 Å, 175.1 Å, α=β=γ=90°	57.2 Å, 57.2 Å, 175.2 Å, α=β=γ=90°
Space group	$I4_122$	$I4_122$	$I4_122$	$I4_122$	$I4_122$
Resolution limits (Å)	36.77 – 1.70	36.78 – 1.86	29.93 – 1.66	36.84 – 1.86	36.70 – 1.86
Highest resolution shell (Å)	1.79 – 1.70	1.96 – 1.86	1.75 – 1.66	1.96 – 1.86	1.96 – 1.86
R_{merge} (%)	9.2 (106.8)	13.1 (130.0)	10.1 (78.0)	25.9 (277.3)	13.9 (136.1)
No unique reflections	16566 (2342)	12534 (1720)	17774 (2543)	12761 (1773)	12709 (1823)
Multiplicity	10.5 (6.9)	11.0 (11.3)	11.1 (10.9)	9.7 (10.2)	10.6 (10.8)
I/sig(I)	13.9 (1.6)	13.1 (2.4)	14.5 (3.1)	6.0 (0.8)	11.0 (1.8)
Completeness (%)	99.9 (99.3)	8.2 (95.5)	100.0 (100.0)	99.7 (98.3)	100.0 (100.0)
CC(1/2)	99.8 (54.1)	n.d.	n.d.	n.d.	99.8 (52.7)
			Data refinement statistics		
Resolution limit (Å)	36.77 – 1.70	12.00 – 1.90	29.93 – 1.66	36.84 – 1.86	36.70 – 1.86
R_{work}/R_{free} (%)	0.21/ 0.23	0.20/ 0.23	0.17/ 0.21	0.23/ 0.27	0.21/ 0.24
R.m.s deviation					
- Bond length (Å)	0.007	0.005	0.012	0.007	0.007
- Bond angles (°)	1.07	1.00	1.24	1.22	1.29
# ligand molecules					
- Cu-cofactor	1	1	1	1	1
- water	37	19	97	65	51
- sulfate	-	3	5	-	-

V. References

1 A. S. Borovik, *Acc. Chem. Res.*, 2005, **38**, 54–61.
2 R. L. Shook and A. S. Borovik, *Inorg Chem*, 2010, **49**, 3646–3660.
3 R. H. Holm and E. I. Solomon, *Chem. Rev.*, 2004, **104**, 347–348.
4 L. L. Welbes and A. S. Borovik, *Acc. Chem. Res.*, 2005, **38**, 765–774.
5 A. C. Sharma and A. S. Borovik, *J. Am. Chem. Soc.*, 2000, **122**, 8946–8955.
6 J. F. Krebs and A. S. Borovik, *J. Am. Chem. Soc.*, 1995, **117**, 10593–10594.
7 C. E. MacBeth, A. P. Golombek, V. G. Young Jr., C. Yang, K. Kuczera, M. P. Hendrich and A. S. Borovik, *Science*, 2000, **289**, 938–941.
8 Y. J. Park, S. A. Cook, N. S. Sickerman, Y. Sano, J. W. Ziller and A. S. Borovik, *Chem. Sci.*, 2013, **4**, 717–726.
9 Y. J. Park, N. S. Sickerman, J. W. Ziller and A. S. Borovik, *Chem. Commun.*, 2010, **46**, 2584–2586.
10 R. L. Shook, W. A. Gunderson, J. Greaves, J. W. Ziller, M. P. Hendrich and A. S. Borovik, *J. Am. Chem. Soc.*, 2008, **130**, 8888–8889.
11 R. L. Lucas, M. K. Zart, J. Murkerjee, T. N. Sorrell, D. R. Powell and A. S. Borovik, *J. Am. Chem. Soc.*, 2006, **128**, 15476–15489.
12 T. Taguchi, R. Gupta, B. Lassalle-Kaiser, D. W. Boyce, V. K. Yachandra, W. B. Tolman, J. Yano, M. P. Hendrich and A. S. Borovik, *J. Am. Chem. Soc.*, 2012, **134**, 1996–1999.
13 D. C. Lacy, R. Gupta, K. L. Stone, J. Greaves, J. W. Ziller, M. P. Hendrich and A. S. Borovik, *J. Am. Chem. Soc.*, 2010, **132**, 12188–12190.
14 C. E. MacBeth, R. Gupta, K. R. Mitchell-Koch, V. G. Young, G. H. Lushington, W. H. Thompson, M. P. Hendrich and A. S. Borovik, *J. Am. Chem. Soc.*, 2004, **126**, 2556–2567.
15 G. K. Y. Ng, J. W. Ziller and A. S. Borovik, *Inorg Chem*, 2011, **50**, 7922–7924.
16 Y. Lu, *Angew. Chem. Int. Ed.*, 2006, **45**, 5588–5601.
17 Y. Lu, N. Yeung, N. Sieracki and N. M. Marshall, *Nature*, 2009, **460**, 855–862.
18 J. R. Carey, S. K. Ma, T. D. Pfister, D. K. Garner, H. K. Kim, J. A. Abramite, Z. Wang, Z. Guo and Y. Lu, *J. Am. Chem. Soc.*, 2004, **126**, 10812–10813.
19 C. Cavazza, C. Bochot, P. Rousselot-Pailley, P. Carpentier, M. V. Cherrier, L. Martin, C. Marchi-Delapierre, J. C. Fontecilla-Camps and S. Ménage, *Nature Chem*, 2010, **2**, 1069–1076.
20 N. Yeung, Y.-W. Lin, Y.-G. Gao, X. Zhao, B. S. Russell, L. Lei, K. D. Miner, H. Robinson and Y. Lu, *Nature*, 2009, **462**, 1079–1082.
21 T. R. Ward and R. Reuter, *e-EROS Encyclopedia of Reagents for Organic Synthesis*, 2014, 1–4
22 C. Letondor, A. Pordea, N. Humbert, A. Ivanova, S. Mazurek, M. Novič and T. R. Ward, *J. Am. Chem. Soc.*, 2006, **128**, 8320–8328.
23 C. Letondor, *Proc. Natl. Acad. Sci. U.S.A.*, 2005, **102**, 4683–4687.
24 C. Letondor and T. R. Ward, *ChemBioChem*, 2006, **7**, 1845–1852.
25 C. Mayer, D. G. Gillingham, T. R. Ward and D. Hilvert, *Chem. Commun.*, 2011, **47**,

12068–12070.
26 M. Creus, T. R. Ward, Design and Evolution of Artificial Metalloenzymes: Biomimetic Aspects in *Progress in Inorganic Chemistry, Volume 57*, K. D. Karlin, Ed., John Wiley & Sons, Inc., New York, USA, 2011, 203–252
27 H. R. Lucas, L. Li, A. A. N. Sarjeant, M. A. Vance, E. I. Solomon and K. D. Karlin, *J. Am. Chem. Soc.*, 2009, **131**, 3230–3245.
28 M. J. Henson, M. A. Vance, C. X. Zhang, H.-C. Liang, K. D. Karlin and E. I. Solomon, *J. Am. Chem. Soc.*, 2003, **125**, 5186–5192.
29 A. Thapper, A. Behrens, J. Fryxelius, M. H. Johansson, F. Prestopino, M. Czaun, D. Rehder and E. Nordlander, *Dalton Trans.*, 2005, 3566–3571.
30 C. Incarvito, M. Lam, B. Rhatigan, A. L. Rheingold, C. J. Qin, A. L. Gavrilova and B. Bosnich, *J. Chem. Soc., Dalton Trans.*, 2001, 3478–3488.
31 J. M. Zimbron, T. Heinisch, M. Schmid, D. Hamels, E. S. Nogueira, T. Schirmer and T. R. Ward, *J. Am. Chem. Soc.*, 2013, **135**, 5384–5388.
32 R. G. Daugherty, T. Wasowicz and B. R. Gibney, *Inorg. Chem.,* 2002, **41**, 2623–2632.
33 J. M. Chambers, L. M. Lindqvist, A. Webb, D. C. S. Huang, G. P. Savage and M. A. Rizzacasa, *Org. Lett.*, 2013, **15**, 1406–1409.
34 T. G. G. Battye, L. Kontogiannis, O. Johnson, H. R. Powell and A. G. W. Leslie, *Acta Crystallogr. D Biol. Crystallogr.*, 2011, **67**, 271–281.
35 M. Creus, A. Pordea, T. Rossel, A. Sardo, C. Letondor, A. Ivanova, I. LeTrong, R. E. Stenkamp and T. R. Ward, *Angew. Chem. Int. Ed.*, 2008, **47**, 1400–1404.
36 A. J. McCoy, R. W. Grosse-Kunstleve, P. D. Adams, M. D. Winn, L. C. Storoni and R. J. Read, *J. Appl. Cryst.,* 2007*,* **40***, 658-674*.
37 P. D. Adams, P. V. Afonine, G. Bunkoczi, V. B. Chen, I. W. Davis, N. Echols, J. J. Headd, L. W. Hung, G. J. Kapral, R. W. Grosse-Kunstleve, A. J. McCoy, N. W. Moriarty, R. Oeffner, R. J. Read, D. C. Richardson, J. S. Richardson, T. C. Terwilliger and P. H. Zwart, *Acta Cryst* 2010, 1–9.
38 P. Emsley and K. Cowtan, *Acta Crystallogr. D Biol. Crystallogr.*, 2004, **60**, 2126–2132.

CHAPTER 3

Investigation of Bis-Biotinylated Salen Compounds

Introduction

Precise control of the secondary coordination sphere surrounding a transition metal ion is an ongoing challenge faced by synthetic chemists.[1] Metalloproteins, which bear metal ions in their active sites, offer unparalleled control of reactivity, in part, through the structure of the protein itself. The metal ion is usually sequestered within the interior of the protein, which isolates it from other metal centers, limits substrate access, and prevents unwanted reactions with the protein. Amino acid residues within the active site surrounding the metal active site provide a number of non-covalent, secondary coordination sphere, interactions which further tune the reactivity and selectivity of the complex.[2-4]

One method of controlling the secondary coordination sphere is to introduce non-native metal ions or prosthetic groups into proteins, thereby engineering artificial metalloproteins for use as biocatalysts. While there are a number of approaches to engineering artificial metalloproteins, the work of Lu and Ward exemplify two different and important design approaches. Lu has demonstrated a number of examples of *de novo* construction of an artificial protein or the creation of a new site within a protein, which can bind a transition metal ion or host a synthetic metal complex. One example is the modification of myoglobin (Mb) to bear the Mn *N,N*'-bis(salicylidene)ethylenediamine (Mn^{III}salen) complex, **1**, which is used for the sulfoxidation of thioanisole (Figure 3-1). When **1** is non-covalently docked in apo-Mb,

no enantioselectivity is observed for the reaction, however, when one covalent tether is introduced, enantiomeric excess (ee) increases to 12%, and two covalent linkages boosts the ee to 51%. Rotational motions are limited by anchoring the metal complex to the protein, which leads to greater control over orientation and placement of the complex, thereby helping to maintain a specific chiral environment around the metal center.[5,6] However, while this method creates a customized site that houses a metal complex, it is exceedingly difficult and time consuming to precisely predict the placement of a metal ion within the protein matrix and subsequently construct such a protein.

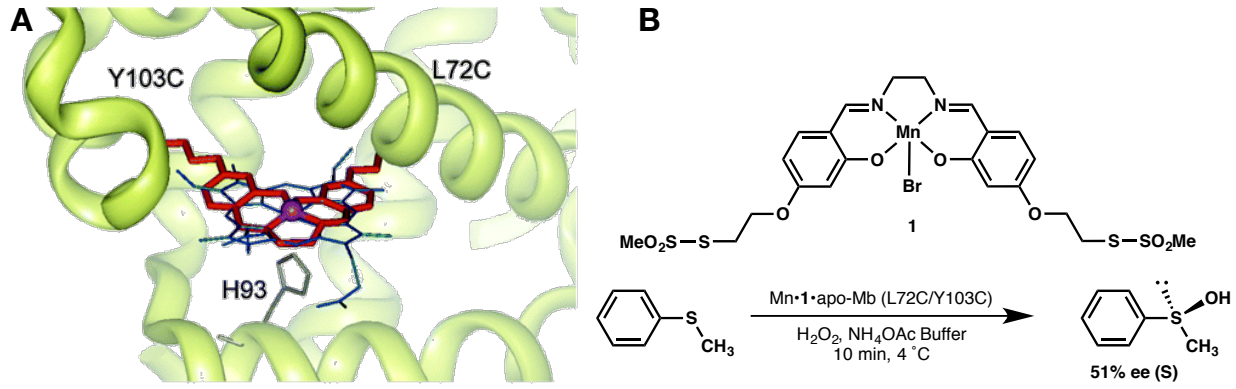

Figure 3-1 (A) Computer model of Mb with covalently attached Mn(salen) complex overlayed with heme. (B) The dually-anchored Schiff base is capable of asymmetric sulfoxidation reactions with moderate ee.[5]

A second method to harness the reactivity of synthetic metal complexes within proteins is the exploitation of the biotin-(strept)avidin interaction. Biotin is a naturally occurring B vitamin which is sequestered by the tetrameric proteins avidin and streptavidin (Sav) in a nearly irreversible process (K_a = ~ 10^{14} M^{-1}).[7] If biotin is conjugated to another compound, such as a metal complex, that moiety would be taken up into the biotin binding site within Sav. In 1977, Whitesides pioneered the use

of this technology as a means of engineering artificial metalloproteins.[8] In the past decade, the Ward lab has explored the use of the inherently chiral microenvironment of the Sav binding site to enact enantioselective transformations for such as asymmetric allyl alkylations,[9] olefin metathesis,[10] and asymmetric transfer hydrogenations (ATH).[11-18] For example, an Ir(III) complex bearing biotinylated aminosulfonamide ligand ([Cp*Ir(Biot-p-L)Cl]) combined with wild type (WT) Sav is capable of producing salsolidine quantitatively with 57% ee (Figure 3-2).

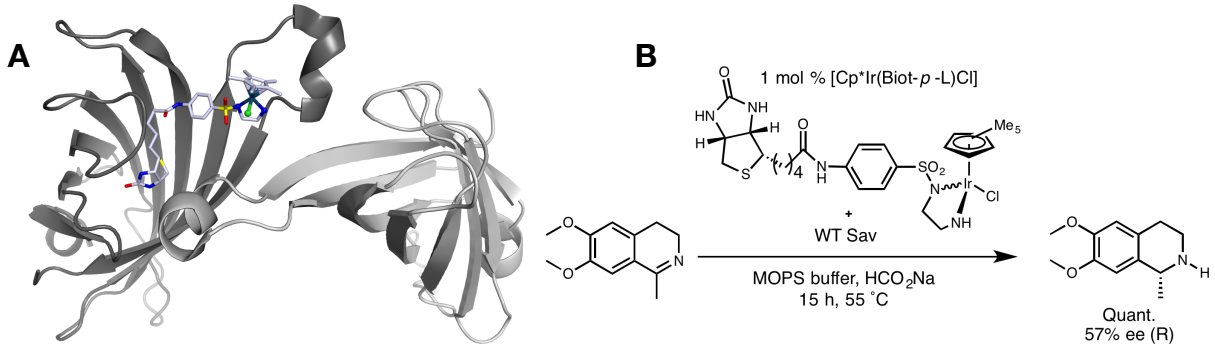

Figure 3-2 (A) X-ray crystal structure (PDB: 3PK2) of complex [Cp*Ir(Biot-p-L)Cl] in the biotin binding pocket of Sav. The other two subunits have been omitted for clarity. (B) Protein-bound [Cp*Ir(Biot-p-L)Cl] serves as a catalyst in asymmetric transfer hydrogenations. [11,12,19]

To date, engineered metalloproteins using biotin-Sav technology feature metal complexes with a single biotin tether. Since Sav forms a functional dimer of dimers with four biotin-binding sites, maximum occupancy is four metal complexes per protein tetramer (Figure 3-3a). Inspired by Lu's example of a dually-anchored Schiff base complex and in collaboration with the Ward lab at the University of Basel, we have prepared bis-biotinylated Schiff base ligands to probe the effects of bridging two adjacent biotin-binding sites in the Sav tetramer (Figure 3-3b). We predict that limiting the freedom of the bound complex will enhance the enantioselectivity of organic transformations. The microenvironment of the metal complex can be further tuned by

site-directed mutagenesis to create new active sites with synthetic metal complexes.[20,21]

This chapter describes the synthesis of a bis-biotinylated ligand, H_2**Sal-2,** and an earlier preparative route for H_2**Sal-1**, which proved to be unsuccessful (Figure 3-3). $[Salen]^{2-}$ was chosen as the base ligand scaffold because of its broad applicability for catalysis and coordination chemistry.[22-24] The key step of the synthetic pathway is the use of Cu-catalyzed alkyne azide cyclization (CuAAC) to form triazoles which will serve as spacers to ensure the positioning of the metal complex between the biotin-binding sites. Additionally, a Cu(II) complex has been prepared with H_2**Sal-2**, which will serve as a probe for studying how Sav binds the bis-biotinylated ligand system.

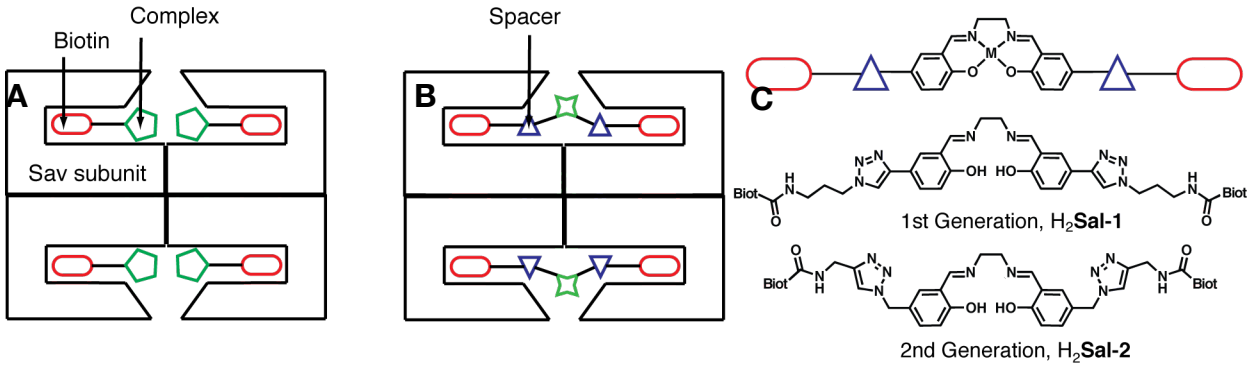

Figure 3 Diagram (a) Depicts Sav as a dimer of dimers with two opposing biotin binding sites per side of the protein. Each binding site is occupied by a biotin bond to one metal complex (b) The proposed dual-anchored system and H_2**Sal-1** and H_2**Sal-2.**

Results and Discussion

First Generation Synthesis

I envisioned the formation of the bis-biotinylated H_2**Sal-1** using the CuAAC between an alkyne substituted salen and an azide tethered to biotin. Bis-alkynyl salen **4** was prepared by modifying a known route.[25] 4-Bromosalicylaldehyde was reacted

with ethynyltrimethylsilane under Sonogoshira conditionsto give the TMS-protected alkyne in 62% yield. Deprotection with potassium carbonate yielded alkyne **3** (45%), which was reacted with ethylene diamine to give salen **4** (61%). The activated succinimide ester **5** was prepared from biotin and N-hydroxysuccinimide with DCC (99%), which was reacted azido propyl amine **6** to give yield azido biotin **7** (Scheme 3-1).[26]

Scheme 3-1 Preparation of precursor salen **4** and biotin alkyne **7**.

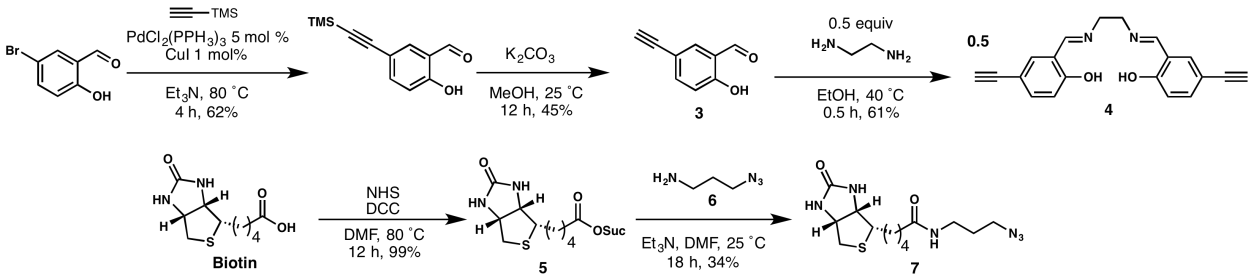

With bis-alkynyl salen **4** and biotin **7** in hand, a standard set of CuAAC conditions in various solvents was examined to effect the desired triazole formation.[27] None of the attempted conditions produced any evidence of triazole formation. Schiff bases are excellent ligands for Cu(II), [28,29]which is the CuAAC precatalyst, therefore it is possible that the Cu(II) ions were being bound by the excess of Schiff base in solution, rendering the Cu(II) ions unreactive to reduction by sodium ascorbate to generate the active Cu(I) catalyst. ESI-MS provided evidence for a [Cu(Salen **4**)+H]$^+$ species with a strong ion peak with a mass-to-charge ratio of 378.06. Even with an excess of $CuSO_4$ and reductant, no triazole product was observed (Table 3-1).

Since Cu(salen) species were observed by mass spectrometry, we thought that it could be possible to perform the triazole formation with the aldehyde **3**, which would not be as good of a ligand for Cu(II). By ^{1}H NMR spectroscopy, one set of conditions

did show evidence of product formation, albeit in low yield (**Table 3-2**). This reaction proved to be difficult to reproduce, and the triazole product **8** was never isolated in sufficient quantity to be a viable building block for the desired ligand.

Table 3-1 CuAAC conditions probed for the formation of H_2**Sal-1**

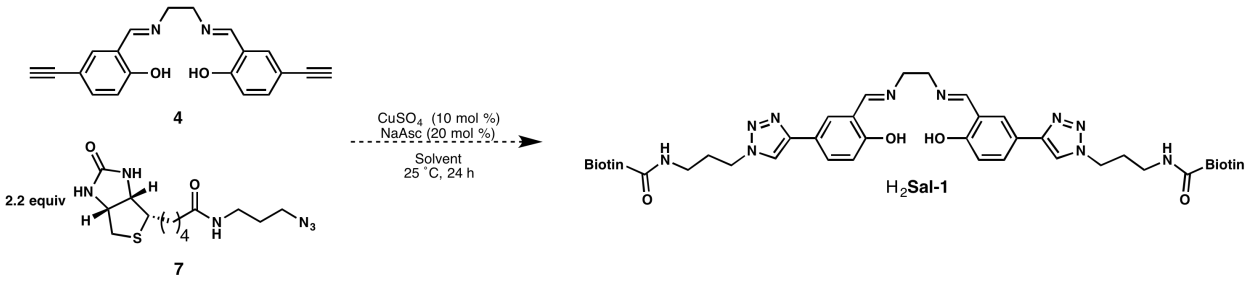

Entry	Solvent	Conversion[a]
1	1:1 H_2O/^{t}BuOH	not observed
2	1:1 H_2O/THF	not observed
3	1:1 H_2O/EtOH	not observed
4	1:1 H_2O/DMF	not observed
5[b]	1:1 H_2O/MeOH	not observed

[a] Determined by ^{1}H NMR spectroscopy. [b] 110 mol % $CuSO_4$, 120 mol % Sodium ascorbate

Table 3-2 CuAAC conditions explored for biotinylated-Salicaldehyde

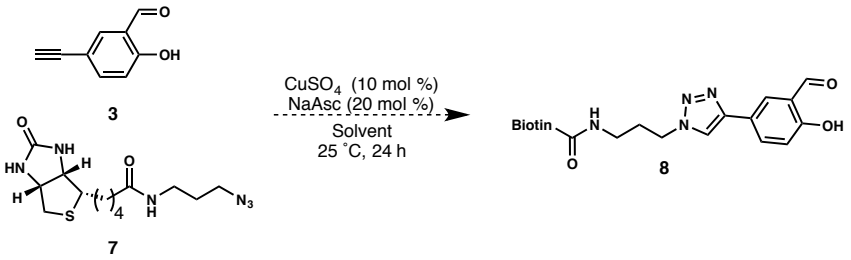

Entry	Cu Source	Additive	Solvent	Conversion[a]
1	$CuSO_4$	-	MeOH	31%
2	$CuSO_4$	110% $CuSO_4$, 120% NaAsc	1:1 H_2O/MeOH	<5%
3	$CuSO_4$	500% $CuSO_4$, 1000% equiv NaAsc	1:1 H_2O/MeOH	<5%
4	Cu(OAc)	1 equiv DIPEA	MeOH	<5%
5	CuI	1 equiv DIPEA	MeOH	<5%

[a] Conversion determined by ^{1}H NMR spectroscopy

Second Generation Synthesis

The second preparative route was designed to provide an improved electronic match between azide and alkyne. I envisioned H_2**Sal-2**, in which aliphatic alkynes and azides would be used, whereas the previous system featured an aryl alkyne. Other benefits include obviating potentially hazardous, low molecular weight alkyl azides, the cross-coupling reaction involving an expensive palladium catalyst, brominated starting compound, and a deprotection step.[30]

Starting from inexpensive salicaldehyde, treatment with formaldehyde in concentrated HCl yielded the 4-chloromethylsalicaldehyde **9** in 25% crystalline yield. In the following step, nucleophilic attack of sodium azide provided the corresponding 4-azidomethylsalicaldehyde **10** in 77% yield (Scheme 3-2).

Scheme 3-2 Synthesis of 4-azidomethylsalicaldehyde **10**.

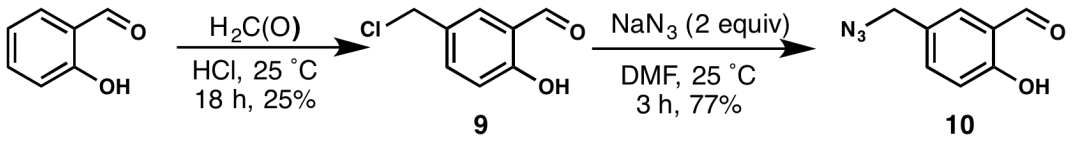

A model system was developed to mimic the electronic properties of the proposed alkynyl biotin in order to conserve difficult to obtain compounds. Benzoyl chloride was treated with propargyl amine according to a known procedure to give the alkyne **11** in good yield.[31] Azide **10** and alkyne **11** were treated with $CuSO_4$, NaAsc, and TBTA to effect the triazole formation in moderate yield. When Schiff-base **16** was treated with alkyne **11** under the same reaction conditions, no triazole formation was observed, suggesting again that the salen is too strong of ligand to allow for CuAAC to function as a catalyst (Scheme 3-3).

The success of the CuAAC model system prompted the synthesis of alkynyl biotin. The pentafluorophenol (PFP) ester of biotin was chosen as synthon due to its greater activity in comparison to the succinimide ester.

Scheme 3-3 CuAAC conditions used for triazole formation between alkyne **11** and salen **10**.

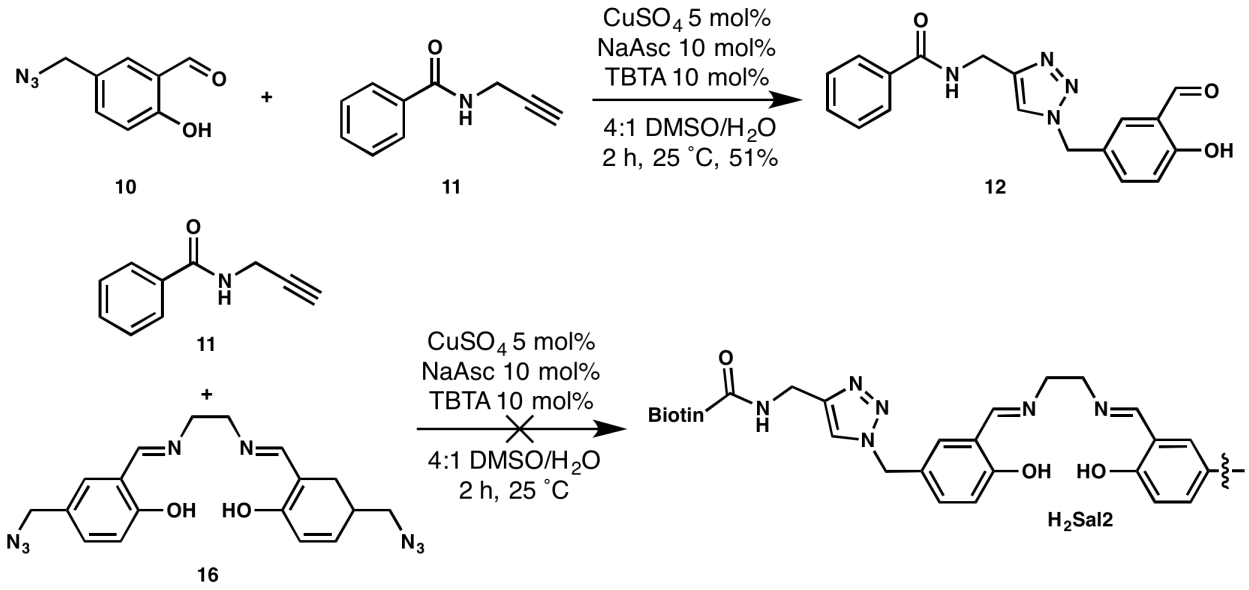

Biot-PFP **13** was prepared from biotin and PFP in the presence of DCC in DMF. The crystalline product was treated with propargyl amine to give biotin **14** in low isolable yield. With the successful preparation of azide **10** and biotin **14**, the CuAAC conditions from the model system were applied to give the desired aldehyde **15**. The aldehyde was carried on with no further purification in the condensation reaction with ethylenediamine to form the bis-biotinylated H_2**Sal-2** in moderate yield (Scheme 3-4).

Scheme 3-4 Synthesis of H_2**Sal-2** from salen **10** and Biotin-Alkyne **14.**

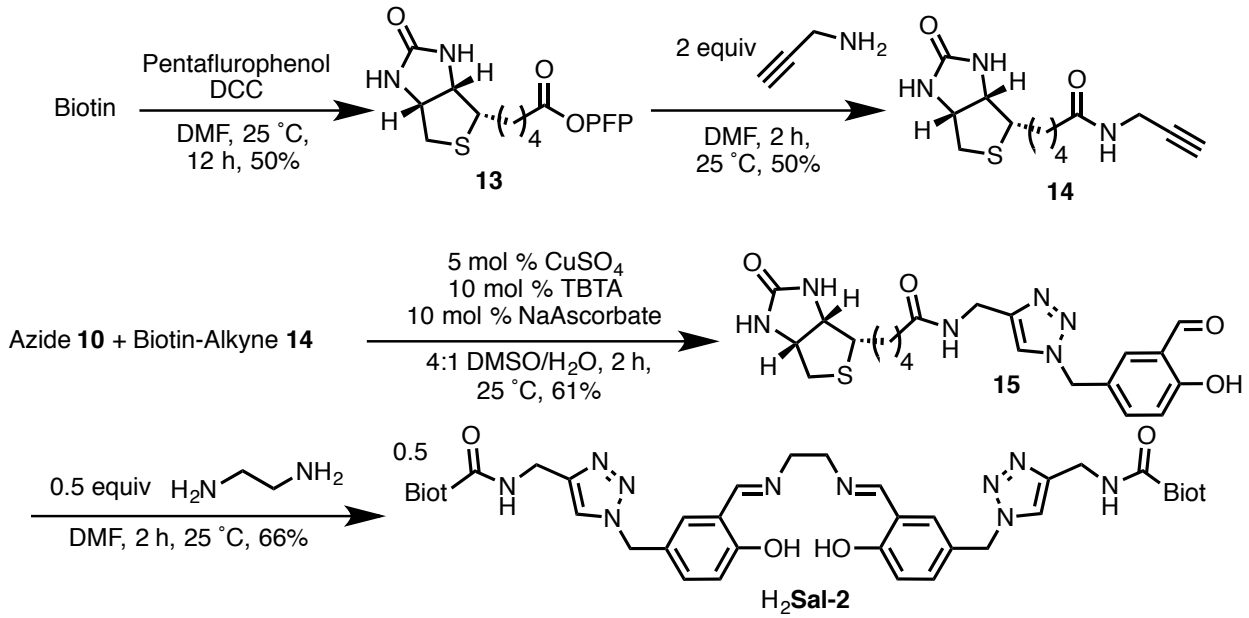

In collaboration with the Ward lab, the interaction of H_2**Sal-2** with Sav was modeled with VMD software, and the result suggested an excellent fit into the cavity. Additionally, the lysine 121 residues of two protein subunits are poised in fashion that could provide for primary or secondary coordination sphere interactions to a metal center (Figure 3-4). The computer model suggested that the developed system could potentially bind in the proposed fashion, so the next step was to prepare a starting metal complex for trials with Sav. Cu(II) was chosen because of its spectroscopic handles; Cu-Schiff base complexes feature distinct electronic characteristics that are evident by UV-vis spectroscopy, and EPR spectroscopy can be used because Cu(II) complexes are paramagnetic. To prepare the complex, H_2**Sal-2** was suspended in DMF and treated with an equivalent of $Cu(OAc)_2$ to generate the corresponding complex Cu(**Sal-2**) in quantitative yield. The electronic absorbance spectrum displayed a LCMT band at λ_{max}= 364 nm (ε = 3100 $M^{-1}cm^{-1}$), and a Cu(II) d-d band at λ_{max}= 585

nm (ε = 110 $M^{-1}cm^{-1}$). EPR spectroscopy gave a signal centered around $g_{\perp}$ = 2.06 G with four-line hyperfine. Both Uv-vis and EPR spectroscopy of the complex are consistent with known Cu(salen) species.[28,29]

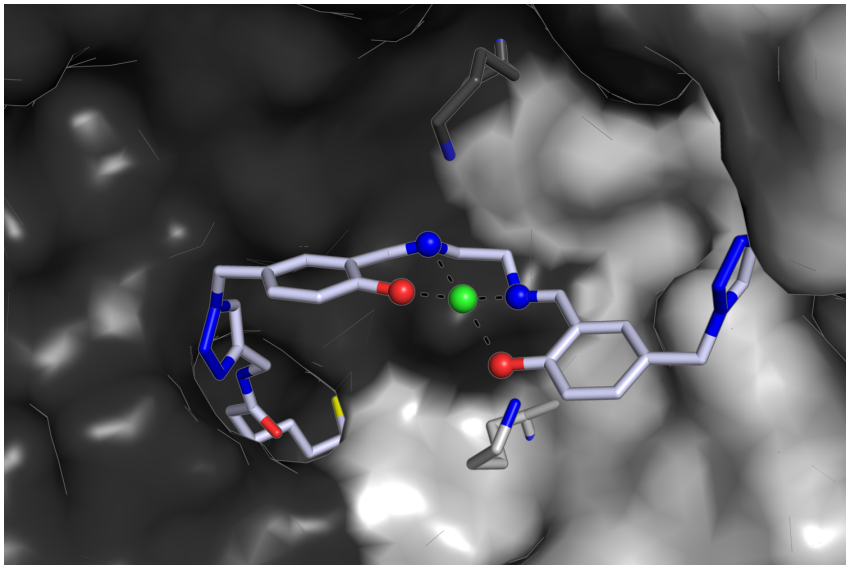

Figure 3-4 Qualitative computer model of **H_2Sal-2** bound to Sav. Two lysines are positioned in fashion to potentially interact with a metal complex. Green sphere represents approximate placing of a metal ion.

HABA Titrations

As previously described in Chapter 2 of this document, HABA titrations are the standard method for determining the binding ratios of biotinylated species to the biotin binding sites of streptavidin. Since our bis-biotinylated species contains two biotin moieties and Sav features four biotin binding sites, the working hypothesis is that Cu(**Sal-2**) should have a binding ratio of 2:1 complex to protein. HABA titrations were performed using solutions of Cu(**Sal-2**) in DMF and WT Sav in phosphate buffer. The binding ratio found required three equivalents of complex to occupy the four binding sites of one Sav tetramer (Figure 3-5). The data suggests that the binding mode is something other than what was predicted, with possible explanations being that

perhaps the bis-biotinylated species are crosslinking multiple Sav tetramers or they are too bulky to fully occupy one Sav tetramer.

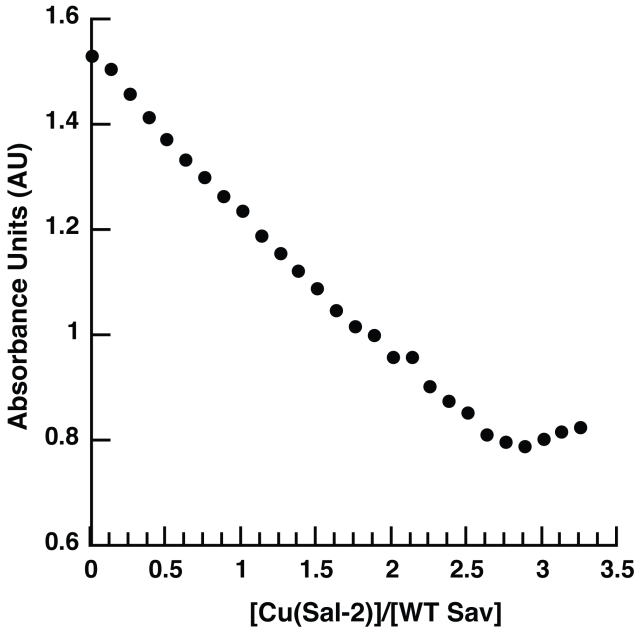

Figure 3-5 Haba titration of Cu(**Sal-2**) with WT Sav. Absorbance measured at 506 nm.

Protein Crystallography

We next sought to perform X-ray crystallographic studies in an attempt to gain further insight into the mode of binding of Cu(**Sal-2**) in Sav. Our collaborators in the Ward lab attempted protein crystallography with our compounds, H_2**Sal-2** and the corresponding Cu(II) complex. However, none of the conditions they explored for co-crystallization of the compound with Sav or soaking of the pre-formed Sav crystals with compound generated crystals that were of X-ray quality. While this evidence does not preclude the ability of the compounds to bridge Sav dimers as expected, it is consistent with multiple binding modes being present that could prevent a regular and ordered crystal lattice from forming.

SDS-Page

HABA titrations failed to reveal a clear correlation between the binding of the bis-biotinylated Salen species and streptavidin. One possible binding mode was for the two biotins from one complex to cross-link separate Sav tetramers. SDS-PAGE was performed using Cu(**Sal-2**) in solution with WT Sav.[32] The result of this experiment showed that even at low ratios of complex to protein, dimers and higher oligomers of streptavidin are observed (Figure 3-6). The experiment was performed with varying concentrations of Sav to determine if there is a concentration dependence of the oligomerization, however significant cross-linking is observed at both concentrations of Sav across all ratios of complex to Sav. It was proposed that two equivalents of ligand would saturate the binding sites of a Sav tetramer, it is evident that significant cross-linking is occurring. These data highlight the limitations of HABA titrations to give conclusive binding ratios, as numerous permutations of complex binding to Sav are possible.

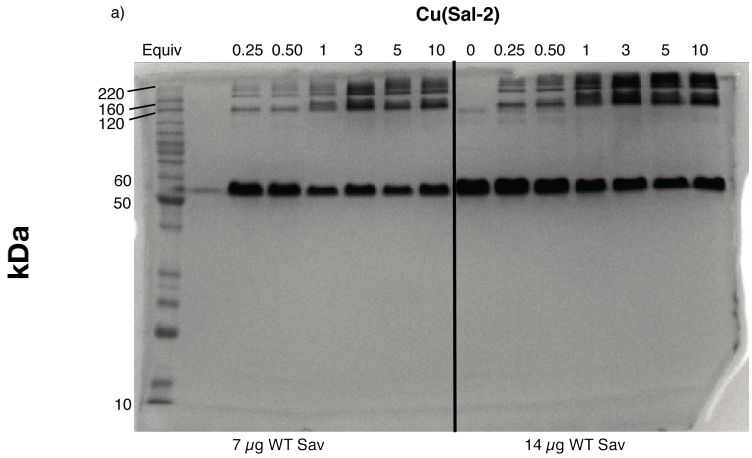

Figure 3-6 Image of SDS-Page of Cu(Sal-2) with WT Sav. Two different concentrations of Sav were used, and for each concentration the ratio of ligand to Sav was varied from 0.25:1 to 10:1. At lower ligand to Sav ratios, mostly monomeric Sav is observed at ~55 Kda. However, even some higher oligomers are observed at ~120 kDa and ~180 kDa. At higher ratios of ligand to Sav, significantly more of the cross-linked Sa is observed.

Conclusions

This investigation has developed a synthesis for the bis-biotinylated Schiff base, H_2**Sal-2**. A Cu(II) complex has been prepared and characterized, and the binding of the complexes to Sav has been studied by means of HABA titrations and gel electrophoresis. The ligand system was designed to bridge two binding sites of a Sav dimer, which would give a complex to Sav ratio of 2:1; two bis-biotinylated complexes to four binding sites. The data from the HABA titrations revealed higher binding ratios (ca 3:1), which suggested that the complexes could cross-link Sav tetramers to form dimers and other oligomers. This premise was supported by SDS-PAGE that revealed that even at low ratios of complex to Sav, various higher molecular mass species were present, which suggested that cross-linked species were present. The soaking method of protein crystallization failed to give crystals suitable for X-ray diffraction, and all attempts at co-crystallization with Sav and biotinylated compound yielded no crystals. Due to the failure of this ligand system to provide well-defined artificial metalloproteins, reactivity studies with organic substrates were not pursued.

A bis-biotinylated species that could link adjacent binding sites in a Sav dimer remains a tantalizing proposition, and a number modifications could be made on this system to make progress toward that goal. The triazole linker formed through CuAAC had been designed as a modular unit, but the size and rigidity of the triazole limits the modularity of the linker. The lack of flexibility of the triazole could contribute to the inability of H_2**Sal-2** and its complexes to bind to Sav as expected. Different alkyl linkers connected through amides or esters (see Chapter 2) could be probed to tune linker length. Additionally, formation of the Schiff-base after binding of a mono-biotinylated

salicylaldehyde could be investigated. This method may avoid cross-linked species, as the formation of the bis-biotinylated Salen species would occur after the binding of the mono-biotinylated species to Sav. Condensation using a linker, such as ethylene diamine, would more likely occur between two salicylaldehydes in a Sav dimer than between two Sav tetramers (Figure 3-5).

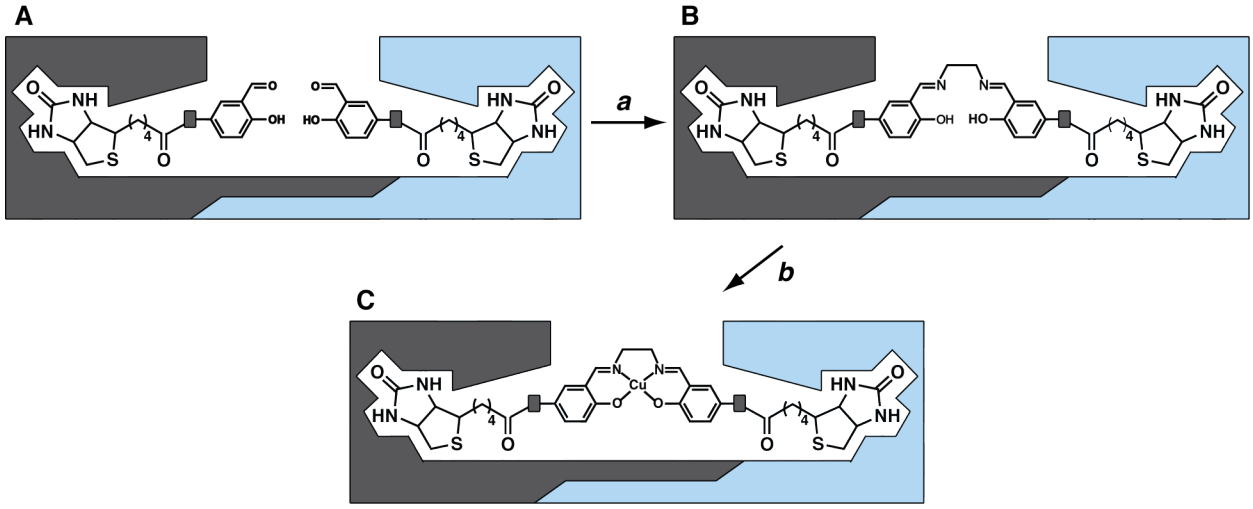

Figure 3-5 Proposed method of in situ formation of Cu(salen) complexes within the Sav dimer. A) Sav would be loaded with biotinylated salicylaldehyde. Treatment with ethylene diamine (a) could form the salen in Sav, and subsequent treatment with a Cu^{2+} source (b) would form the TM complex in solution.

Experimental Conditions.

General Experimental Details. All commercially available reagents were used as received except the following: dimethylsulfoxide, *N,N*-dimethylformamide, toluene, and ether were degassed with argon and dried by vacuum filtration through activated alumina according to the procedure by Grubbs.[33] Triethylamine, *N,N*-diisopropylethylamine, and ethylenediamine were distilled from CaH_2. Thin-layer chromatography (TLC) was performed on Whatman 250 μm layer 6 Å glass-backed silica gel plates. Eluted plates were visualized using either UV light, I_2, or potassium

permanganate stains. Silica gel chromatography was performed with the indicated solvent system using Fisher reagent silica gel 60 (230-400 mesh).

Instrumentation: Fourier Transform infrared spectra were collected on a Varian 800 Scimitar Series FTIR spectrometer. ^{1}H and ^{13}C,NMR spectra were recorded at 500/600 and 125 MHz, respectively. ^{1}H NMR spectra were reported in ppm on the δ scale and referenced to tetramethylsilane. The data are presented as follows: chemical shift, multiplicity (s = singlet, d = doublet, t = triplet, q = quartet, m = multiplet, br = broad, app = apparent), coupling constant(s) in Hertz (Hz), and integration. ^{13}C NMR spectra were reported in ppm relative to $CDCl_3$ (77.23 ppm) or DMSO (39.52 ppm). Mass spectra were measured on a MicroMass AutoSpec E, a MicroMass Analytical 7070E, or a MicroMass LCT Electrospray instrument. Electronic absorbance spectra were recorded with a Cary 50 spectrophotometer. X-band EPR spectra were collected using a Bruker EMX spectrometer equipped with an ER041XG microwave bridge.

Preparative Methods

General CuAAC Conditions

CuAAC Reactions with $CuSO_4$

Stock solutions of $CuSO_4$ were prepared fresh with deionized water. Sodium ascorbate was added as a solid. All reactions took place in in dry, screw-cap vials without the exclusion of air unless stated otherwise noted. See synthesis of triazole **12** for example conditions (*vida infra*).

CuAAC *Reactions with Cu(I) Precursors*

Cu(I) salts were stored in a drybox under an argon atmosphere. All reactions were conducted in oven-dried glassware under an N_2 atmosphere with rigorous exclusion of air.

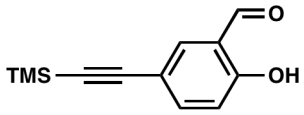

5-Trimethylsilyethynylsalicaldehyde (2).[25] To a mixture of 5-bromosalicylaldehyde (5.00 g, 24.9 mmol), $PdCl_2(PPH_3)_2$ (0.515 g, 0.734 mmol), and copper(I) iodide (0.153 g, 0.803 mmol) in 80 mL Et_3N, trimethylsilylacetylene (5.50 mL, 38.7 mmol) was added drop-wise via syringe pump over the course of 1 h. The mixture was heated to 80 ˚C and stirred for 3 h. After cooling, the mixture was filtered through a pad of Celite to remove the ammonium salts, and the crude residue was purified via column chromatography on silica gel with THF/hexanes (1:2) as eluent. Solvent was removed under reduced pressure and aldehyde **2** was afforded as a yellow solid (3.398 g, 62% yield). ^{1}H NMR (500 Mhz, $CDCl_3$) δ: 11.15 (s, 1H), 9.90 (s, 1H), 7.75 (d, 1H, *J* = 1.8 Hz), 7.65 (dd, 1H, *J* = 8.4, 1.8 Hz), 6.99 (d, 1H, *J* = 8.4 Hz), 0.29 (s, 9H).

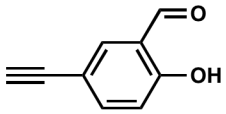

5-Ethynylsalicylaldehyde (3).[25] A methanol solution (50 mL) of aldehyde **2** (2.293 g, 10.50 mmol) and K_2CO_3 (1.454, 10.52 mmol) was stirred for 12 h at 25 ˚C. The resulting precipitate was filtered, and the solvent was removed under vacuum. To the residue

was added water and DCM (50 mL each). The resulting biphasic mixture was neutralized by addition of 10% aq NH_4Cl and 10% aq HCl. The aqueous layer was extracted twice more with 50 mL DCM, and the combined organic layers were washed with H_2O and brine, dried over MgSO4, and the solvent was removed in vacuo. The crude solid was purified via column chromatography with DCM/hexanes (1:2) as the eluent (r.f. = 0.24). Aldehyde **3** was afforded as an ivory solid (0.690 g, 45% yield). ^1H NMR (500 Mhz, $CDCl_3$) δ 11.13 (s, 1H), 9.87 (s, 1H), 7.72 (s, 1H), 7.63 (dd, 1H, *J* = 9.7, 1.1 Hz), 6.96 (d, 1H, *J* = 8.6 Hz), 3.04 (s, 1H).

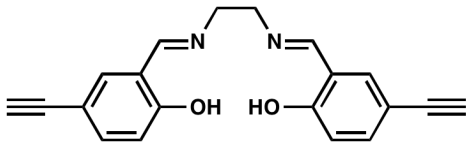

H_2(5-Ethynylsalen) (4): To a solution of 5-ethynylsalicylaldehyde (0.279 g, 1.91 mmol) in 5 mL EtOH was added ethylenediamine (59 µL, 0.87 mmol) with stirring. The reaction mixture was heated to 50 ˚C for ca 30 min, at which point a yellow precipitate formed. The precipitate was isolated via filtration, washed with ice cold ethanol and dried *in vacuo* to give salen **4** as a bright yellow solid (0.167 g, 61%).

^1H NMR (500 MHz, $CDCl_3$) δ 13.44 (s, 2H), 8.32 (s, 2H), 7.42 (app. dd, *J* = 8.6 Hz, 2H), 7.40 (app. d, 2H), 6.90 (d, *J* = 8.5 Hz, 2H), 3.96 (s, 4H), 2.98 (s, 2H); ^{13}C NMR (125 MHz, $CDCl_3$) δ 165.9, 161.7, 136.2, 135.5, 118.4, 117.6, 112.4, 75.8, 59.6; IR (KBr) 3295, 2963, 1638, 1484, 1384 cm^{-1}; HRMS (ES, MeOH) *m / z* calcd for $C_{20}H_{16}O_2N_2$ $[M + Na]^+$ 339.1110, found 339.1108.

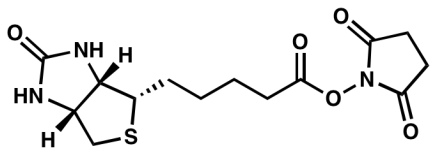

Biotin-succinimide ester (5) Biotin (2.6571 g, 10.876 mmol) and *N*-hydroxysuccinimide (1.2549g, 10.904 mol) were dissolved in hot DMF (75 mL) in a 500-mL round-bottom flask with stirring. *N*,*N*'-Dicyclohexylcarbodiimide (DCC) (2.91 g, 14.1 mmol) was added, and the solution was stirred overnight at room temperature, during which time a white precipitate was formed. The reaction mixture was filtered, and the filtrate was evaporated and triturated with ether. The white precipitate was filtered and washed with ether to give **5** a white powder (3.694 g, 99%). ^{1}H NMR (500 MHz, DMSO-d_6)DCl): δ 5.23 (s, 1H), 4.96 (s, 1H), 4.52 (m, 1H), 4.33 (m, 1H), 3.16 (m, 1H), 2.87-2.97 (m, 1H), 2.86 (s, 4H), 2.75 (d, 1H) 12.8 Hz), 2.58-2.70 (m, 2H), 1.6-1.9 (m, 4H), 1.5-1.6 (m, 2H).

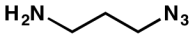

3-Azidopropyl-1-amine (**6**) was prepared according to the method of Sasake.[34] *Note: Low-molecular weight azides are extremely dangerous and provide significant risk of explosion. Although no complications arose in this study, such compounds should always be handled with great care.* A solution of 3-chloropropyl-1-amine (5.213 g, 40.09 mmol) and NaN_3 (7.843 g, 12.96 mmol), in water 40 mL, was heated at 80 ˚C for 15 h. Half of the water was removed under vacuum. The resulting solution was cooled in an ice bath and diethyl ether (50 mL) and KOH (2 g) were added, keeping the

temperature under 10 ˚C. After separation, the aqueous phase was extracted with diethyl ether (2 x 50 mL) The combined organic layers were dried with Na_2SO_4 and concentrated to give azide **6** in 41% yield (1.643 g). IR (thin film, cm^{-1}): 3368, 2941, 2872, 2518, 2098. ^1H NMR (500 MHz, $CDCl_3$) δ 3.38 (t, 2H, *J* = 6.7 Hz), 2.81 (t, 2H, *J* = 6.8 Hz), (p, 2H, *J* = 6.8 Hz), 1.32 (bs, 2H). ^{13}C (126 MHz, $CDCl_3$) δ 49.4, 39.5, 32.7.

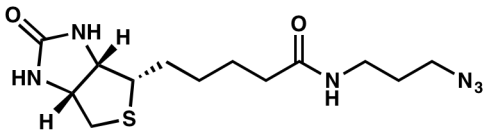

Biotin azide (7).[35] Succinimide **5** (1.071 g, 3.137mmol), azide **6** (0.433 g, 4.33 mmol), and triethylamine (0.78 mL) were suspended in 50 mL DMF and the reaction mixture was allowed to stir at 25 ˚C, under nitrogen, overnight. The reaction was filtered, and the filtrate concentrated to dryness. The residue was purified using flash chromatography eluting 10% MeOH/DCM to afford **7** (0.640 g, 63%) as waxy solid. R.f.: 0.50. ^1H NMR (500 Mhz, $CDCl_3$) δ 1.28 (q, 2H, *J* = 7.5 Hz), 1.50 (m, 4H), 1.62 (m, 2H, *J* = 6.9 Hz), 2.04 (t, 2H, *J* = 6.6 Hz), 2.57 (d, 1H , *J* = 12.9 Hz), 2.76 (dd, 1H, *J* = 13.2 Hz, 5.1 Hz), 3.01 (m, 1H), 3.11 (q, 2H, *J* = 6.0 Hz), 3.19 (t, 2H, *J* = 6.9 Hz), 4.15 (dd, 1H, *J* = 7.8 Hz, 4.5 Hz), 4.35 (dd, 1H, *J* = 7.8 Hz, 4.2 Hz), 7.21 (br, 1H).

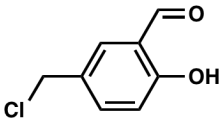

5-Chloromethyl-2-hydroxybenzaldehyde (9). To a stirred mixture of concentrated HCl (150 mL) and formaldehyde 37 wt% in H_2O (11 mL), salicaldehyde (15 mL, 141.49 mmol) was added drop-wise over approximately ten minutes. The solution

immediately turned bright yellow, and a fine precipitate gradually formed. The solid was filtered and dissolved in diethyl ether and concentrated. The crude material was recrystallized from hexanes to afford the product aldehyde **9** as white crystals (6.120 g, 25%). ^{1}H (500 MHz, $CDCl_3$) δ: 11.06 (s, 1H), 9.90 (s, 1H), 7.59 (d, 1H, *J* = 2.0), 7.50 (dd, 1H, *J* = 9.5 Hz, 2.0 Hz), 7.00 (d, 1H, 9.5 Hz) 4.59 (s, 2H).

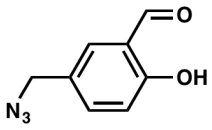

5-Azidomethyl-2-hydroxybenzaldehyde (10). Aldehyde **9** (2.840 g, 16.65 mmol) was dissolved in 5 ml dimethylformamide at room temperature. Then, sodium azide (2.175 g, 33.46 mmol) was slowly added while stirring. The reaction was monitored with TLC, and upon completion (ca 3 h), the mixture was diluted with 15 ml of water and extracted with ethyl acetate (3 × 10 ml). The combined organic extracts were washed successively with water (10 ml) and brine (10 ml). The organic layer was dried over anhydrous magnesium sulfate and the solvent evaporated under reduced pressure. The crude product was purified by column chromatography with ethyl acetate/hexanes (1:4) as eluent (rf = 0.39) to afford the product **10** as a pale orange oil in (2.262 g, 77%). ^{1}H and ^{13}C NMR spectra matched those previously reported for this compound.

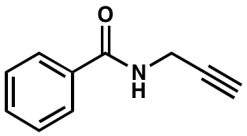

N-Prop-2-ynylbenzamide (11) was prepared according to the method of Wipf.[31] To a solution of 0.192 g (3.49 mmol) of propargyl amine in 8 mL DCM was added 0.5 g (4

mmol) of benzoyl chloride and 0.56 mL of triethyl amine at 0 ˚C. The reaction mixture was stirred at room temperature for 1 h, poured into 1.0 M HCl (50 mL), and extracted with DCM. The combined organic layers were washed with brine (100 mL), dried over magnesium sulfate, and concentrated under reduced pressure, and purifed via column chromatography (20% EtOAc in hexanes) to give the product in 70% yield (0.566 g). ^{1}H NMR (500, $CDCl_3$) δ 7.79 (d, 2 H, *J* = 7.3 Hz), 7.56-7.40 (m, 3 H), 6.35 (br, 1 H), 4.26 (dd, 2 H, *J* = 5.1, 2.5 Hz), 2.29 (t, 1 H, *J* = 2.4 Hz).

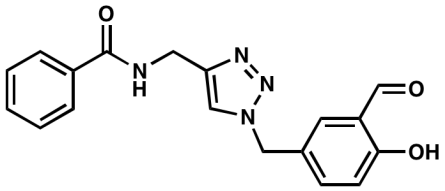

***N*-((1-(3-Formyl-4-hydroxybenzyl)-1H-1,2,3-triazol-4-yl)methyl)benzamide (12)** In a screw cap vial, Alkyne **11** (0.1157 g, 0.7269 mmol) and azide **10** (0.1295 g, 0.7310 mmol) were dissolved in 1 mL DMSO/H_2O (4:1). To this was added TBTA (0.173 mM in DMSO, 211 µL, 0.0365 mmol), sodium ascorbate (0.0191 g, 0.0964 g), and $CuSO_4$(aq) (0.108 mM, 337 µL, 0.0364 mmol). The vial was sealed, and the reaction was allowed to stir at room temperature for two hours while monitoring by TLC. The reaction mixture was added to H_2O (5 mL), and the resulting precipitate was collected on a frit, washed three times with diethyl ether, and dried under reduced pressure. Triazole **12** was collected as a yellow-green powder (0.124 g, 51%). MP 166-169 ˚C; ^{1}H (600 MHz, DMSO-d_6) δ 10.82 (bs, 1H), 10.25 (s, 1H), 9.00 (t, *J* = 5.4 Hz, 1H), 8.00 (s, 1H), 7.86 (d, *J* = 7.8, 2H), 7.66 (s, 1H), 7.53–7.50 (m, 2H), 7.45 (t, *J* = 9.6 Hz, 2H), 6.99, (d, *J* = 8.4 Hz, 1H), 5.75 (s, 1H), 5.50 (s, 2H), 4.49 (d, *J* = 6.0 Hz, 2H); ^{13}C NMR (125

MHz, DMSO-d_6) δ 190.6, 166.1, 160.6, 145.4, 136.3, 134.1, 131.3, 128.4, 128.3, 127.3, 127.2, 122.9, 122.2, 117.8, 51.8, 35.9; IR (KBr): v 3425, 3295, 3138, 3070, 2955, 2864, 1654, 1546, 1488, 1425, 1384, 1309, 1281, 1235, 1209, 1152, 787, 394 cm^{-1}; HMRS (ES, MeOH) *m / z* calcd for $C_{18}H_{16}N_4O_3$ $[M + Na]^+$ 359.1120, found 359.1120.

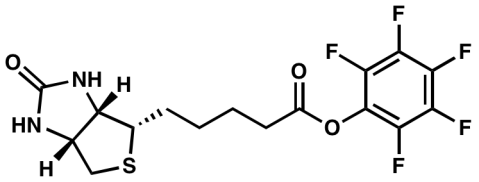

Biotin–PFP ester (13). Biotin-PFP ester was prepared as described in Chapter 2.

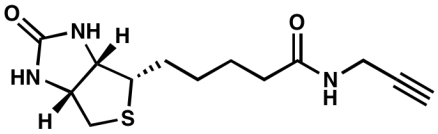

Biotin alkyne (14). Biotin Alkyne **14** was synthesized following the method of Hest.[36] To a solution of biotin-PFP (0.200 g, 0.487 mmol) and 66 uL propargyl amine (0.056 g, 1.0 mmol) in DMF was added 180 uL of triethyl amine (1.3 mmol) After being stirred for 24 h at room temperature, the reaction mixture was concentrated in vacuum and the resulting residue was diluted with DCM. The organic layer was washed with water, dried over sodium sulfate, and purified with column chromatography ($CHCl_3$/MeOH/H_2O 65:25:4) to give the product in 66% yield (0.090g). p.12185: Biotin 53 (40 mg, 0.16 mmol), propargylamine 41 (15 μL, 0.21 mmol), HATU (68 mg, 0.18 mmol), and HOBt monohydrate (27 mg, 0.18 mmol) were combined and dissolved in dry DMF (3 mL). DIPEA (85 μL, 0.50 mmol) was added, and the reaction was allowed to stir for 4 hours. The solvent was removed under reduced pressure to yield a crude oil

which and purified by column chromatography (CH2Cl2 to 12.5% MeOH/CH2Cl2) to yield 10 (34 mg, 74%), a white precipitate with limited organic solubility. ^{1}H NMR (500 MHz, DMSO-d_6) δ 8.21 (bs, 1H), 6.42 (s, 1H), 6.35 (s, 1H), 4.28 (t, *J* = 6.4 Hz, 1H), 4.10 (q, *J*= 3.2 Hz, 1H) 3.81 (d, *J* = 2.4 Hz, 2H), 3.06 (m, 1H), 2.80 (dd, *J*= 4.8, 12.4 Hz, 1H), 2.55 (d, *J* = 12.4 Hz, 1H), 2.06 (t, *J* = 7.2 Hz, 2H), 1.59-1.24 (m, 6H).

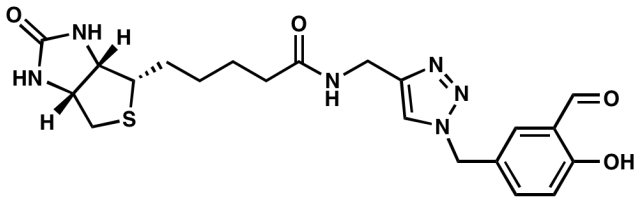

***N*-((1-(3-Formyl-4-hydroxybenzyl)-1H-1,2,3-triazol-4-yl)methyl)-5-((3aS,4S,6aR)-2-oxohexahydro-1H-thieno[3,4-d]imidazol-4-yl)pentanamide (15).** Aldehyde **15** was synthesized following the same procedure as triazole **12** (*vida supra*) and isolated as a light green-tinged powder, 61%. ^{1}H NMR (500 MHz, DMSO-d_6) δ 10.85 (bs, 1H), 10.26 (s, 1H), 8.26 (t, *J* = 5.3 Hz, 1H), 7.92 (s, 1H), 7.65 (d, *J* = 1.9 Hz, 1H), 7.49 (dd, *J* = 8.5, 1.9 Hz, 1H), 6.99 (d, *J* = 8.5 Hz, 1H), 6.42 (s, 1H), 6.37 (s, 1H), 5.49 (s, 2H), 4.30 (t, *J* = 7.1 Hz, 1H), 4.25 (d, *J* = 5.5 Hz, 2H), 4.11 (app. t, 1H), 3.08 (m, 1H), 2.81 (dd, *J* = 12.4, 5.02 Hz, 1H), 2.57 (d, *J* = 12.4, 1H), 2.54 (s, 1H), 2.07 (t, *J* = 7.4, 2H), 1.60–1.27 (m, 6H); ^{13}C NMR (125 MHz, DMSO-d_6) δ 190.6, 172.0, 162.7, 160.6, 145.4, 136.3, 128.3, 127.1, 122.6, 122.2, 117.8, 61.0, 59.2, 55.4, 51.8, 40.4, 35.0, 34.1, 28.2, 28.0, 25.2; IR (KBr pellet) 3358, 3307, 3070, 2940, 2836, 1701, 1682, 1653, 1644, 1617, 1546, 1449, 1253, 779 cm^{-1}. HRMS (ES, MeOH) *m* / *z* calcd for $C_{21}H_{26}N_6O_4S$ $[M+Na]^+$ 481.1634, found 481.1648.

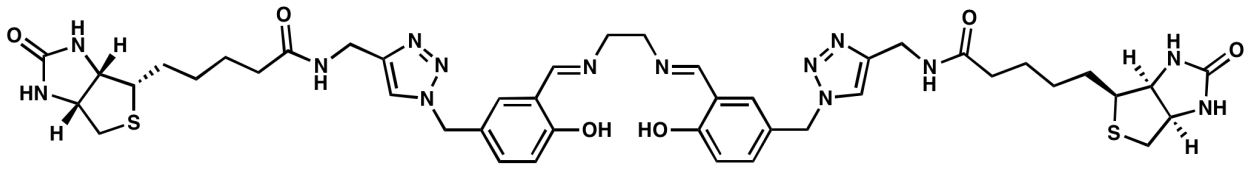

H_2Sal-2. Aldehyde **15** (0.0541 g, 0.118 mmol) was suspended in 1 mL DMF. To this was added ethylene diamine, (4.0 µL, 0.060 mmol) and the mixture was allowed to sir for two hours. The residue was collected on a fine frit, washed three times with diethyl ether, and allowed to dry under vacuum overnight. H_2**Sal-2** was collected as a light green powder (0.035 g, 66%). ^{1}H NMR (500 MHz, DMSO-d_6) δ 13.48 (bs, 2H), 8.57 (s, 2H), 8.25 (app. t, 2H), 7.89 (s, 2H), 7.44, (s, 2H), 7.31 (d, *J* = 7.9 Hz, 2H), 6.86 (d, *J* = 8.45, 2H), 6.42 (s, 2H), 6.37 (s, 2H), 5.47 (s, 4H), 4.29 (app. t, 2H), 4.25 (d, *J* = 5.0 Hz, 4H), 4.11 (app. t, 2H), 3.91 (s, 4H), 3.07 (m, 2H), 2.81 (dd, *J* = 12.6, 4.81 Hz, 2H), (d, *J* = 12.6 Hz, 2H), 2.01 (t, *J* = 7.3 Hz, 4H), 1.58–1.28 (m, 12H); NMR (125 MHz, DMSO-d_6) δ 172.5, 167.0, 163.2, 161.2, 145.8, 133.1, 132.0, 123.0, 118.8, 117.5, 61.5, 59.7, 59.0, 55.9, 52.6, 35.4, 34.6, 28.7, 28.5, 25.7; IR (KBr) 3422, 3286, 3080, 2926, 2858, 2392, 1696, 1638, 1497, 1384 cm^{-1}; HRMS (ES, MeOH) *m* / *z* calcd for $C_{44}H_{56}N_{14}O_6S_2$ [M + Na]$^+$ 963.3846, found 963.3853.

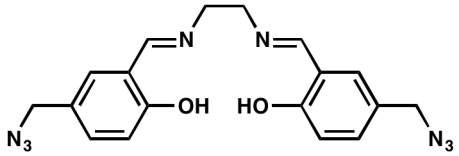

H_2(5-azidomethylsalen) (16). To a solution of azide **15** (0.102 g, 0.575 mmol) in 2.5 mL EtOH was added ethylenediamine (18 µL, 0.27 mmol). The reaction mixture was heated to 50 ˚C with stirring for 30 min. The resulting precipitate was isolated via vacuum filtration and washed with ice cold ethanol. Upon drying, **16** was afforded as a

bright yellow powder (0.071 g, 68%). ^{1}H NMR (600 MHz, $CDCl_3$) δ 13.26 (s, 2H), 8.37 (s, 2H), 7.25 (d, *J* = 1.8 Hz, 2H), 7.19 (d, *J* = 1.8, 2H), 6.96 (d, *J* = 8.4 Hz), 4.26 (s, 4H), 3.97 (s, 4H); ^{13}C (125 MHz, $CDCl_3$) δ 176.7, 166.4, 161.3, 132.8, 131.6, 125.8, 118.7, 117.8, 59.9, 54.4); IR (KBr) 3442, 3007, 2917, 2868, 2122, 1638, 1587, 1493 cm^{-1}; HRMS (m/z) calcd for $C_{18}H_{18}N_8O_2$ $[M + H]^+$ 379.1631, found 379.1630

Cu(Sal-2). H_2**Sal-2** (0.0098 g, 10 μmol) was dissolved in 300 μL H_2O/DMSO (1:1). To this was added $Cu(OAc)_2$ (0.0026 g, 13 μmol). The reaction mixture was heated to 65 ˚C and stirred for 2 h. The resulting precipitate was collected on a fine frit and washed successively with ice cold H_2O and diethyl ether (3x), and dried over night under reduced pressure. **Cu(Sal-2)** was afforded as a purple solid (0.010 g, 98%). IR (KBr) 3422, 3303, 2926, 2856, 1700, 1632, 1467, 1384, 1117, 1051; HRMS (m/z) calcd for $C_{44}H_{54}N_{14}O_6S_2Cu$ $[M + Na]^+$ 1024.2986, found 1024.2976; UV-vis λ_{max} (DMSO, nm (ε, $M^{-1}cm^{-1}$)): 364 (3100), 585 (110). EPR: (DMSO, 77 K), $g_{\perp}$ = 2.06 G, $g_{\parallel}$ = 2.21 G, A = 618 MHz (Figure 3-6).

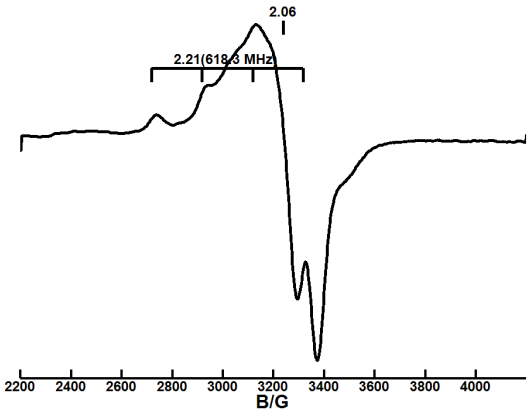

Figure 3-6 Perpendicular-mode X-band EPR spetrum of Cu(Sal-2) in DMSO at 77 K.

HABA Titrations. A solution of protein (1 mg/mL) was prepared in 200 mM phosphate buffer at pH 7 and transferred to a 1 cm cuvette. 150 equivalents of a 20 mM solution of HABA in phosphate buffer were added. A solution of metal complex in DMF was added in 4 μL portions until 5 equivalents had been added. The titration was monitored by UV-visible spectroscopy at λ_{max} = 506 nm.

References

1 R. L. Shook and A. S. Borovik, *Inorg. Chem.*, 2010, **49**, 3646–3660.
2 Y. Lu, N. Yeung, N. Sieracki and N. M. Marshall, *Nature*, 2009, **460**, 855–862.
3 Y. Lu, *Inorg. Chem.*, 2006, **45**, 9930–9940.
4 Y. Lu, *Angew. Chem. Int. Ed.*, 2006, **45**, 5588–5601.
5 J. R. Carey, S. K. Ma, T. D. Pfister, D. K. Garner, H. K. Kim, J. A. Abramite, Z. Wang, Z. Guo and Y. Lu, *J. Am. Chem. Soc.*, 2004, **126**, 10812–10813.
6 D. K. Garner, L. Liang, D. A. Barrios, J.-L. Zhang and Y. Lu, *ACS Catal.*, 2011, **1**, 1083–1089.
7 K. Oohora, S. Burazerovic, A. Onoda, Y. M. Wilson, T. R. Ward and T. Hayashi, *Angew. Chem. Int. Ed.*, 2012, **51**, 3818–3821.
8 M. E. Wilson and G. M. Whitesides, *J. Am. Chem. Soc.*, 1978, **100**, 306–307.
9 J. Pierron, C. Malan, M. Creus, J. Gradinaru, I. Hafner, A. Ivanova, A. Sardo and T. R. Ward, *Angew. Chem.*, 2008, **120**, 713–717.
10 C. Mayer, D. G. Gillingham, T. R. Ward and D. Hilvert, *Chem. Commun.*, 2011, **47**, 12068–12070.
11 C. Letondor, A. Pordea, N. Humbert, A. Ivanova, S. Mazurek, M. Novič and T. R. Ward, *J. Am. Chem. Soc.*, 2006, **128**, 8320–8328.
12 M. Dürrenberger, T. Heinisch, Y. M. Wilson, T. Rossel, E. Nogueira, L. Knörr, A. Mutschler, K. Kersten, M. J. Zimbron, J. Pierron, T. Schirmer and T. R. Ward, *Angew. Chem. Int. Ed.*, 2011, **50**, 3026–3029.
13 T. R. Ward, *Acc. Chem. Res.*, 2011.
14 M. R. Ringenberg and T. R. Ward, *Chem. Commun.*, 2011, **47**, 8470–8476.
15 J. Steinreiber and T. R. Ward, *Coord. Chem. Rev.*, 2008, **252**, 751–766.
16 M. Creus and T. R. Ward, *Org. Biomol. Chem.*, 2007, **5**, 1835–1844.
17 C. Letondor, *Proc. Natl. Acad. Sci. U.S.A.*, 2005, **102**, 4683–4687.
18 C. Letondor and T. R. Ward, *ChemBioChem*, 2006, **7**, 1845–1852.
19 M. Creus, A. Pordea, T. Rossel, A. Sardo, C. Letondor, A. Ivanova, I. LeTrong, R. E. Stenkamp and T. R. Ward, *Angew. Chem. Int. Ed.*, 2008, **47**, 1400–1404.
20 A. Pordea and T. R. Ward, *Chem. Commun.*, 2008, 4239.
21 G. Klein, N. Humbert, J. Gradinaru, A. Ivanova, F. Gilardoni, U. E. Rusbandi and T.

R. Ward, *Angew. Chem. Int. Ed. Engl.*, 2005, **44**, 7764–7767.
22 T. Katsuki, *Coord. Chem. Rev.*, 1995, **140**, 189–214.
23 N. S. Venkataramanan, G. Kuppuraj and S. Rajagopal, *Coord. Chem. Rev.*, 2005, **249**, 1249–1268.
24 J. F. Larrow and E. N. Jacobsen, *Organometallics in Process Chemistry*, 2004, 123–152.
25 K.-H. Chang, C.-C. Huang, Y.-H. Liu, Y.-H. Hu, P.-T. Chou and Y.-C. Lin, *Dalton Trans.*, 2004, 1731.
26 J. L. Meier, A. C. Mercer, H. Rivera and M. D. Burkart, *J. Am. Chem. Soc.*, 2006, **128**, 12174–12184.
27 M. Meldal and C. W. Tornøe, *Chem. Rev.*, 2008, **108**, 2952–3015.
28 M. M. Bhadbhade and D. Srinivas, *Inorg Chem*, 1993, **32**, 6122–6130.
29 A. Boettcher, H. Elias, E. G. Jaeger, H. Langfelderova, M. Mazur, L. Mueller, H. Paulus, P. Pelikan, M. Rudolph and M. Valko, *Inorg. Chem.*, 1993, **32**, 4131–4138.
30 Lwoski, W. Azides and Nitrous Oxide. In *1,3-Dipolar Cycloaddition Chemistry*, A. Padwa, Ed. Wiley, New York, 1984, 559–651.
31 P. Wipf, Y. Aoyama and T. E. Benedum, *Org. Lett.*, 2004, **6**, 3593–3595.
32 N. Humbert, A. Zocchi and T. R. Ward, *Electrophoresis*, 2005, **26**, 47–52.
33 A. B. Pangborn, M. A. Giardello, R. H. Grubbs, R. K. Rosen and F. J. Timmers, *Organometallics*, 1996, **15**, 1518–1520.
34 K. Onizuka, A. Shibata, Y. Taniguchi and S. Sasaki, *Chem. Commun.*, 2011, **47**, 5004–5006.
35 A. J. Lampkins, E. J. O'Neil and B. D. Smith, *J. Org. Chem.*, 2008, **73**, 6053–6058.
36 J. A. Opsteen, R. P. Brinkhuis, R. L. M. Teeuwen, D. W. P. M. Löwik and J. C. M. van Hest, *Chem. Commun*, 2007, 3136–3138.

CHAPTER 4

Investigation of a Transition Medal-Mediated C–H Bond Amination Reaction

I. Introduction

The ubiquity of C–H bonds in organic compounds leads them to be attractive targets for chemical transformations. However, the selective functionalization of unactivated C–H bonds remains a challenge for the modern synthetic chemist.[1-3] In recent years, great effort and significant progress have been made towards activating C–H bonds, especially in the field of metal-mediated functionalization. An important transformation that falls under this umbrella is the direct formation of C–N bond from C–H bonds, or C–H bond amination.[4] This family of transformations represents a valuable set of techniques that can be applied to the synthesis of natural products and biologically active compounds, many of which are nitrogen-containing species.[5]

Numerous methods have been developed to perform C–H bond aminations on unactivated substrates using transition metal catalysts. Several of the key contributors in this area include Du Bois (Rh)[6-9], White (Fe,[10] Pd[11-13]), Blakey (Ru[14-16]), Driver (Ir,[17] Rh[18-20]), Yu (Pd,[21,22] Cu [23,24]), Warren (Cu[25]), Cundari (Cu[26]), and Betley (Fe[27-30]). The substrate of these reactions usually contains an organic azide or sulfamate, which generates a metallonitrene when treated with a transition metal complex. These species are highly reactive and can insert into C–H bonds to form new C–N bonds. The transition metal

ion and the ligand framework around it are essential for tuning the reactivity, selectivity, and stereochemistry of the transformation.

One example is a system developed by the Blakey group that utilizes a chiral ruthenium(II) pybox (pybox = pyridine bisoxazoline) complex that can catalyze asymmetric intramolecular amination of benzylic and allylic C–H bonds using sulfamate ester substrates (Figure 4-1).[14-16] Blakey chose the pybox ligand framework for its modularity, which allows for rapid development of numerous ligand substitutions to optimize the reaction conditions as well as chiral options to investigate enantioselective transformations. Additionally, the neutral nature of pybox allows for cationic metal complexes, which would favor electrophilic metallonitrenes, which have been suggested to be the active oxidant in C–H amination reactions.[7]

Blakey proposes that a bis-ruthenium(VI) metallonitrene is the active species in the reaction, which is consistent with known ruthenium porphyrin chemistry.[31] Under Blakey's conditions, the sulfamate ester is oxidized to a nitrene by $PhI(O_2C\textit{t}Bu)_2$. Abstraction of a bromide by the addition of silver triflate (triflate = trifluoromethanesulfonate) from $[RuBr_2(C_2H_4)pybox]$ opens a coordination site cis to the pyridine of the pybox ligand and allows for the formation of the first metallonitrene. Dissociation of the ethylene ligand followed by isomerization of the remaining bromide opens a vacant site for the formation of the second metallonitrene. The bulky ligand enforces a specific orientation of the sulfamate ligand, causing the aromatic group of the substrate to orient away from the complex and positioning one of the two enantiotopic H-atoms in close proximity to the reactive metallonitrene (Figure 4-2).

H-atom abstraction followed by recombination of the new carbon-based with an electron from the metallonetrene (radical rebound) forms the new C–N bond. Under these conditions, benzylic and allylic C–H bonds were aminated with yields ranging from 42–71% and *ee* up to 92%. Both electron-donating and –withdrawing substituents off the aromatic ring were tolerated.

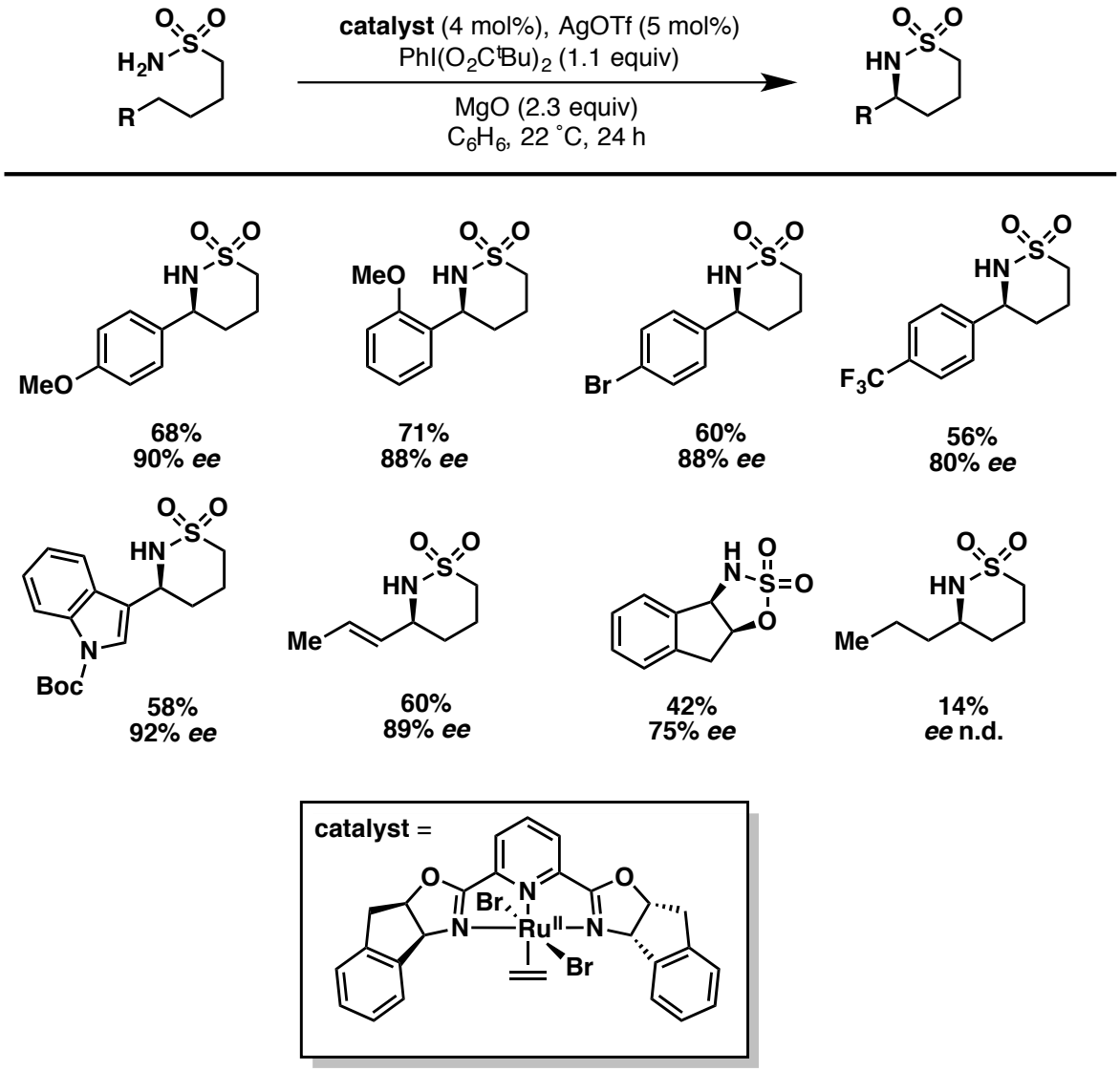

Figure 4-1. Blakey and co-works have demonstrated intramolecular C–H bond amination using a Ru-pybox catalyst with sulfonamide substrates.

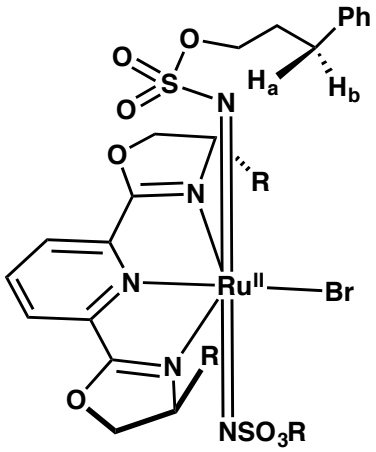

Figure 4-2. Stereochemical model for Blakey's Ru(pybox) catalyzed C—H bond amination reaction. The bulky R group off the pybox ligand causes the aromatic substituent of the substrate to orient away from the metal center and exposes one of the enantiotopic H-atoms toward the metallonitrene.

Organic azides have also proven to be useful substrates in C–H bond aminations and present several advantages over sulfamate esters. Sulfamate esters require sacrificial oxidants to form the metallonitrene and further deprotection to reveal the amine product, organic azides generate only N_2 as a byproduct and require no further deprotection.[32,33] The work of Driver and coworkers has shown $[(cod)Ir(OMe)]_2$ as a competent catalyst for intramolecular C–H amination of *ortho*-homobenzyl-substituted aryl azides (Figure 4-1). The reaction is sensitive to the electronic properties of the aryl azide. Electron-donating groups cause no reaction (Table 4-1, entry 1), whereas electron-withdrawing groups improve yield and selectivity (entries 3–7). The electronic properties of the homobenzylic aryl group did not greatly affect the reaction outcome (entries 8–10), and the reaction will not proceed with aliphatic or tertiary C–H (entries 11 and 12). Driver postulates the reaction proceeds through an Ir

metallonitrene which can abstract an H-atom and then form a C–N bond through radical rebound, or insert across the benzylic C–H bond in a concerted, two electron process.

Table 4-1. Scope of Driver's Ir-catalyzed indoline formation. Indole, the overoxidation product, is also shown.

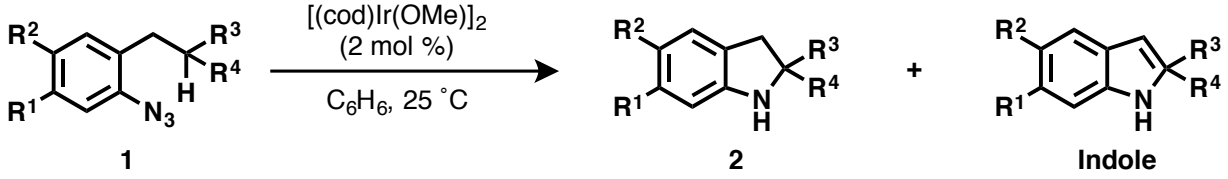

1 **2** **Indole**

Entry	**1**	**2** yield, %	Indole yield, %	Entry	**1**	**2** yield, %	Indole yield, %
1	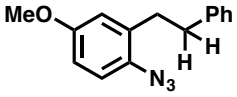	no reaction		7	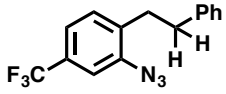	93	4
2	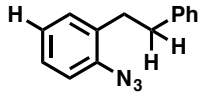	58	11	8	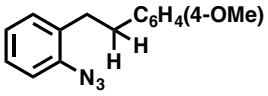	53	15
3	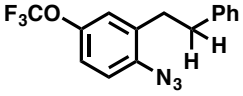	75	13	9	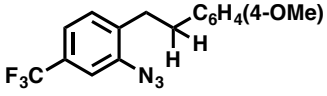	81	39
4	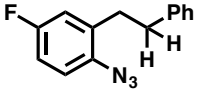	72	21	10	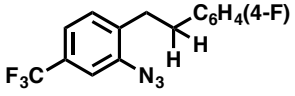	85	8
5	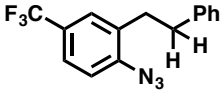	91	2	11	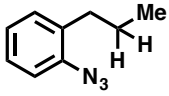	no reaction	
6	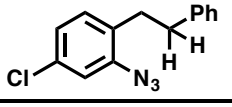	81	13	12	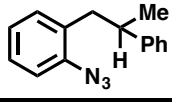	no reaction	

Both examples of C–H amination shown thus far are based off of precious metal catalysts (e.g. ruthenium and iridium). Although these and many other precious metal catalysts have rich chemistry and utility, they are limited by their cost and relatively low natural abundance. First row transition metals (TM) provide an attractive alternative, as they are far less expensive and earth-abundant. In contrast to second and third row TM, the first row metals have a tendency to react via one-electron processes, and while this is still is capable of promoting C–H amination pathways such as the step-wise H-atom abstraction followed by radical rebound, great care must be taken to avoid undesired functionalization of the ligand scaffold. For example, the Betley lab has demonstrated that an Fe^{II}(dipyrrinato) construct can activate organic azides and catalyze intramolecular C–H amination to form pyrrolidine products in good yield (Scheme 4-1).[27-30] Treatment of the pyrrolidine-coordinated complex with Boc_2O under elevated temperatures liberates the Boc-protected amine and allows the Fe complex to participate in successive catalytic cycles. This methodology can tolerate a variety of substitutions along the aliphatic chain and can be extended to the formation of piperidines and azetidines. The reaction is proposed to proceed through coordination of the azide to the iron center followed by extrusion of N_2. This intermediate forms a high spin (S = 5/2) Fe(III) center that antiferromagnetically couples to an imido radical (S = 1/2) to give an overall S = 2 ground state. It is this imido-radical character along both the π and σ components of the Fe–N bond that is proposed to promote the H–atom abstraction and subsequent radical recombination.

Scheme 4-1. Intramolecular C–H bond amination using an Fe(II) complex as a catalyst.

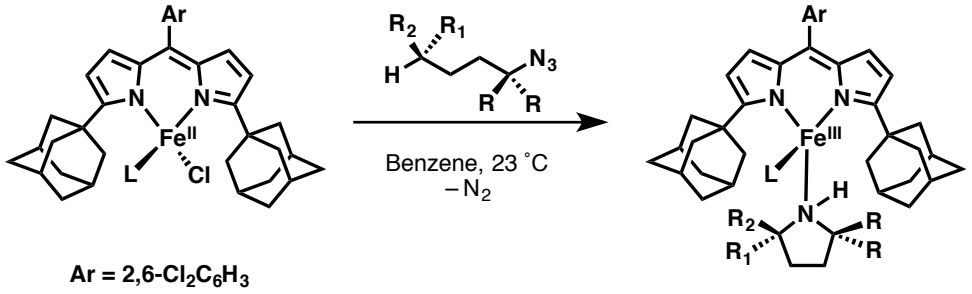

Ar = 2,6-$Cl_2C_6H_3$

R_1, R_2, R = **Ph, H, H**
C_2H_3, H, H
Me, Me, H
Et, H, H
H, H, Me

Previous Work Within this Group

The Borovik lab has not previously researched C–H amination reactions, however, prior studies within the lab have revealed TM complexes that react with aryl azides and generate C–H bond activation products. Previous group member Robie Lucas prepared the ferrous complex of the diurea monoamide scaffold, $[Fe^{II}(H_2dima)]^-$ and treated it with *p*-tolyl azide to generate a ferric amido complex whose molecular structure was confirmed by X-ray diffraction methods.[34] It was proposed that that the azide coordinated to the Fe(II) complex followed by extrusion of N_2 to generate an Fe(IV)-imido intermediate. This highly reactive species presumably abstracted an H-atom from a solvent molecule or the ligand to generate the stable $[Fe^{III}(H_2dima)NHTol]^-$ amido species (Scheme 4-3).

Scheme 4-2. Proposed mechanism for forming an Fe(III)-amido species via an Fe(IV)-imido intermediate.

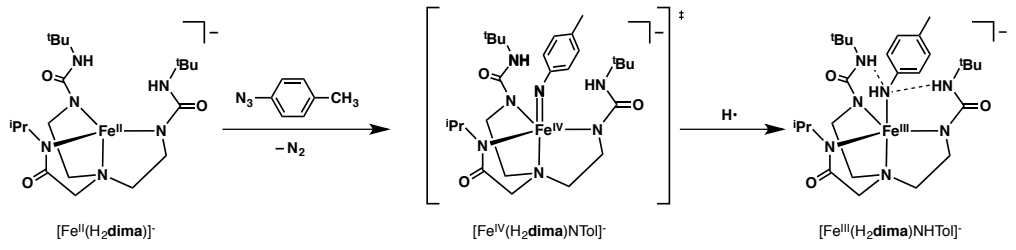

Lucas investigated the proposed mechanism of $[Fe^{II}(H_2\mathbf{dima})(HNTol)]^-$ formation by treating the Fe(II) starting compound with *p*-tolyl azide in the presence of external H-atom sources. Addition of 0.5 equiv of 1,2-diphenylhydrazine to the reaction of $[Fe^{II}(H_2\mathbf{dima})]^-$ with *p*-tolyl azide afforded the Fe(III)-amido product as well as azobenzene in 91% yield. The analogous reaction with half an equivalent of 9,10-dihydroanthrocene demonstrated intermolecular C–H bond activation to give small amounts of anthracene and the coupled product 9,9',10,10'-tetrahydro-9,9'-bianthracene; however, 73% of unreacted DHA was recovered (**Figure 4-3**). The results of Lucas's mechanistic study highlighted the ability of $[Fe^{II}H_2\mathbf{dima}]^-$ to perform C–H bond activation.

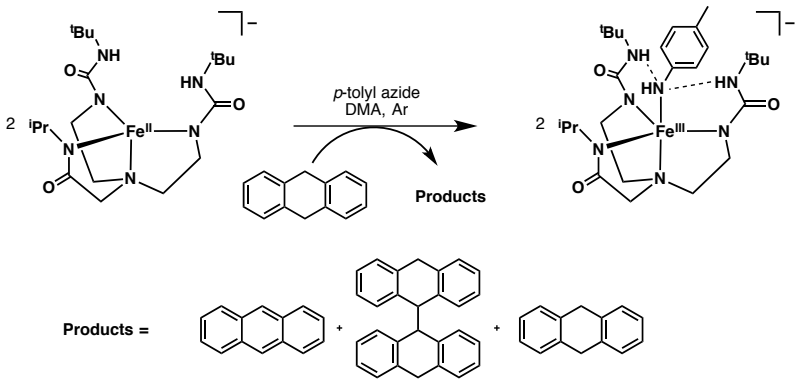

Figure 4-3. Formation of the Fe(III)-amido in the presence of an H-atom source demonstrates C–H bond activation.

This Study

This study focused on the application of Borovik group chemistry toward the goal of developing a C–H amination catalyst. This approach focuses on the use of H-bond donors or acceptors on a ligand, which can stabilize reactive intermediates, enhance reactivity, or directs the position of substrates. The ortho-homobenzyl aryl azide was selected as a substrate based on the success of the Driver group as well as the established precedent of the reactivity of Lucas's complexes with aryl azides.

In the initial phase of the research, the ligand **NAO** was prepared as an analog to pybox ligands and was screened with TM salts for reactivity with the aryl azide substrate. (Figure 4-4).[35] **NAO** was inspired by the ligand **TAO**, which had been previously developed in the Borovik lab as a neutral ligand capable of enforcing local three-fold symmetry around the metal ion and promoting intramolecular hydrogen bonding. By synthesizing **NAO** as a hybrid with one fewer arm, a binding environment similar to pybox-type ligands would be achieved. This was thought to be an advantage over **TAO** as it would allow sufficient binding sites for bis-metallonitrene species such as those proposed by Blakey. Although the **NAO** ligand as used lacks the chirality of pybox, it contributes H-bond donor groups, which could be useful in stabilizing reactive intermediates and studying reaction mechanisms.

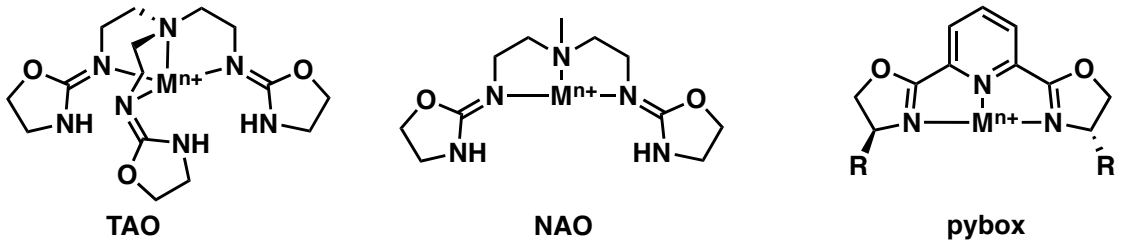

Figure 4-4. Comparison of the previously reported TAO, NAO (this work), and a generic pybox ligand.

The second phase of this study employed two ligands from the Borovik repertoire based on the platform used by Lucas. The first, H_6**buea**, has been previously shown to stabilize high-valent metal species, which would be useful in studying potential reaction intermediates such as the proposed Fe(IV)-imido species.[36-38] The second ligand precursor, H_3**0**, lacks the H-bonding capabilities of H_6**buea** and features a potentially more accessible cavity that would allow access for substrates (Figure 4-5).[39] The *ortho*-homobenzyl-subsituted aryl azide was selected because if the azide were to coordinate and extrude N_2 to form an Fe(IV) metallonitrene, a benzylic C–H bond would be poised for H-atom abstraction and subsequent radical rebound (Figure 4-6).

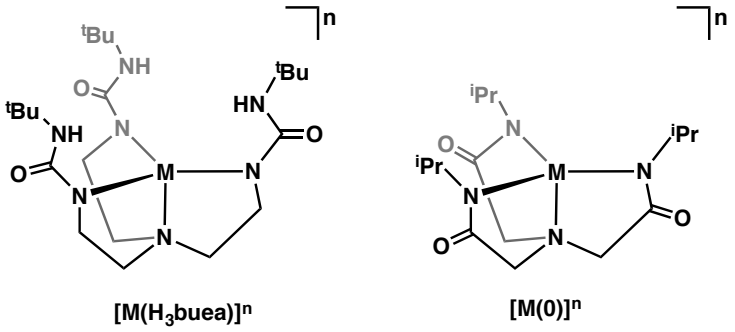

Figure 4-5. Generic TM complexes derived from H_6buea and H_30.

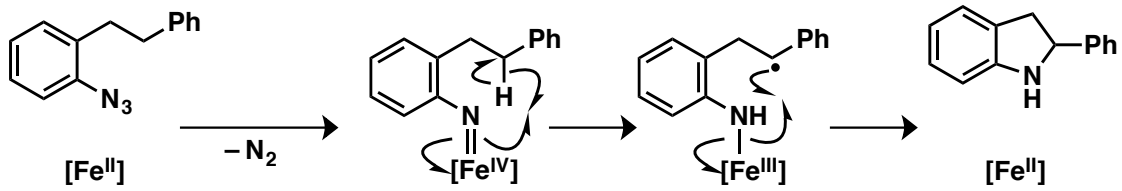

Figure 4-6. Proposed C–H amination pathway involving an Fe(II) catalyst.

II. Results and Discussion

Preparation of NAO

Initial studies focused on the use of the ligand **NAO** to prepare transition metal complexes capable of performing C–H bond amination reactions. **NAO** was readily synthesized in 76% yield over two steps (**Scheme 4-3**). *N,N*-(diaminoethyl)methylamine was treated with 1-chloro-2-isocyanatoethane in diethyl ether at 25 °C. A white powder precipitated immediately upon mixing, and **3** was isolated via filtration in 98% yield. Urea **3** was subsequently suspended in methanol and treated with an excess of $NaHCO_3$ under reflux in methanol. After filtering through a pad of Celite, the reaction mixture was concentrated *in vacuo* and heated to reflux in

methylene chloride (DCM) so as to remove the remaining bicarbonate salts from solution. **NAO** was collected as a pale yellow oil in yield of 89%.

Scheme 4-3. Preparation of NAO.

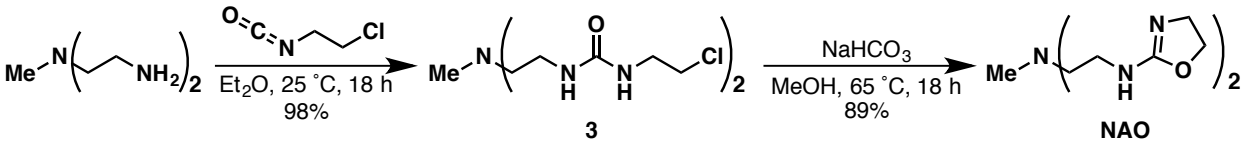

Substrate Synthesis

Azide **1** was prepared from a literature procedure in three steps from commercially available materials (Scheme 4-6).[17] 2-Nitrobromobenzene was subjected to Sonogoshira cross-coupling conditions with phenylacetylene, which afforded crude **4** as a deep, red-orange oil, which was purified by column chromatography in yields of up to 94%. Alkyne **4** was then dissolved in THF and reduced with hydrogen gas in the presence of catalytic amounts of Pd/C to furnish crude **5** in 90% yield. Aniline **5** was carried on without further purification in a diazotization-azidation sequence, affording crude **1**. Purification by column chromatography gave pure azide **1** as a yellow oil in 61% overall yield.

Scheme 4-4. Synthetic pathway for preparing azide 1.

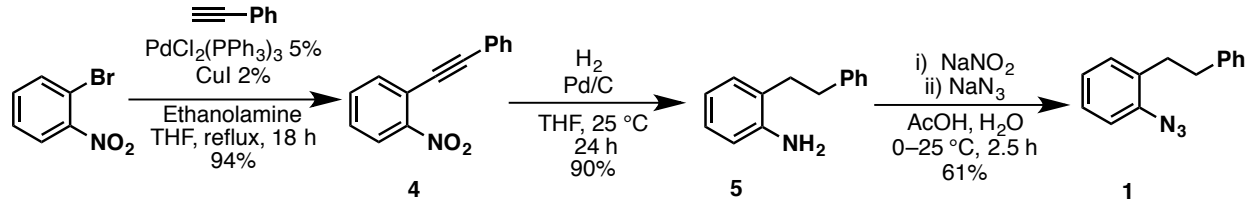

Catalyst Screens

In order to probe the viability of **NAO** as a ligand capable of supporting transition metal complexes in C–H amination reactions, catalyst screens were performed on a series of metal salts employing conditions similar to those used by Driver (Table 4-1). All reactions were prepared in a dry box under an argon atmosphere, sealed and then removed to atmospheric conditions. The reaction mixtures were heated to reflux for 18 h. Afterward the crude reaction mixture was filtered through a pad of Celite, and the solvent was removed *in vacuo*. The resulting residue was analyzed by ^{1}H NMR spectroscopy. Product ratios were calculated based on the comparison of the indoline **2** NH peak at ~4.9 ppm, the aniline **12** aliphatic CH_2 signal at ~2.79 ppm, and the aliphatic CH_2 signal of azide **1** starting material at ~2.87 ppm.

Table 4-2 Catalyst screen results

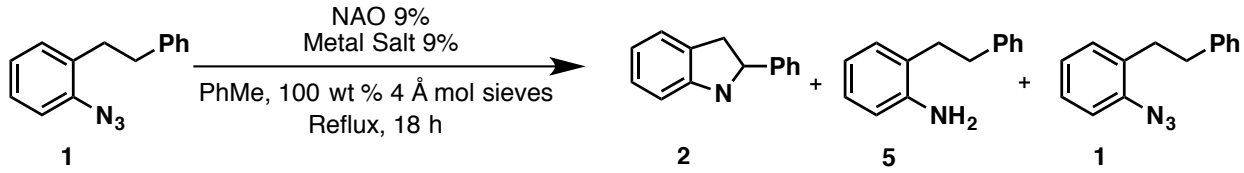

Entry	Metal Salt	Ligand	Product Ratio [%] (2:5:1)[a]
1	$Co(OAc)_2$	NAO	no reaction
2	$Mn(OAc)_2$	NAO	no reaction
3	$MnCl_2$	NAO	no reaction
4	$FeSO_4 \cdot H_2O$	NAO	no reaction
5	$Cu(OAc)_2$	NAO	no reaction
6	$Ni(OAc)_2$ [b]	NAO	no reaction
7	$NiBr_2$ [b]	NAO	no reaction
8	$RuCl_3 \cdot 3H_2O$	NAO	0:42:68
9	$RuCl_2(PPh_3)_3$	NAO	71:18:12
10	$RuCl_2(PPh_3)_3$	none	73:20:06

[a] As determined by NMR Spectroscopy [b] MeOH used as solvent

Nine different metal salts were screened, of which only two ruthenium salts displayed any reactivity under the test conditions (Table 4-2). $RuCl_3 \cdot 3H_2O$ and $RuCl_2(PPh_3)_3$ gave partial conversion to aniline **5** (entries 8 and 9), and $RuCl_2(PPh_3)_3$ also produced target indoline **2** (entry 9). However, control reactions with $RuCl_2(PPh_3)_3$ alone under the same reaction conditions (Entry 10, Table 1) afforded the same products as the previous ruthenium tests with slightly improved yield of indoline **2**, demonstrating that **NAO** does not significantly affect the reaction. This result is supported by the work Jia which demonstrates ruthenium salts are capable of performing similar reactions with *o*-aryl phenylazides to form carbazoles via a ruthenium nitrenoid intermediate.[40] When azide **1** was subjected to the test conditions with **NAO** in absence of metal, no reaction was observed. Moreover, when azide **1** was heated to reflux in toluene in the absence of both **NAO** and any metal salt, only starting material was recovered.

Investigation of urea and carboxamide based ligands

Based on the precedent within the Borovik group of tripodal Fe(II) systems capable of reacting with aryl azides, first row TM complexes of tripodal urea and carboxamide based ligands were investigated as reagents for C–H amination. The pre-ligand (H_6**buea** or H_3**0)** was deprotonated in the dry box with three equivalents of KH in DMA and metallated with $Fe^{II}(OAc)_2$ or $Mn^{II}(OAc)_2$ (Scheme 4-7)). After filtration of two equivalents of potassium acetate, the resulting pale yellow solution was treated with an equivalent of the substrate in a DMA stock solution. In the case of systems using the urea-based H_6**buea**, the reaction mixture would immediately turn dark amber.

However, when the analogous carboxamide H_3**0** system was treated with substrate, the reaction mixture would quickly turn dark blue-green, and then over the span of five to ten minutes would become the same dark amber, which is consistent with Lucas's observations in the formation of putative Fe(IV) imido species—the proposed reactive intermediate along the C–H amination pathway.[34] The solvent was removed *in vacuo* with the aid of diethyl ether as a coevaporator. The crude residue was taken up in $CDCl_3$ and passed through a plug of Celite before being analyzed by ^{1}H NMR spectroscopy for organic products. In no case was there any evidence of formation of indoline **2**. The Fe(II) systems gave partial conversion of the starting material to the aniline **5** decomposition product. The corresponding Mn(II) system bearing the carboxamidate **0** gave a modest conversion to the aniline; however, the analogous $[Mn^{II}(H_3\textbf{buea})]^-$ complex was completely unreactive towards azide **1.**

The urea-based ligand system is limited to DMA as a solvent because it decomposes in other media, but the salt of $[Fe^{II}(\textbf{0})]^-$ can be isolated after metallation and then be taken up in acetonitrile (CH_3CN), dichloromethane (DCM), or dimethylformamide (DMF) for treatment with azide **1**. The complex was only sparingly soluble in DCM, and no transformation was observed. CH_3CN and DMF provided for slightly enhanced degradation of the starting azide into the corresponding aniline. The observation of aniline is suggestive of the formation of a metallonitrene in situ. If formation of an Fe(IV)-imido occurs followed by H-atom abstraction from the solvent or intramolecularly from the substrate to form an Fe(III)-amido, a second H-atom abstraction event in situ or from the reaction work-up would form the aniline. This is

suggestive that ligand environment around the metal center in both $[Fe^{II}(H_3\textbf{buea})]^-$ and $[Fe^{II}(\textbf{0})]^-$ is too crowded to allow the approach of the benzylic C–H bond to the reactive metallonitrene. Additionally, it could indicate that the reduction back to an Fe(II) center to facilitate the bond formation is two difficult; the ligands are designed to stabilize high-valent metal centers.

Scheme 4-5. In situ formation of Mn and Fe complexes with H_6buea or $H_3$0 followed by addition of azide 1 afforded aniline 5 in addition to starting material.

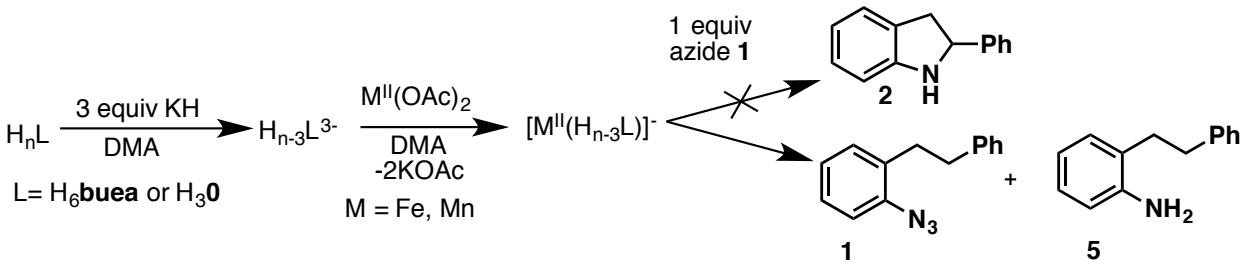

Table 4-3. Results of Fe(II) and Mn(II) chemistry.

Entry	Metal Salt	Ligand	Solvent	Product Ratio, % (**1**:**5**)[a]
1	$Fe(OAc)_2$	H_3**0**	DMA	48:52
2	$Fe(OAc)_2$	H_3**0**	DMF	66:34
3	$Fe(OAc)_2$	H_6**buea**	DMA	55:45
4[b]	$Fe(OAc)_2$	H_3**0**	CH_3CN	38:62
5[b]	$Fe(OAc)_2$	H_3**0**	DCM	no reaction
6[b]	$Fe(OAc)_2$	H_3**0**	DMF	47:53
7	$Mn(OAc)_2$	H_3**0**	DMA	42:68
8	$Mn(OAc)_2$	H_6**buea**	DMA	no reaction

a As determined using 1H NMR spectroscopy. b Metal complex isolated from DMA and redissolved in indicated solvent before treatment with substrate.

III. Conclusions

The ligand **NAO** was combined with various transition metal salts in an effort to generate conditions for C–H amination suitable for transforming *ortho*-homobenzyl aryl azide **1** into indoline **2**. Initial screens with first row transition metal salts provided none of the desired reactivity. $RuCl_3 \cdot 3H_2O$ and $RuCl_2(PPh_3)_3$ exhibited reactivity with azide **1** both in the presence and the absence of NAO, however this is a previously demonstrated transformation.

The chemistry of Fe(II) and Mn(II) complexes bearing tripodal anionic ligands was also explored. Although there is precedence of these Fe(II) complexes performing C–H activation, the experimental results suggest that this system is not amenable to the intramolecular cyclization of phenthylazobenzene **1**. Variation of solvent and use of Mn(II) in place of Fe(II) demonstrated little to no improvement.

IV. Experimental

General Procedures

^1H NMR and ^{13}C NMR spectra were recorded at ambient temperature at 500 MHz and 125 MHz, respectively, on a Bruker DRX500 NMR instrument. ^1H and ^{13}C NMR data are reported as follows: chemical shifts are reported in ppm on a δ scale and referenced to internal tetramethylsilane or residual solvent (TMS: δ 0.00; $CHCl_3$: δ 7.27), multiplicity (s = singlet, bs = broad singlet) d = doublet, t = triplet, q = quartet), coupling constants (Hz), and integration. Liquid chromatography was performed using forced flow (flash chromatography) of the indicated solvent system on Sorbent

Technologies silica gel (SiO_2) 60 (230–400 mesh). High-resolution mass spectra (HRMS) were recorded on a Waters LCT Premier quadrupole time-of-flight spectrometer and were obtained by peak matching. Gas chromatography/mass spectrometry (GC/MS) was performed with a Waters GCT Premier orthogonal acceleration time-of-flight spectrometer using chemical ionization. Fourier transform infrared spectra were collected on a Varian 800 Scimitar Series FTIR spectrometer. Preparation of ligand was performed in oven-dried glassware under atmospheric conditions. The synthesis of substrate and all intermediates was performed under an atmosphere of nitrogen in glassware that had been oven-dried. The preparation of all catalysis screening reactions was performed in a Vacuum Atmospheres, Co. dry box under an argon atmosphere. All reagents were purchased from commercial sources and used as received, unless otherwise noted. Solvents were sparged with argon and dried over columns containing Q-5 and molecular sieves. Ligands H_6**buea** and H_3**0** were obtained from Dr. David C. Lacy.

Ligand Synthesis

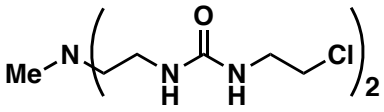

Ligand Precursor 12. To a 500 mL round-bottom flask containing N,N-(diaminoethyl)methylamine (1.06 g, 9.01 mmol) in diethyl ether (100 mL) was added 2.2 equiv 1-chloro-2-isocyanatoethane (2.10 g, 19.9 mmol) dissolved in diethyl ether (100 mL) via dropwise addition. Upon mixing, a white solid precipitated. After allowing the reaction mixture to stir overnight, the white solid was collected on a glass frit, washed

with diethyl ether (50 mL), and dried under reduced pressure to yield **12** (98%): mp 92–95 °C. ^{1}H NMR (500 MHz, $CDCl_3$) δ 5.64 (t, *J* = 5.5, 2H), 5.55 (bs, 2H), 3.63 (t, *J* = 5.5, 4H), 3.56 (q, *J* = 5.4), 3.27 (q, *J* = 5.0, 4H), 2.52 (bt, *J* = 5.0, 4H), 2.29 (s, 3H); ^{13}C NMR (500 MHz, $CDCl_3$) δ 159.1, 57.6, 45.5, 42.9, 42.4, 38.3; FTIR (KBr pellet) 3333, 2959, 1703, 1623, 1575, 1568, 1481 cm^{-1}; HRMS (ESI) *m* / *z* calcd for $C_{11}H_{23}O_2N_5Cl_2H$ $(M + H)^+$ 328.1307, found 328.1307.

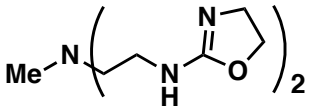

Preparation of *N*-methyl(2-amino-oxazoline) (NAO) compound 13. Compound **12** (2.90 g, 8.83 mmol) and $NaHCO_3$ (3.01 g, 35.8 mmol) were suspended in MeOH (100 mL) and heated to 90 °C (silicon oil bath) overnight. The reaction mixture was initially clear with some insoluble $NaHCO_3$, but over 1-3 h additional salts precipitated. Upon completion of reaction, the precipitate was removed via frit filtration, and the filtrate was concentrated *in vacuo* to give a viscous white residue. This residue was dissolved in CH_2Cl_2 (100 mL) and brought to reflux for ca 1 h to extract the product from the residue. Upon cooling, the resulting solution was filtered through a pad of Celite. The pale yellow filtrate was evaporated under reduced pressure to give **13** (**NAO**) as an extremely viscous pale yellow oil (89%): ^{1}H NMR (500 MHz, $CDCl_3$) δ 4.63 (bs, 2H), 4.26 (t, *J* = 8.5, 4H), 3.78 (t, *J* = 8.5, 4H), 3.28 (t, *J* = 5.5, 4H), 2.54 (t, *J* = 6.0), 2.23 (s, 3H); ^{13}C NMR (500 MHz, $CDCl_3$) δ 161.8, 77.4, 68.1, 56.7, 53.0, 41.9, 40.6; FTIR (thin film) 3436, 2972, 2881, 2807, 2208, 1668, 1517 cm^{-1}; HRMS (ESI) *m* / *z* calcd for $C_{11}H_{21}O_2N_5H$ $(M + H)^+$ 256.1773, found 256.1769.

Substrate Synthesis[17,40]

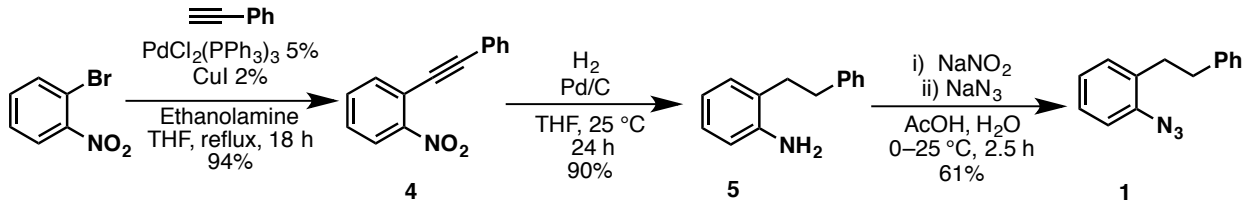

Azide **1** and all intermediates were prepared according to literature procedures from the Driver lab and Murata and coworkers.

Procedure for Catalysis Screens with NAO

In a 0.5 mL conical screw cap reaction vessel, metal salt (9 mol%), 4 Å molecular sieves (100 wt%), and toluene (0.24 mL) were weighed out in a dry box under an atmosphere of argon. To this was added ligand NAO in toluene (9 mol%, 0.029 mM), followed by 1 equiv of azide **1** via syringe. The vial was sealed and removed to atmospheric conditions. The reaction vessel was heated to reflux in a sand bath. After heating overnight, the reaction mixture was cooled to room temperature and solids were removed via filtration through a pipette column of Celite. The resulting crude solution was dried *in vacuo*. The residue was taken up in $CDCl_3$ and analyzed with ^1H NMR. The areas of the N-H signal in **2**, the aliphatic C-H signal in **5**, and the aliphatic C-H signal in **1** were compared to determine the ratio of products.

General Procedure for M(II) Chemistry

To a solution of H_6**buea** (0.387 g, 0.0872 mmol) in DMA (5 mL) in a 20 mL scintillation vial was added 3 equiv KH (0.102 g, 0.254 mmol) in a dry box under an atmosphere of

argon. Vigorous bubbling ensued as H_2 gas evolved, causing the reaction mixture to become opaque. Once the bubbling ceased (ca 1 h), $Fe^{II}(OAc)_2$ (0.015 g, 0.087 mmol) was added to the reaction mixture, resulting in the precipitation of KOAc. The solid was removed via filtration through a glass frit, and the resulting pale yellow filtrate was collected in a second 20 mL scintillation vial. To this was added azide **1** in DMA (0.31 μL, 0.28 M). The reaction mixture immediately turned deep amber. After 1 h, the reaction mixture was concentrated *in vacuo*, and the residue was washed portion-wise with diethyl ether (3 x 2 mL) until all remaining DMA was removed and a red-brown powder remained. The powder was suspended in diethyl ether (5 mL) and was filtered through a glass frit to give a pale yellow filtrate. This solution was evaporated under reduced pressure, and the residue was dissolved in $CDCl_3$ and analyzed by ^1H NMR spectroscopy for C–H amination reaction products.

References

1 J. A. Labinger and J. E. Bercaw, *Nature*, 2002, **417**, 507–514.
2 R. G. Bergman, *Nature*, 2007, **446**, 391–393.
3 A. E. Shilov and G. B. Shul'pin, *Chem. Rev.*, 1997, **97**, 2879–2932.
4 T. G. Driver, *Nature Chem*, 2013, **5**, 736–738.
5 C. Kibayashi, *Chem. Pharm. Bull.*, 2005, **53**, 1375–1386.
6 D. N. Zalatan and J. Du Bois, *J. Am. Chem. Soc.*, 2009, **131**, 7558–7559.
7 K. W. Fiori and J. Du Bois, *J. Am. Chem. Soc.*, 2007, **129**, 562–568.
8 C. G. Espino, K. W. Fiori, M. Kim and J. Du Bois, *J. Am. Chem. Soc.*, 2004, **126**, 15378–15379.
9 K. W. Fiori, C. G. Espino, B. H. Brodsky and J. Du Bois, *Tetrahedron*, 2009, **65**, 3042–3051.
10 S. M. Paradine and M. C. White, *J. Am. Chem. Soc.*, 2012, **134**, 2036–2039.
11 G. T. Rice and M. C. White, *J. Am. Chem. Soc.*, 2009, **131**, 11707–11711.
12 S. A. Reed and M. C. White, *J. Am. Chem. Soc.*, 2008, **130**, 3316–3318.
13 K. J. Fraunhoffer and M. C. White, *J. Am. Chem. Soc.*, 2007, **129**, 7274–7276.
14 D. G. Musaev and S. B. Blakey, *Organometallics*, 2012, **31**, 4950–4961.
15 S. B Blakey and J. L Bon, *Heterocycles*, 2012, **84**, 1313.
16 E. Milczek, N. Boudet and S. Blakey, *Angew. Chem. Int. Ed.*, 2008, **47**, 6825–6828.

17 K. Sun, R. Sachwani, K. J. Richert and T. G. Driver, *Org. Lett.*, 2009, **11**, 3598–3601.
18 C. Jones, Q. Nguyen and T. G. Driver, *Angew. Chem. Int. Ed.*, 2014, **53**, 785–788.
19 Q. Nguyen, K. Sun and T. G. Driver, *J. Am. Chem. Soc.* 2012, **134**, 7262–7265.
20 C. Kong, N. Jana and T. G. Driver, *Org. Lett.*, 2013, **15**, 824–827.
21 T.-S. Mei, X. Wang and J.-Q. Yu, *J. Am. Chem. Soc.*, 2009, **131**, 10806–10807.
22 E. J. Yoo, S. Ma, T.-S. Mei, K. S. L. Chan and J.-Q. Yu, *J. Am. Chem. Soc.*, 2011, **133**, 7652–7655.
23 M. Shang, H.-L. Wang, S.-Z. Sun, H.-X. Dai and J.-Q. Yu, *J. Am. Chem. Soc.*, 2014, **136**, 11590–11593.
24 M. Shang, S.-Z. Sun, H.-X. Dai and J.-Q. Yu, *J. Am. Chem. Soc.*, 2014, **136**, 3354–3357.
25 Y. M. Badiei, A. Krishnaswamy, M. M. Melzer and T. H. Warren, *J. Am. Chem. Soc.*, 2006, **128**, 15056–15057.
26 T. R. Cundari, A. Dinescu and A. B. Kazi, *Inorg Chem*, 2008, **47**, 10067–10072.
27 E. T. Hennessy and T. A. Betley, *Science*, 2013, **340**, 591–595.
28 E. T. Hennessy, R. Y. Liu, D. A. Iovan, R. A. Duncan and T. A. Betley, *Chem. Sci.*, 2014, **5**, 1526–1532.
29 E. R. King, E. T. Hennessy and T. A. Betley, *J. Am. Chem. Soc.*, 2011, **133**, 4917–4923.
30 E. R. King and T. A. Betley, *Inorg Chem*, 2009, **48**, 2361–2363.
31 S. K.-Y. Leung, W.-M. Tsui, J.-S. Huang, C.-M. Che, J.-L. Liang and N. Zhu, *J. Am. Chem. Soc.*, 2005, **127**, 16629–16640.
32 H. M. L. Davies and J. R. Manning, *Nature*, 2008, **451**, 417–424.
33 S. Cenini, E. Gallo, A. Caselli and F. Ragaini, *Coord. Chem. Rev.,* 2006, **250**, 1234–1253.
34 R. L. Lucas, D. R. Powell and A. S. Borovik, *J. Am. Chem. Soc.*, 2005, **127**, 11596–11597.
35 Y. J. Park, N. S. Sickerman, J. W. Ziller and A. S. Borovik, *Chem. Commun.*, 2010, **46**, 2584–2586.
36 A. S. Borovik, *Chem. Soc. Rev.*, 2011, **40**, 1870.
37 D. C. Lacy, R. Gupta, K. L. Stone, J. Greaves, J. W. Ziller, M. P. Hendrich and A. S. Borovik, *J. Am. Chem. Soc.*, 2010, **132**, 12188–12190.
38 C. E. MacBeth, A. P. Golombek, V. G. Young Jr., C. Yang, K. Kuczera, M. P. Hendrich and A. S. Borovik, *Science*, 2000, **289**, 938–941.
39 R. L. Lucas, M. K. Zart, J. Murkerjee, T. N. Sorrell, D. R. Powell and A. S. Borovik, *J. Am. Chem. Soc.*, 2006, **128**, 15476–15489.
40 S. Murata, R. Yoshidome, Y. Satoh, N. Kato and H. Tomioka, *J. Org. Chem.*, 1995, **60**, 1428–1434.